A Histological Investigation into the Temporal Development of Respiratory Muscle Dysfunction in a Murine Model of Pressure-Overload Heart Failure

By
Alicia Maria Arkell

A Thesis
Presented to
The University of Guelph

In partial fulfillment of requirements
set forth for the degree of
Master of Science
in
Human Health and Nutritional Science

Guelph, Ontario, Canada

ABSTRACT

A Histological Investigation into the Temporal Development of Respiratory Muscle Dysfunction in a Murine Model of Pressure-Overload Heart Failure

Alicia Maria Arkell

University of Guelph, 2017

Advisor:

Professor Jeremy A. Simpson

Heart failure is one of the leading causes of morbidity and mortality worldwide. One of the chief complaints of heart failure patients is exercise intolerance, characterized by fatigue and dyspnea. Currently, there are two theories meant to explain respiratory dysfunction in heart failure (HF). First, pulmonary edema increases the relative work of breathing, which predisposes the diaphragm to fatigue related injury (Ingram & Braunwald, 2005; Mulrow, Lucey & Farnett, 1993). Second, a HF induced catabolic state results in skeletal muscle atrophy, increasing ventilation via an over active ergo-reflex. Importantly, to date, only end stage HF has been examined, leaving incipient events in the pathogenesis of respiratory dysfunction unknown. Therefore, we sought to characterize the temporal development of respiratory muscle dysfunction during pressure-overload HF. We hypothesized that neither pulmonary edema, nor limb muscle myopathy were involved in the onset of respiratory dysfunction. Indeed, similar to clinical HF, animals displayed increased work of breathing in the absence of pulmonary edema. Diaphragmatic weakness occurred quickly following transverse aortic constriction (TAC) and was strongly correlated with muscle cell atrophy, preceding limb muscle myopathy. Further, chronic blockade of β-adrenergic signaling for four weeks prevented dysfunction and atrophy within the diaphragm. This work provides evidence towards the mechanism and preventable nature of HF-induced respiratory dysfunction.

Acknowledgements

First and foremost, I would like to express my endless gratitude to my advisor, Dr. Jeremy Simpson. The time you have invested in me has certainly been considerable. I cannot say what prompted you to take a chance on me, but I am eternally grateful. Your patience, guidance and support have been the cornerstone of my education; which definitely goes far beyond what is contained in the following pages. Successfully navigating the roles of mentor, boss and friend is a difficult task, but you somehow manage to do it *and* make it look easy.

To my committee, Dr. David Wright. Thank you for including me in your work and trusting me with your samples. Thank you for your encouragement, and most importantly for your time. Above all, thank you for caring enough to be tough on me when needed, that is no easy thing.

Dr. Lawrence Spriet, thank you for the talks, the jokes and all you do to keep our department running smoothly and successfully.

The A-Team, Andra, Anne S and Anne LH, thank you for your dedication to HHNS and your amazing spirits. You are the Atlas to the department, always in the know and always ready to support. There would be chaos without you! Diana, Andy and Becky, if the A-team were the soul of the department, you would be the heart. There would be no research without everything you do. Thank you for caring for our animals, their home and the students who need them. You are all absolutely wonderful.

The Simpson Lab, past and present. Laura, Gillian and Melissa C. You girls where there to welcome me from day one. Laura, nobody would have found anything without you. You were always the one organizing an ready to help whenever needed. Gillian, thank you for adopting me that very first day. I felt so out of place and so much like I didn't belong there and you helped me fit. You will likely never know how much your support means to me. Melissa C, thank you for sharing your time, your poster and your knowledge with me. My first project in lab was with you and I can't think of a better person to help me cut my teeth in research. Your dedication to your work is such an inspiration.

Laelie Snook, you are one of the smartest people I know. Thank you for your friendship, support, and for nurturing me when I was just an insecure summer student with a bad case of imposter syndrome.

Matt Platt, my lab brother. We started the very same day and look where we are now! Certainly not as far along as we dreamed, but truly it doesn't matter how long it takes to reach a destination, but what we gain along the way. Above your integral role in the lab, I'll most remember what an outstanding person you are. Even considering your 'Matt facts', you are still one of the most intelligent people I have ever had the pleasure of knowing. You are a rare find in this world, a person whose smarts is equaled by his humility and I am proud to have worked with you. Nadya, would there be any posters, papers or talks without your contribution? I think not. But more than that, you have nurtured and strengthened my confidence as a bourgeoning young scientist, and for that I am so grateful. Jason, my grasshopper. Looking back at how much we taught each other is so exciting. That is, to me, what grad school is really all about. You are a jack of all trades, and a master of science (literally). Your thirst for knowledge is inspiringly strong. I am excited to see where life takes you next, I think yours will be a wild and fantastic ride. Andrew Foster, you are athletic, hilarious, witty and have a massive heart. It has been one of the highlights of my scholastic career not only knowing you, but working closely with you. Thank you for your kindness, laughs, help and friendship. Finally, Melissa Allwood (Seabiscuit). Of all of the things I knew I would gain from my graduate degree, a sister was not one I was expecting. You are a force, an inspiration and one of the best friends I've ever had. I am not sure that anyone can understand how you managed to do all of the things you did in a day, month or year and still have time to bond with all of us in lab, but we are all grateful that you did. I have no doubt that we will be friends forever, and I am so excited to see what you conquer next.

To my mother, thank you for making me. If raising a child takes a village, then you are a village. Thank you for being everything I ever needed, mother father, sister and best friend. I love you and owe my life to you.

To my husband, a more supportive and loving partner does not exist in the world. There is no hyperbole in saying that this work would have never been accomplished without you. You have bolstered and encouraged me every step of the way with your selfless and endless love. You have taught me

everything I know about commitment, relationships and perseverance. You inspire me to love more, push harder and to be happy, every single day.

Finally, to my son, Emmett. Some may say that it took me too long to graduate because of you. The real truth is, you gave me the will and courage to finally finish. I love you more than life its self.

LIST OF FIGURES

LIST OF TABLES

LIST OF ABBREVIATIONS

Abdominal Aortic Constriction	AAC
Abdominal Pressure	Pab
American Heart Association	AHA
Cardiac Output	CO
Cross Sectional Area	CSA
Diastolic Blood Pressure	DBP
Esophageal Pressure	Pes
Expiratory Time	T_E
Heart Rate	HR
Heart Failure	HF
Inspiratory Pressure	PI
Inspiratory Time	T_I
Left Ventricular End Diastolic Pressure	LVEDP
Mean Arterial Pressure	MAP
New York Heart Association	NYHA
Stroke Volume	SV
Systolic Blood Pressure	SBP
Trans-diaphragmatic pressure	Pdi
Maximal Trans-diaphragmatic pressure	Pdi_{MAX}
Transverse Aortic Constriction	TAC
Total Breath Time	T_{TOT}

TABLE OF CONTENTS

STATEMENT OF CONTRIBUTIONS

I am exceedingly grateful to Matt J. Platt and Andrew J Foster for their contributions to my project. Matt is responsible for all of the TAC and sham surgeries; as well as collecting and analyzing the hemodynamic data. Figure 12 B, C & D were generated by Matt, as wells as Tables 7 & 8.

Andrew J Foster performed both the *in vivo* and *in vitro* diaphragm function data collection and analysis. Andrew created Figure 14 and 15D, as well as Table 9. Without them, this work could never have been completed. My sincerest thanks.

CHAPTER I: REVIEW OF LITERATURE

Introduction

Heart failure (HF), is defined as the inability of the heart to provide sufficient blood supply to meet the body's metabolic demands (Denolin et al., 1983). Currently, over 500,000 Canadians are living with HF and 50,000 new patients are diagnosed annually (Ross et al., 2006). That figure is projected to triple over the next three decades (Health Canada, 2002; Johansen et al., 2003). There are several known causes of HF (Table 1), such as myocardial infarction, hypertension and valvular disease (Ho et al., 1993). Regardless of its incipient cause, HF negatively impacts quality of life, exercise tolerance and lifespan

Pathological	Physiological
Volume	
Acute Myocardial Infarction	Pregnancy
Aortic regurgitation	Endurance Training
Anemia	
Pressure	
Chronic Hypertension	Resistance Training
Aortic Stenosis	
Coronary Artery Disease	
Endocrine	
Obesity	
Thyroid Disease	
Infection	
Septic Shock	
Viral/ Bacterial Cardiomyopathy	
Myocarditis	
Pericarditis	
Idiopathic	
Valve Disease	
Arrhythmias	
Takostobu	
Dilated/Hypertrophic Cardio Myopathy	

Table 1. Known causes of heart failure.

Hypertension, defined as systolic blood pressure > 140 mmHg, is one of the most common causes of HF (Ho et al., 1993); it is estimated that upwards of 30% of adults in North America have hypertension, with an additional 20% being pre-hypertensive (systolic blood pressure 120-139 mmHg) (Wilkins et al., 2010). HF is one of the leading causes of morbidity and mortality, and puts significant economic and clinical strain on the Canadian healthcare system, with 50% of patients dying within five years of diagnosis (Ahmed, 2009). Critically, HF is on the rise owing primarily to three factors: First, an aging population as the risk of HF increases with age (Roth et al., 2015). Second, there is an increased prevalence of comorbidities associated with an increased risk of developing HF such as obesity (Flegal et al., 2015) and type II diabetes (Bilandzic & Rosella 2017). Finally, recent improvements in detection of MI (eg. cardiac TnI) results in earlier treatment and lower incidences of misdiagnosis. This substantially increases the survival rate of myocardial infarction, resulting in more people living with HF. Considering this, there seems to be no prospect for the decline in rates of HF.

Pathology of Hypertensive Heart Failure

The primary clinical characteristic of HF is reduced cardiac output, which is a product of stroke volume (SV) and heart rate (HR).

Cardiac Output = SV*HR

Stroke volume is the amount of blood ejected from the heart with each beat (~70 mLs per beat) while HR is the number of times the heart beats per minute (~72 beats per minute). Together, these variables result in a cardiac output of approximately 5L per minute at rest in adults. Often, stroke volume is the primary component that is compromised in HF. The three variables that contribute to determining stroke volume are: preload, afterload, and contractility.

Preload is peak wall stress during diastole (which occurs at end diastole and is often likened to ventricle filling) and after load is peak LV wall stress during systole (and is often likened to blood pressure). Ventricle wall stress is the tension generated by cardiomyocytes, which is proportionate to the product of left ventricular pressure (P) and inner radius of the left ventricle (r) divided by the left ventricle wall thickness (t).

Wall Stress = P*r/t

Pressure-overload (e.g. exercise, hypertension or valvular disease) increases peak wall stress, causing remodeling of the heart to increase wall thickness (Figure 1). Increased pressure will cause the addition of sarcomeres (the smallest contractile unit of muscle) in parallel, resulting in concentric hypertrophy. This will effectively decrease the size of the left ventricle chamber and increase ventricular wall thickness. Collectively, these changes normalize wall stress. (Smart, Knickelbine, Malik, & Sagar, 2000). While increased wall thickness is an adaptive response meant to normalize wall stress, over time it becomes maladaptive leading to HF. Specifically, pathological remodeling resulting from pressure-overload HF is associated with the excessive accumulation of fibroblasts and extracellular matrix proteins along with concentric hypertrophy of the heart. This fibrosis results in a stiffer ventricle, interfering with ventricular relaxation and increasing preload (Bernardo et al., 2010). In summary, although hypertrophy develops initially as a compensatory response to high blood pressure, over time, it becomes maladaptive, leading to contractile dysfunction and heart failure.

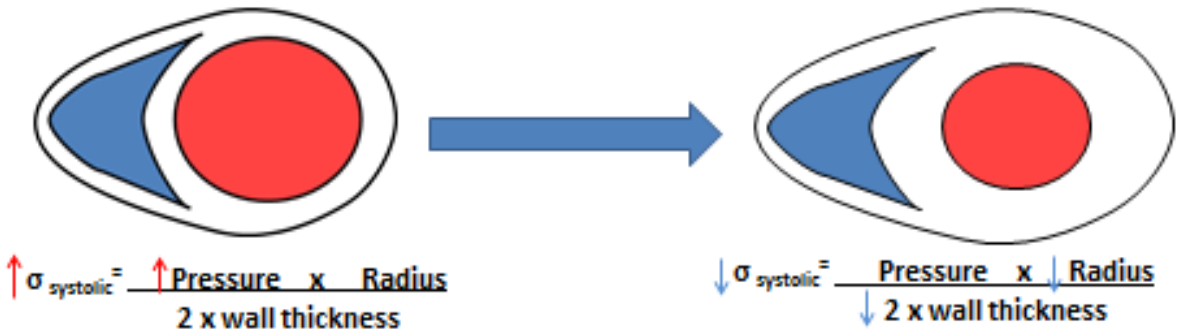

Figure 1. Cardiac remodeling as governed by La Place's law. Increased systolic wall stress results in ventricular hypertrophy, increasing wall thickness to normalize wall stress. Adapted from Maillet, van Berlo, & Molkentin (2013).

Contractility is the degree to which muscle fibers can shorten. In instances when demand for cardiac output increases, such as during exercise, the autonomic nervous system releases catecholamines, epinephrine and norepinephrine. The effects of catecholamines on the heart, mainly norepinephrine, are mediated primarily by β_1 receptors. Although α_1, α_2 and β_2 receptors also exist in modest amounts on cardiac tissue. Cardiac β -receptor activation by catecholamines has lusitropic, ionotropic and chronotropic effects. However, unlike exercise, HF creates an unrelenting pathological stress which results in chronic over stimulation of the sympathetic nervous system (Colucci et al., 1988). Infusion of norepinephrine or a nonselective β adrenergic receptor agonist results in myofilament damage, impaired calcium handling and formation of reactive oxygen species in the heart (Todd et al., 1985) and incubation of cardiomyocytes with norepinephrine *in vitro* causes a concentration-dependent decrease in cell viability (Mann et al., 1992). Moreover, chronic catecholamine administration

in animals causes fibrosis, apoptosis and left ventricular dilation (Brouri et al., 2004; Osadchii et al., 2007). Indeed, circulating catecholamines are significantly higher in HF patients that in healthy age matched individuals (Colucci et al., 1988) and serum norepinephrine concentrations represent a stronger prognostic indicator for survival than indices of cardiac function (Cohn et al., 1984; Rengo et al, 2014). Clearly, adrenergic overdrive is a central factor in the pathogenesis of HF as it affects cardiac function and correlates with mortality.

Classification of HF

The cardinal feature of HF is exercise intolerance, characterized by dyspnea and exertional fatigue. Exercise intolerance is quantified by peak oxygen consumption ($VO2_{MAX}$), which is substantially lower in HF patients (Piepoli, Ponikowski & Clark, 1999). Importantly, peak oxygen consumption correlates with low quality of life and poor prognosis (DeGroote et al., 2004). In fact, exercise intolerance is often the first noticeable symptom of HF, prompting patients to seek medical attention. It is because of this, that the degree of exercise limitation is used by primary care givers to diagnose HF. As such, the New York Heart Association (NYHA) developed a four-stage HF classification system. Class I-III are defined as asymptomatic at rest, with progressive fatigue upon exercise and limitation in activities of daily living. Patients in class IV exhibit marked exercise intolerance as well as symptoms at rest and a severely decreased capacity to perform normal daily activities. Recently, the American Heart Association developed a complimentary ranking system (Figure 2) to include patients that are at high risk for developing HF, while also including structural characteristics of the heart (Hunt et al., 2009). Interestingly, while these symptoms are characteristic of HF, they are not solely caused by impairments in central hemodynamics (Franciosa, Park & Levine, 1981; Josiak et al., 2014; Lipkin et al., 1986; Metra et al, 1990; Weber et al, 1982;), indicating that while HF and exercise intolerance occur concomitantly, they are not directly related.

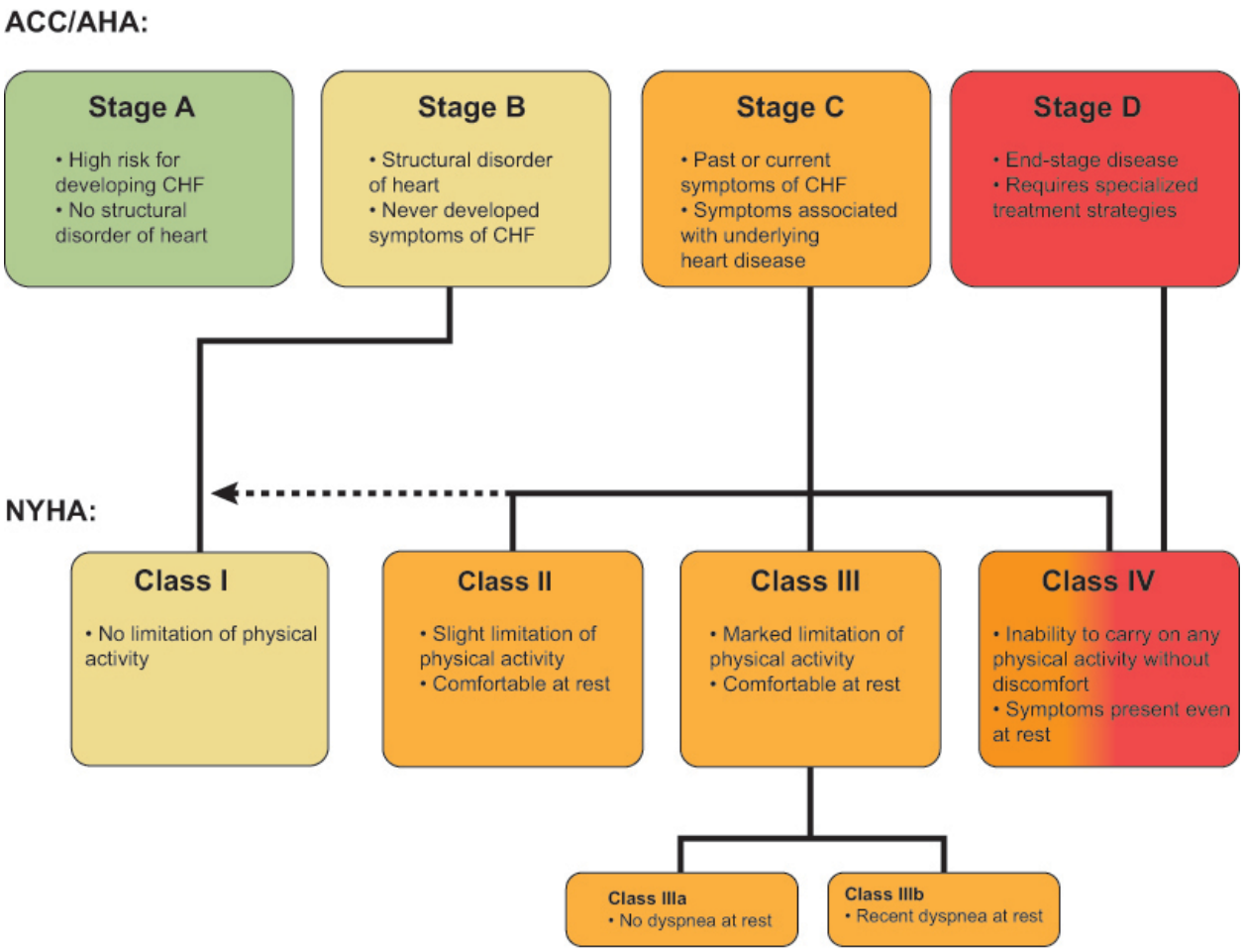

Figure 2. Comparison of NYHA and AHA heart failure rating systems. Retrieved from: http://www.heartfailure.org/wpcontent/uploads/2015/03/www.HF-Stages1.jpg

Several groups have attempted to improve exercise capacity by acutely improving hemodynamics with vasodilators, (Drexler et al., 1989; Maskin et al., 1983; Wilson, Ferraro & Weiner, 1985; Wilson & Ferraro, 1985;). Although subjects in these studies did improve cardiac output and blood flow to working muscles, no improvements in maximal oxygen consumption, or sensed fatigue were achieved, suggesting that reduced exercise capacity is not directly related to limitations in blood flow, but to dysfunction within peripheral muscles themselves.

Skeletal Muscle

Structure and Function

Skeletal muscle is comprised of bundles of muscle cells; owing to their elongated shape, they are commonly referred to as fibers instead of cells. These cells/fibers often span the entire length of the muscle, are multinucleate and the cytoplasm is tightly packed with contractile proteins. The smallest contractile unit of muscle is called a sarcomere. Within each sarcomere, the two primary contractile proteins, actin and myosin are oriented parallel to each other and anchored to z-disks. Muscle contraction is accomplished by the binding of myosin heads to stationary actin filaments, to form a cross-bridge. In the presence of calcium, the myosin binding sites on actin are exposed, permitting the binding of myosin heads. Upon binding, ADP and Pi are released from the myosin head causing it to pivot, thus producing a power stoke. In the presence of abundant energy, ATP binds the myosin head and is cleaved to form ADP and Pi, a process which re-positions the myosin head to bind to actin again. As this process continues, the myosin heads “walk” towards the center of corresponding actin filaments, shortening the sarcomere, and thus the muscle fiber, producing a contraction.

Fiber Typing

Skeletal muscle is comprised of both slow twitch and fast twitch muscle fibers. Slow twitch muscle fibers, also referred to as type I, are associated with low force output and fatigue resistance. Fast twitch, or type II muscle fibers, are able to achieve high force outputs and reach fatigue faster. Type II muscle fibers can be further distinguished into type IIa and type IIb, the former being more fatigue resistant than the latter. While all skeletal muscle expresses both type I and type II fibers, the relative proportion in each is specific to several factors, including the primary function of the muscle, genetics and the physical demands placed upon the muscle. For example, postural muscles such as the soleus, tend to express a higher proportion of type I muscle fibers than non-postural muscles. Experimentally, skeletal muscle fiber types can be distinguished by the isoform of myosin they express and their metabolic properties. Myosin heavy chain is directly related to fiber type, where slow fibers express myosin heavy chain type I and fast fibers express type II isoforms.

Limb Muscle in Heart Failure

Patients with HF are severely limited in their daily life because of dyspnea and fatigue. While central hemodynamic abnormalities are the trademark feature of HF, a direct link between central hemodynamics and functional exercise capacity does not exist (Lipkin et al., 1986; Franciosa, Park & Levine, 1981). Specifically, the maximum achievable workload ($VO2_{peak}$) in a graded exercise test in HF patients is significantly reduced, but is not related to resting indices of cardiac function (Cohen-Solal, Beauvais, & Tabet, 1994). In healthy individuals, maximal exercise tests are generally terminated when maximal aerobic capacity is achieved, but if HF, tests are most often terminated due to dyspnea and fatigue (Wilson, Mancini & Dunkman 1993). Moreover, while blood flow to working muscles is reduced in

HF, it is not the cause of limitation. During a treadmill based maximal exercise test, when blood flow to working muscles is increased to levels comparable to healthy age matched individuals, HF patients still exhibit exercise intolerance, reduced exercise capacity and fail to achieve higher workloads than without improved flow (Wilson, Mancini & Dunkman 1993). This indicates that exercise intolerance is independent of central hemodynamics, and involves skeletal muscle myopathy.

Changes in Muscle Strength and Endurance

HF is associated with marked reductions in skeletal muscle function. In a study done by Minotti et al. (1991), dynamic endurance during a loaded knee extensor activity was significantly lower in HF compared to healthy subjects. This was demonstrated by a greater decline in torque generation during the final repetitions of knee extension compared to the initial torque produced. Static muscle endurance, defined as the length of time required for initial force to decline to 60% of maximum, was also significantly decreased. Many groups since (Chua et al., 1995; Minotti et al., 1993; Panizzolo et al, 2015; Toth et al., 2006 & Toth et al., 2010) have confirmed the finding. Muscle strength, on the other hand, as indicated by peak torque in the first three repetitions of knee extension, was not affected by HF. In contrast, Lipkin et al., (1988) did find reduced strength in the quadriceps of HF patients, however, this result could be attributed to their use of more physically active control subjects and more advanced HF patients (NYHA class 3 versus a mean class of 2.4 in Minotti's study). Since then, several groups have also found reduced skeletal muscle strength (Kitzman et al., 2014; Saval et al., 2010; Selig et al., 2004). Interestingly, one research group (Buller, Jones & Poole-Wilson, 1991) did find reduced strength in large locomotor muscles, but not small upper limb muscles, suggesting that deconditioning could play a role in loss of strength in HF. While exercise intolerance certainly encourages a sedentary lifestyle, changes in skeletal muscle of

HF patients is not entirely owing to disuse. Both Simonini et al (1996) and Vescovo et al. (1996) found different patterns of atrophy in HF versus disuse subjects. Specifically, subjects exposed to bed rest showed reductions in type II glycolytic fibers, whereas HF patients increase proportions of type II fibers (Mancini et al., 1989; Mancini et al., 1992; Simonini et al., 1996; Sullivan, Green & Cobb, 1990; Vescovo et al., 1996). Impaired muscle function in HF is characterized by decreased strength and endurance, and while a sedentary lifestyle is a likely characteristic of HF patients due to exercise intolerance, muscle atrophy and fiber type data suggests there is more to skeletal muscle myopathy then simply disuse.

Changes in Muscle Metabolism

In HF, skeletal muscle metabolism during exercise is impaired. Wilson, Fink & Marris (1985) reported that graded exercise resulted in decreased phospho-creatine and pH in the skeletal muscle of HF patients compared to healthy age matched subjects, a finding confirmed by Massie, Conway and Younge (1985) and Mancini et al. (1988). These findings indicate a greater reliance on anaerobic metabolic pathways in HF. Critically, these differences were noted in spite of normal perfusion, and remained when experiments were performed under ischemic conditions (Minotti et al., 1993) reinforcing the distinction between impaired central hemodynamics and skeletal myopathy.

Changes in Muscle Morphology

Atrophy of peripheral skeletal muscle is a prominent feature of HF (Josiak et al, 2014; Minotti et al., 1993; Stassijins, Lysens & Decramer, 1996). Atrophy can be described as either decreased cross sectional area of the total muscle, or a decrease in the cross sectional area of individual muscle fibers. Critically, cross sectional area is a strong determinant of muscle strength (Minotti et al., 1996) meaning that in HF, atrophy directly impacts force generation.

In addition to reduced muscle size, limb muscles of HF patients exhibit a greater proportion of type II muscle fibers, with decreased type I fibers (Mancini et al., 1989; Mancini et al., 1992; Simonini et al., 1996; Sullivan, Green & Cobb, 1990; Vescovo et al., 1996), suggesting decreased oxidative capacity. Indeed, HF patients produce more lactate at a given workload then healthy invidiuals, indicating a greater reliance on anaerobic metabolism (Wilson, Mancini & Dunkman 1993), indicative of a slow to fast fiber type shift. Moreover, decreased activity of mitochondrial enzymes such as cytochrome oxidase, citrate synthetase and succinate dehydrogenase of HF patients have been observed by several groups (Drexler et al., 1992; Sullivan, Green & Cobb 1990) further decreasing oxidative capacity. HF induced changes in muscle morphology include decreased cross sectional area, increased proportion of type II muscle fibers and a decrease in oxidative enzymes.

Limb muscles of HF patients are characterized by decreased strength and endurance, general atrophy and type II fiber dominance with reduced oxidative capacity with the exact cause not yet fully understood.

The Muscle Theory

One dominant hypothesis in the understanding of exercise intolerance in HF is the Muscle Theory (Figure 3). According to this hypothesis, left ventricular dysfunction causes a cascade like response in which reduced blood flow causes extreme muscle wasting (cardiac cachexia) and dyspnea upon exertion. Muscle myopathy and dyspnea then feed forward to sympathetic excitation and vasoconstriction which then loop back to further disrupt ventricular dysfunction creating a vicious cycle.

Central to the muscle theory is the exaggerated ergo-reflex, meant to explain exercise induced dyspnea. Ergo-receptors are afferent nerves within skeletal muscle that are sensitive

to metabolic activity and muscle contraction, which inform the brainstem of muscular movement. This causes sympathetic nerve excitation, to provoke necessary changes in ventilation and hemodynamics to support the increased demand for oxygenated blood in response to increases in physical activity (Scott et al., 2003). In HF, reduced peripheral blood flow and skeletal muscle myopathy cause ergo receptor over-excitation (Roberto et al., 2017). This leads to (1), an increased ventilatory response to exercise, contributing to the sense of dyspnea, and (2), over stimulation of the sympathetic nervous system with subsequent generalized vasoconstriction (Piepoli et. al., 1996; 2007; Roberto et al., 2017). These alterations reduce exercise capacity by causing an early onset of anaerobic metabolism and decreased strength and endurance, further activating the ergo reflex which then feeds back to further deconditioning by exacerbating exertional discomfort, promoting a sedentary lifestyle. According to the muscle hypothesis, dyspnea and exercise intolerance is caused by peripheral limb muscles. What the muscle theory fails to acknowledge is the contribution of the diaphragm in particular to exercise intolerance. It is well accepted that the diaphragm develops a myopathy distinct from other skeletal muscles (Mancini et al., 1992), indicating that dyspnea extends beyond the influence of peripheral muscle ergo receptors.

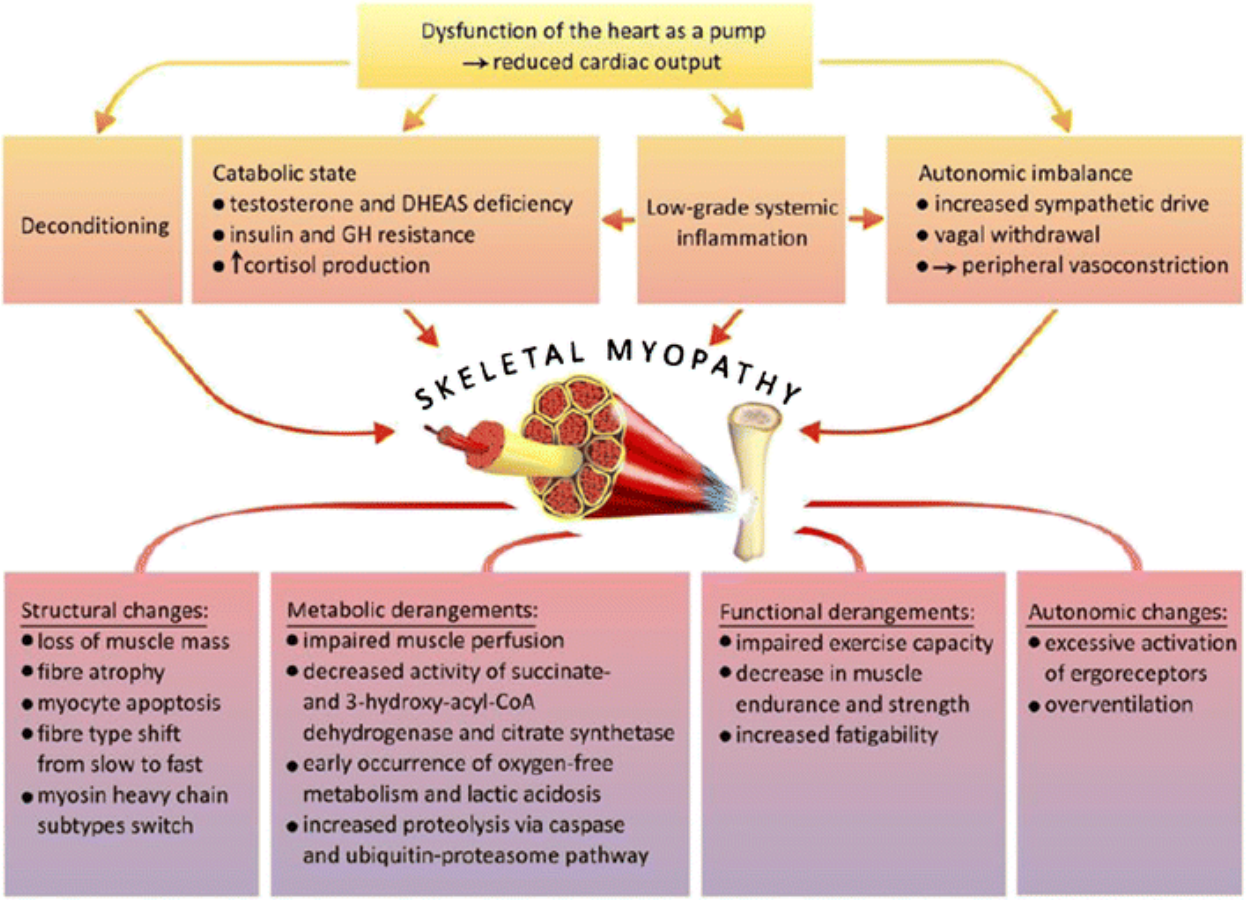

Figure 3. The Muscle hypothesis attributes dyspnea and increased ventilatory drive to limb muscle changes in structure and metabolism. From Josiak et al., 2014.

Diaphragm Dysfunction in Heart Failure

The diaphragm is a dome shaped skeletal muscle, located at the most inferior aspect of the ribcage and is the primary muscle for inspiration. As the diaphragm contracts, it moved downwards, increasing the volume of the thoracic cavity, creating a negative pressure which expands the lungs. During quiet expiration, the diaphragm passively returns to resting muscle length. The diaphragm arises from 3 peripheral origins: (1) the arcuate ligaments on the lumbar vertebrae L1-3, (2) the costal cartilage of ribs 7 to 12, (3) the xyphoid process of the sternum. The fibers that originate from the lumbar make up the crural region, while the fibers originating from the ribs and xyphoid comprise the costal region (Figure 4) with the former being responsible for inspiration. The muscle fibers of the diaphragm converge and form the central tendon, which is fused with the pericardium.

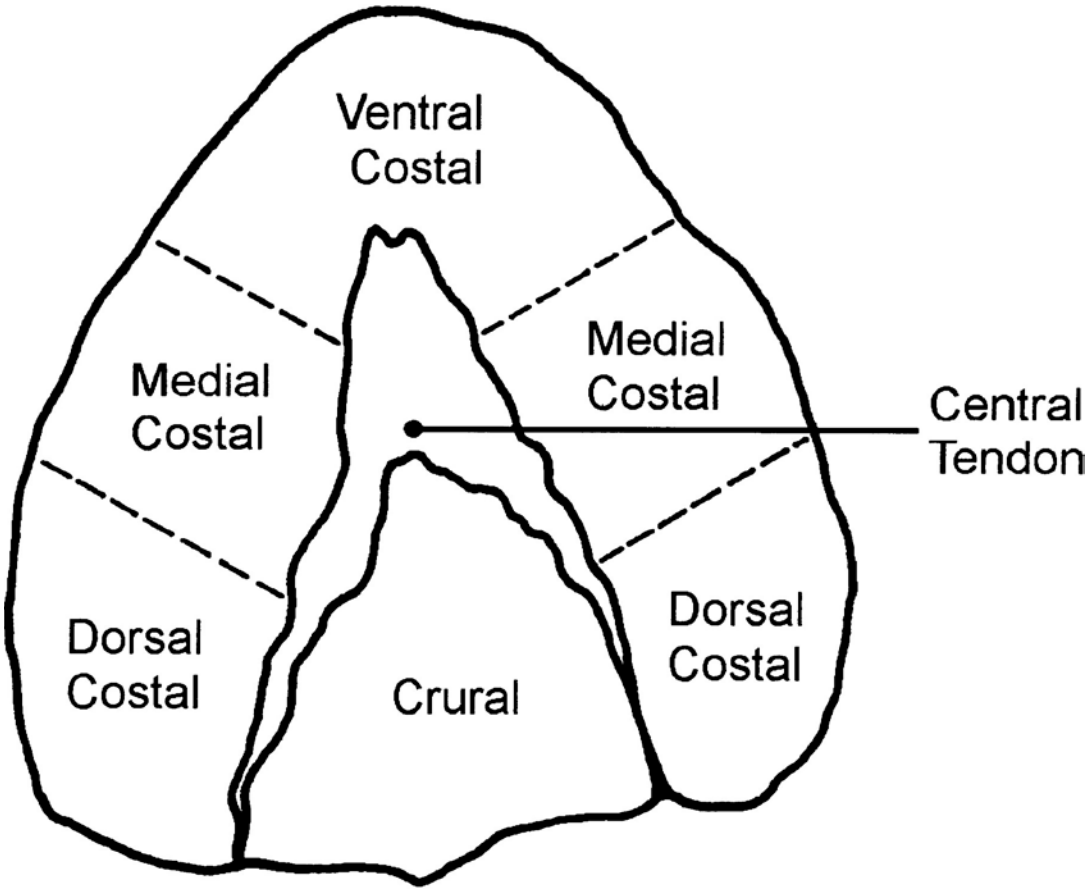

Figure 4. Abdominal view of diaphragm depicting the costal, crural and central tendon regions. From Sexton & Poole, 1998

While the diaphragm is classified as a skeletal muscle, it is the only skeletal muscle that is under both voluntary and involuntary control. Moreover, it is constantly contracting, from birth until death unlike limb muscles which, by comparison, are easily rested. It is because of this, Mangner et al. (2015) postulated that the diaphragm would be more sensitive to intrinsic stimuli (such as atrophy signaling) as well as fatigue-related injury. Indeed, significant diaphragmatic atrophy occurs with as little as 18 hours of mechanical ventilation (Levine et al., 2008), whereas limb immobilization results in atrophy after 36-48 hours (Booth et al., 1977), reinforcing the sensitivity of the diaphragm compared to peripheral limb muscles.

DeTroyer and colleagues first noted respiratory muscle dysfunction (inclusive terminology for any deficit in respiratory muscle pressure generation, including, for example, atrophy, dysfunction, myopathy) in HF over thirty years ago, and several studies since have confirmed this finding as a phenomenon separate from limb muscle dysfunction (Coirault et al., 1999; Lecarpentier et al., 1999; Mancini et al, 1992; Supinski et al, 1994). Clinically, respiratory muscle dysfunction manifests as reduced maximal diaphragmatic strength and endurance, which is found in approximately 50% of HF patients (Dall'Ago et al., 2006). The direct measurement of diaphragmatic strength is difficult since the muscle is essentially inaccessible. Instead, trans-diaphragmatic pressure (Pdi) was used since it is linearly related to force output. For maximal diaphragmatic strength, trans-diaphragmatic pressure generated during a maximal inspiratory effort (Pdi_{MAX}) from resting muscle length was measured. Measuring maximal trans-diaphragmatic pressure is accomplished by calculating the difference between abdominal pressure (Pab) and esophageal pressure (Pes) during an inspiratory effort (Caruso et al., 2015).

Pdi= Pab-Pes

Several groups have observed atrophy and decreased function in both clinical (DeTroyer

et al., 1980; Dimopoulou et al, 1998; Lindsay et al., 1996) and experimental HF (Coirault et al., 1999; Klawitter et al., 2004; Lecarpentier et al., 1999; Mancini et al, 1992; Supinski et al, 1994). Critically, despite the substantial body of research produced to date, there is still little known about the initial cause and progression. It is generally believed that diaphragm dysfunction is a result of fatigue related injury, caused by a chronic load placed on the diaphragm throughout the development of heart failure (Wilson & Mancini, 1993). The tension time index (TTI) is used to evaluate mechanical loads on skeletal muscle. It is the product of duty cycle, contraction or inspiratory time (T_I) divided by total breath cycle time (T_{TOT}) and the ratio of mean Pdi per breath to maximal Pdi (Pdi_{MAX}).

$$\mathbf{TTI = (T_I/T_{TOT})\ (Pdi/Pdi_{MAX})}$$

While HF patients do show tension-time index values more than double those of age matched healthy subjects, it is not due to changes in duty cycle (Mancini et al., 1992). In fact, the change in tension-time index is solely owing to increased Pdi and reduced Pdi_{MAX} (Mancini et al., 1992 & 1994), indicating an increase in work of breathing and a decrease in contractile reserve, respectively. It is generally thought that respiratory muscle dysfunction is caused by pulmonary edema, which increases resting Pdi, and results in hypoxia. Decreased oxygen availability causes an adaptive response within the muscle towards increased anaerobic metabolism, shifting from type I slow oxidative fibers to type II fast glycolytic. Importantly, the clinical manifestation of respiratory dysfunction in HF is not in alignment with the fatigue related injury theory. First, clinical incidence of pulmonary edema in HF is rare, which is why it is no longer commonly referred to as congestive HF (Piepoli & Coats, 2007). Second, should hypoxia be contributing to muscle alterations, it would be expected that the observed shift would be towards a glycolytic phenotype, when in fact, the diaphragm increases the proportion of oxidative fibers (Coirault et al., 2007; Supinski et al., 1994; Stassijins et al., 1998). In clinical HF, there is a ~30% reduction in diaphragmatic strength (Hughes et al., 1999) and

reports from various animal models range from 40-60% reduced strength (Coirault et al., 1999; Supinski et al., 1994; Stassijins et al., 1998). The force capabilities of a muscle are primarily determined by : force-length relationship, muscle architecture, fiber type, muscle cross sectional area and contractile function. Interestingly, the observed fiber type shift in the diaphragm is opposite of that observed in limb muscle (Coirault et al., 1999 & 2007; Howell et al., 1995). In limb muscle, metabolism shifts towards a glycolytic phenotype owing to reduced perfusion (Coats, Clark & Piepoli, 1994), inflammation (Lima et al., 2014) and a sedentary lifestyle (Josiak et al, 2014). The diaphragm, however, presents with an increased proportion of slow twitch fibers, implying fatigue resistance at the expense of force generation. In this instance, chronically elevated tension-time index is analogous to endurance training. The diaphragm of HF patients also shows signs of atrophy and apoptosis leading to decreased myofibril cross sectional area (Lindasy et al., 1996; Stassijns et al., 1998). In the diaphragm, it is predominantly type IIb fibers that atrophy (Coirault et al., 2007; Howell et al., 1995; Stassijins et al, 1998). Type IIb muscle fibers are capable of producing high forces but also fatigue quickly, it is believed that selective atrophy of IIb fibers is the reason for the observed increase in slow twitch fiber proportion (Howell et al., 1995).

In HF, there is a marked reduction in cross bridge formation, and impairments in calcium handling which collectively result in poor contractile performance (Coirault et al., 2007; Lecarperntier et al., 1999; Middlekauff et al., 2012). Interestingly, decreased diaphragmatic strength correlates well with dyspnea (Mancini et al., 1992), but not indices of left ventricular function or lung function, furthering the distinction of a myopathy unique to the diaphragm in HF.

Animal Models of Heart Failure

Animal models are an invaluable component of HF research. They are designed to mimic the clinical presentation of HF in order to identify potential treatment targets and strategies. Since the etiology of HF is exceedingly variable, there are several well established surgical models. Transverse aortic constriction (TAC) and myocardial infarction are two of the most commonly used surgical models of HF.

TAC seeks to recapitulate HF resulting from hypertension and is achieved by banding the aortic arch (Figure 5, top), inducing a significant increase in intracardiac pressure. Initially, a surgically-induced constriction leads to hypotension distal to the tie resulting in decreased perfusion to tissues and organs distal to the band. In response to low pressures, the kidney increases sodium and water reabsorption to return blood pressure towards normal values by increasing blood volume. To accommodate the increased blood volume, the blood pressure from the left ventricle to the constriction has to increase, which eventually leads to pressure-overload HF (van Oort & Wehrens, 2010).

Experimentally, myocardial infarctions are surgically-induced, typically done by ligation of a coronary artery, often the left anterior descending (Figure 5, bottom) and completely occluding blood flow inferior to the tie. Without perfusion, the affected cardiomyocytes become necrotic. The lost cardiomyocytes are then replaced by scar tissue, which has no contractile ability, contributing to depressed cardiac output. Reduced cardiac output causes a proportional decrease in mean arterial pressure which causes the kidneys to increase sodium and water reabsorption to return blood pressure towards normal values by increasing blood volume. The subsequent increase in blood volume further impairs the heart's ability to function by increasing preload. Chronically elevated preload causes chamber dilation to accommodate increased filling volume, resulting in eccentric hypertrophy.

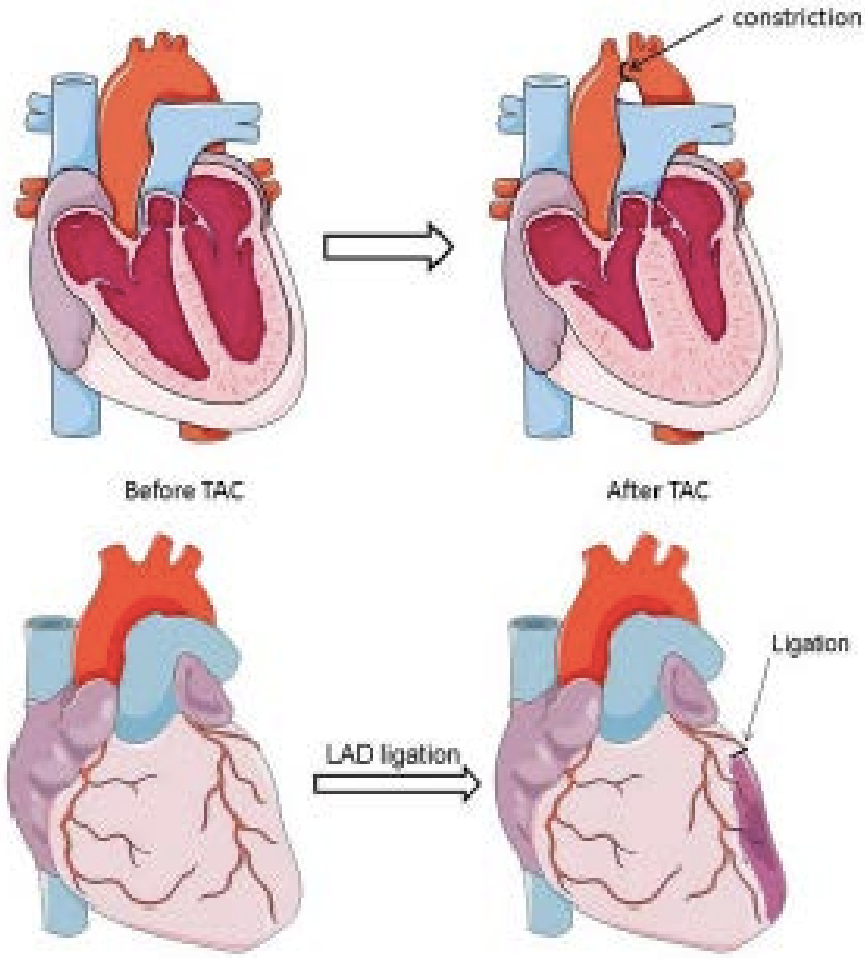

Figure 5. Surgical induction of heart failure.
Top- Location of band for TAC, between brachiocephalic and left common carotid artery. Bottom – myocardial infraction induced by ligation of left anterior descending artery.
Retrieved from https://www.unil.ch/caf/en/home/menuinst/services/micro-surgery.html

While mice are currently the most commonly used animals in HF research today, much of the early work done on respiratory muscle dysfunction in HF was done in high order animals such as dogs and pigs (Howell et al., 1995; Supinski et al., 1994). The cardiac physiology of larger animals holds more similarities with humans than that of rodents, meaning a more direct translation of findings to clinical populations. However, decreased costs associated with the care and housing of rodents and increased availability of non-invasive imaging methods and hemodynamic assessment tools (Patten & Hall-Porter, 2009) spurred a transition from the use of larger animals to rodents in HF research. Additionally, the development of transgenic mice and the continuing advancements in technology available for cardiovascular diagnostics have enabled the opportunity to examine HF to a depth and detail not possible in clinical research; leading to the development of several effective pharmaceutical interventions responsible for improving the length and quality of life for patients.

Treatment of HF

Currently, treatment for HF is aimed at managing symptoms, as there is no cure. In HF, there is a reduction in cardiac output leading to hypotension that causes a reflex increase in sympathetic nervous system activity (Gheorghiade, Colucci & Swedberg, 2003; Stassijins, Lysens & Decreamer, 1996). With enhanced sympathetic activity follows an increase of catecholamines, epinephrine and norepinephrine, released primarily by sympathetic nerve endings and the adrenal medulla. Serum catecholamine concentrations in HF patients are markedly higher than healthy age matched subjects (Colucci et al., 1988). Epinephrine and

norepinephrine bind to β-adrenergic receptors on cardiac muscle, increasing heart rate and accelerating ventricular relaxation which aids in increasing cardiac output. Peripheral muscle vasculature also possesses β receptors which, when stimulated by catecholamines, cause vasoconstriction. The consequences of chronic long-term β receptor activation, as outlined by Piepoli et al. (1996), are reduced peripheral blood flow, vagal withdrawal, desensitizing of the β-adrenergic system, increased likelihood of arrhythmias (Hunt et. al, 2001) and an imbalance of anabolic and catabolic processes in favor of the latter (Josiak et al., 2014). If left untreated, over activation of the sympathetic nervous system contributes to skeletal myopathy and cardiac remodeling (Maak & Elter, 2003). Therefore, the significant impact of sympathetic over activation in HF makes it a crucial target for complete treatment.

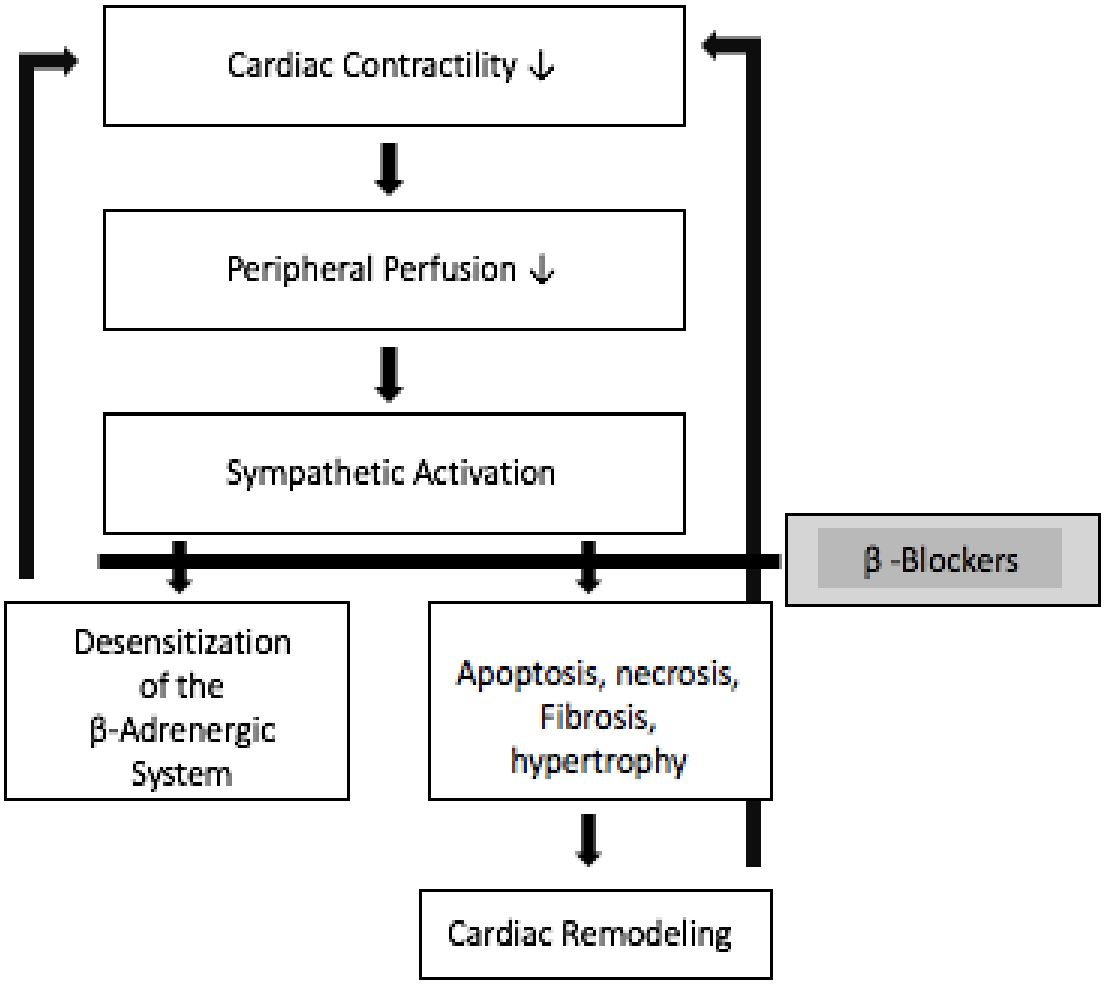

Figure 6. Effect of β-adrenergic blockade on the pathogenesis of heart failure. Decreased cardiac contractility results in decreased peripheral perfusion. A reflex increase in sympathetic output occurs resulting in cardiac remodeling and desensitization of β-adrenergic receptors. β blockers prevent overstimulation of receptors, preventing desensitization and cardiac remodeling. Adapted from Maak & Elter, 2003.

β -blockers were one of the first class of drugs shown to directly reduce both morbidity and mortality in HF patients (Bristow, 1997). By antagonizing the effects of autonomic stimulation on adrenergic receptors, β-blockers reduce HR, contractility, lessening the energetic demand on the heart. β –blocker therapy also lowers blood pressure by decreasing renin release from the kidney, (Gheorghiade, Colucci & Swedberg, 2003).

Because of their efficacy, β-blockers are recommended for all stable HF patients, including those on other medications such as digoxin and angiotensin converting enzyme inhibitors (AHA, 2016). Despite this, β-blockers continue to be grossly under-prescribed. According to the PURE study, (Yusuf et al., 2011) only 47.6% of HF patients in North America are being treated with β-blockers. Clearly, clinical treatment of HF differs from guidelines, and is characterized by underuse of β-blockers, which likely results in increased mortality and hospitalizations (Fonarow et al., 2011).

HF represents a significant medical and economic burden globally. Reduced exercise capacity negatively impacts both quality of life and disease prognosis (Riberio et al., 2009). While the contribution of limb muscle myopathy towards exercise intolerance is well defined, many aspects of diaphragmatic myopathy have yet to be fully explored. The progression of diaphragm dysfunction in HF is largely unknown, as studies investigating diaphragm dysfunction are relegated to a single time point in end stage HF. Without defining the temporal development of respiratory myopathy, it is not possible to identify the incipient cause.

CHAPTER II: HYPOTHESIS & AIMS

The contribution of limb muscle myopathy to exercise intolerance has been well established. Patients with HF are limited in their daily living by dyspnea and fatigue, thought to be caused by pulmonary edema and altered skeletal muscle metabolism, respectively. However, pulmonary edema is rare in clinical HF, making it an unlikely cause of dyspnea. Also, limb and respiratory muscles adapt differently in HF, which raises doubt in a common mechanism and concomitant progression. Critically, all investigations into exercise intolerance in HF to date have been completed at a single time point in end stage HF, making it impossible to elucidate the time-course development, and therefore the cause, of these symptoms.

Aims

1. Characterize changes in diaphragm structure and function at 2, 4, 9 and 18 weeks of TAC.
2. Characterize changes in limb muscle structure relative to the diaphragm in TAC induced HF.
3. Delineate the time course between the development of pulmonary edema and respiratory muscle dysfunction.
4. Compare effects of pressure-overload HF caused by TAC and abdominal aortic constriction on diaphragm structure.
5. Evaluate effect of β-blockade on TAC diaphragm function and morphology.

Hypothesis

HF induced respiratory muscle weakness is a progressive phenomenon, caused by atrophy, in the absence of pulmonary edema and preceding limb muscle alterations.

CHAPTER III: METHODS

Animals

CD1 Male mice were obtained from Charles River Laboratory International Inc. (Canada). at 7-8 weeks of age. Animals were stored in cages of 3-4 housed in a 12:12 light dark facility with access to food and water *ad libitum*, and monitored twice daily according to the policies set forth by Guelph Animal Care Facilities. Mice were acclimatized for 1 week prior to surgical intervention. All experimental procedures were approved by the institutional animal care and use committee and conducted in accordance with the guidelines of the Canadian Council on Animal Care as set out in the Guide to the Care and Use of Experimental Animals.

Pressure-overload Induced by Transverse Aortic Constriction

9 week-old mice (~35 g body weight) were anesthetized with a minimum alveolar concentration of 5% isoflurane in 100% oxygen and were maintained in the surgical plane of anesthesia (lack of reflex or response to toe pinch) with a minimum alveolar concentration of 2% isoflurane (CDMV, Canada) in 100% oxygen. Mice were then orotracheal intubated using a 20 gauge angio-catheter (Dickinson and Company, USA) and mechanically ventilated with a rodent microvent (Harvard Apparatus, Canada) at an approximate tidal volume of 300µl and 200 breaths/min. Next, mice were placed in a supine position and body temperature was maintained at 37^{o}C with a hot water pad. Chest hair was shaved to expose the skin and a 1centimeter horizontal incision was made at the second intercostal space. Ribs were separated from the sternum at their cartilaginous insertions and the transverse aorta was isolated. A 7-0 Sofsilk ® (Coviden Tech, USA) thread was tied around the transverse aorta between the innominate and left common carotid artery to the diameter of a 26-gauge needle (Figure 1 & 7). The needle was quickly removed, leaving the suture to constrict the aorta. The incision was

closed using 5-0 Sofsilk ® (Coviden Tech, USA) to suture the ribs and skin. Mice were then allowed to recover on a warming pad until fully awake. Sham operated mice underwent an identical procedure omitting the suture around the aorta.

Nota bene: Preliminary experiments confirmed identical histomorphometric, hemodynamic and functional values among animals at 2, 4, 9 and 18 weeks following sham surgery. Therefore, to limit the use of animals for this thesis, sham animals were not age matched and a single group of sham animals were used for comparison throughout this thesis.

Pressure-overload by Abdominal Aortic Constriction

In a subset of animals, the abdominal aorta was constricted in a similar fashion to TAC, between the supra renal and renal arteries (Figure 7), to investigate the effects of HF and diaphragmatic hypertension on the morphology of diaphragm muscle. Animals were sacrificed at 18 weeks of abdominal aorta constriction.

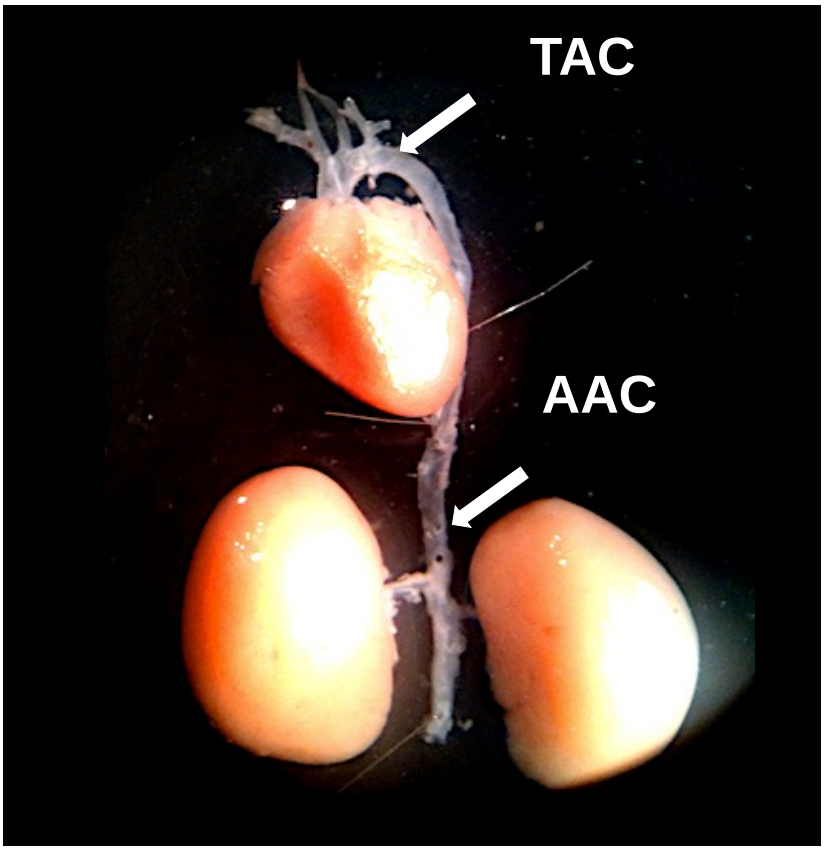

Figure 7. Point of constriction on the transverse and abdominal aorta for experimental cardiac pressure-overload.

Experimental Timeline

Following surgical induction of HF, mice were left to progress to either 2, 4, 9 or 18 weeks of TAC. Prior to sacrifice, mice underwent hemodynamic and *in vivo* respiratory function analysis. Following sacrifice, heart, lung, gastrocnemius, soleus and diaphragm were harvested for histological analysis. A portion of diaphragm was also dissected for *in vitro* function analysis. A summary of experiments at each time point can be found in table 2.

	2 wk TAC	**4 wk TAC**	**9 wk TAC**	**18 wk TAC**	**18 wk AAC**	**2 wk TAC + Pro**	**4 wk TAC + Pro**
Histology							
Heart				✓			
Diaphragm	✓	✓	✓	✓	✓		✓
Lung		✓	✓	✓	✓		
Limb Muscle		✓					
Hemodynamics				✓	✓	✓	✓
In Vivo Function	✓	✓	✓	✓			
In Vitro Function	✓	✓	✓	✓			

Table 2. Summary of analyses performed at each experimental time point.

Ventricular Hemodynamic Function

Hemodynamic analysis was performed under previously described anesthesia procedures. Ventricular function was determined by advancing a 1.2F catheter (Transonic, Canada) through the right common carotid artery or jugular vein and into the left ventricle. Physiologic LV and aortic pressure measurements were recorded and digitized at 2KHz using Labscribe2 analytic software (iWorx, USA). Left ventricular end diastolic pressure (LVEDP), and maximum and minimum first derivative of LV pressure (dP/dtmax; dP/dtmin), systolic blood pressure (SBP) and diastolic blood pressure (DBP) were recorded. Mean arterial blood pressure (MAP) was calculated as:

$$\mathbf{SBP(1/3) + DBP(2/3)}$$

Following hemodynamic function, animals were euthanized and tissues were used for histology, *in vitro* function or morphometric analysis.

Tissue Weights

Following euthanasia, hearts and lungs were quickly excised, rinsed in saline and placed in trays. Lungs were weighted and then left to dry at room temperature for 7 days. Once dry, lungs were weighted and recorded again. Hearts were also rinsed in saline and weighted. Then the right and left ventricle were dissected and weighted individually. Heart samples were then frozen at -80^{o}C for use in another study.

Respiratory Measurements

Animal Preparation

Induction of anesthesia was achieved in mice with a minimum alveolar concentration of 5% isoflurane in 100% oxygen and were maintained in the surgical plane of anesthesia (lack of reflex or response to toe pinch) with a minimum alveolar concentration of 2% isoflurane

(CDMV, Canada) in 100% oxygen. Body temperature was monitored and maintained at 37ºC. To ensure an unobstructed airway all mice were orotracheal intubated using a 20 gauge angio-catheter (Dickinson and Company, USA) retrofitted with compressible tubing to facilitate inducible airway occlusions.

In vivo Diaphragm Function

To assess indices of respiratory function and diaphragmatic strength we measured esophageal pressure in anaesthetized mice during two protocols: 1) eupneic breathing and 2) during 25 second airway occlusion.

In both protocols, mice were anesthetized with a minimum alveolar concentration of 5% isoflurane in 100% oxygen and were maintained in the surgical plane of anesthesia (lack of reflex or response to toe pinch) with a minimum alveolar concentration of 2% isoflurane (CDMV, Canada) in 100% oxygen. Mice were then orotracheal intubated using a 20 gauge angio-catheter (Dickinson and Company, USA) to maintain an open airway and to facilitate tracheal occlusions.

1. *Eupneic breathing*

In sham and all time points of TAC, raw measurements were recorded of respiratory pressure and timing during stable eupneic breathing; inspiratory, expiratory and total breath time (T_I, T_E, T_{TOT}) and inspiratory pressure (PI). From these raw measurements indices of respiratory drive (PI/T_I), duty cycle (T_I/T_{TOT}) and respiratory frequency ($60s/T_{TOT}$) were calculated.

Baseline data was considered appropriate if; (1) physiologic body temperature of 37ºC remained stable, (2) recordings were free from equipment malfunction, (3) pressure readings indicated that probe placement was stable. Figure 8 displays inclusion criteria for adequate baseline data recordings for eupenic breathing.

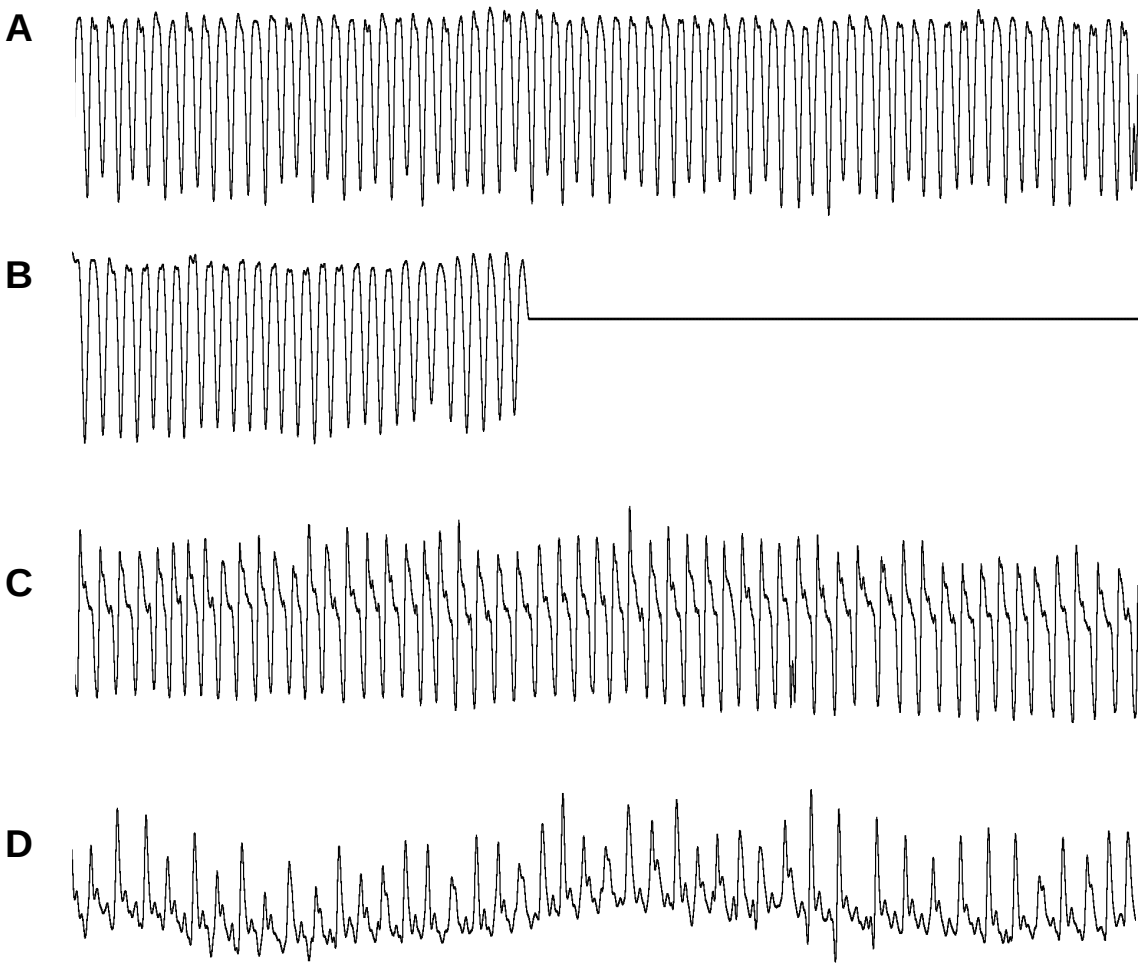

Figure 8. Representative respiratory tracings illustrating exclusion measures
(**A)** Representation of useable esophageal pressure tracing. **(B)** Pressure tracing including probe failure **(C)** Pressure tracing with probe slipping between abdominal and thoracic cavities. **(D)** Tracing of abdominal pressure.

Baseline data were analyzed by random sampling of data points. Inspiratory time was represented by the time of the beginning of an inflection, to the time of the peak inflection. Expiratory time was the time from the peak of an inflection, to the time of the beginning of the next. Total breath time was measured as the sum of both components (Figure 9). Inspiratory pressure was the difference between the base and peak of a given inflection (Figure 9).

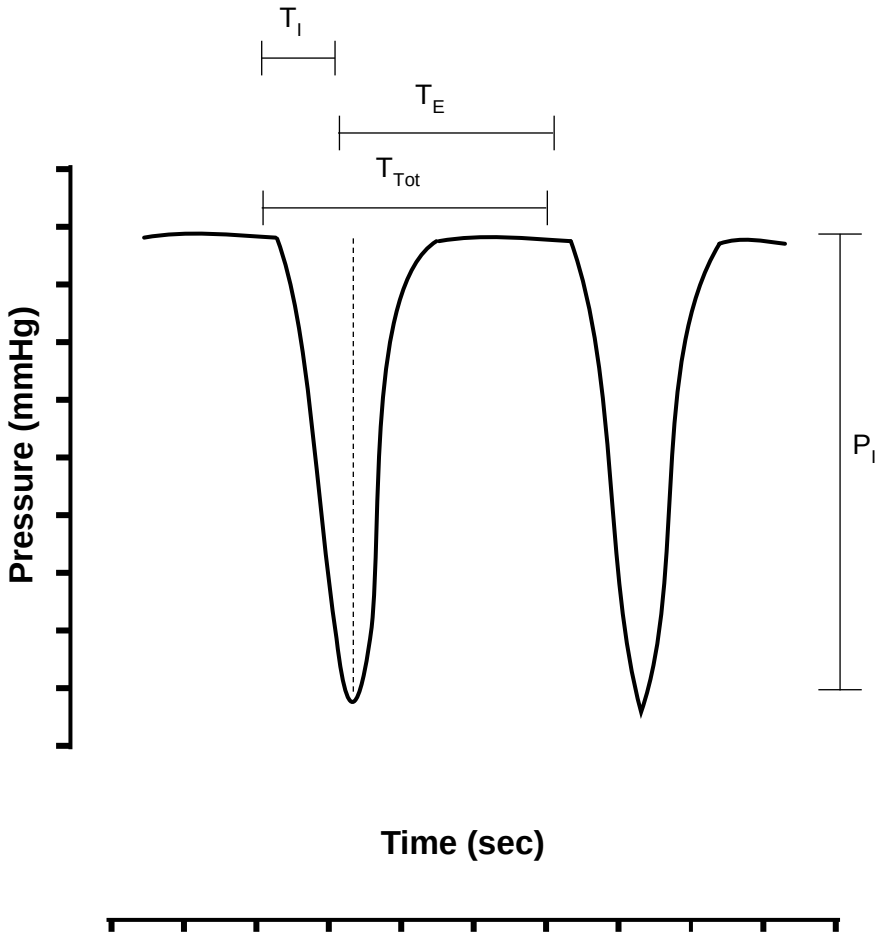

Figure 9. Representative respiratory tracing illustrating breath time and force measures, inspiratory time (T_I), expiratory time (T_E), total breath cycle (T_{TOT}) and inspiratory pressure (PI)

Total breath time was measured as the sum of both components (Figure 9). Inspiratory pressure was the difference between the base and peak of a given inflection (Figure 9).

2. *Tracheal occlusions*: Muscle strength is a key factor of muscle function. The ability of the diaphragm to generate pressure is therefore of importance. Clinically, diaphragm strength is determined by measuring esophageal pressure during a maximal voluntary inspiratory effort (Caruso et al., 2015). Since volitional tests are not feasible, inspiratory esophageal pressure (PI) during 25 second tracheal occlusions were measured instead.

Once intubated, two minutes of eupenic breathing were recorded to establish baseline data. Following baseline measurement, the trachea was occluded at end expiratory volume, to ensure consistency of the diaphragm length-tension relationship. Maximum inspiratory pressure (PI_{OCC}) was determined as the point at which pressure generation plateaued.

To account for any time of day variation in ventilatory drive, all PI measurements were conducted between 9am and 11am.

In Vitro Diaphragm Function

Immediately following euthanasia, intact whole diaphragms were quickly excised from the animal and placed in Krebs-Henseleit solution (Table 2) at room temperature and pH 7.4.

Compound	mM/L
NaCl	118
KCl	4.7
KH_2PO_4	1.2
$MgSO_4 \cdot 7H_2O$	1.2
$NaHCO_3$	27.26
Glucose	11.1
CaCl2·2H2O	2.3
Insulin	10 units/L
Curare	$3.0x10^{-4}$ g/L

Table 3. Recipe for 1 liter of Krebs-Henseleit solution

A section of muscle was removed from the costal portion of the right hemi-diaphragm with rib and central tendon intact. Silk ties were secured to both the central tendon and ribs and attached to a force transducer (Grass instruments, USA) and stationary hook, respectively. Stainless steel stimulating electrodes connected to a Grass electrical stimulator were placed on either side of the muscle section and used to elicit contractions via field stimulation. Tissue baths were placed such that each muscle was immersed in Krebs-Henseleit bicarbonate buffer (Table 2) continuously warmed to 27°C and aerated with 95% O_2:5%CO_2. This maintains the viability of the muscle sample by providing electrolytes, substrates and gas aeration thereby maintaining physiologic pH. Next, optimal muscle length was established by recording force output to electric stimulation during increasing muscle lengths. Optimal muscle length was defined as the length of muscle that produced the greatest amount of force. Following setting optimal muscle length and a 45-minute thermo equilibration period, peak force was determined during a force-frequency test (1 contraction every 30s with 250ms train duration at increasing stimulation frequencies: 1,5,10,20,30,40->120hz). A schematic of the described protocol can

be found in Figure 10. Isometric contractility data was collected using AcqKnowledge software (BIOPAC systems, Goleta, CA, USA) and analyzed using Spike2 software. Force production and contractility were normalized to muscle weight (mg) to account for differences in diaphragm tissue size.

Figure 10. Graphical representation of *in vitro* muscle function protocol.

Propranolol Treatment

In a subset of TAC mice, the β-blocker propranolol (Sigma-Aldrich, Canada) was administered by intraperitoneal injection twice daily (at 8am and 6pm) at a dose of 15mg/kg. Treatment began immediately following surgery and continued for 4 weeks. *In vivo* diaphragmatic function and occlusions performed as described above, followed by hemodynamic measurements. Animals were then sacrificed and tissues harvested for histological analysis to determine fibrosis and cross sectional area.

Histological Analysis

For animals designated to be histologically examined, an intraperitoneal injection of 500IU Heparin (Sigma-Aldrich, Canada) /kg body weight was administered after animals were anaesthetized as described above. The right common carotid artery was exposed and cannulated, the abdominal aorta was exposed and severed. The body was flushed first with 10 mL of phosphate buffered saline, (recipe in Table 4, Bioshope, Canada) at low pressure. In order to preserve muscle morphology, several steps were taken. First, after sacrifice, each animal was perfused with 50 mM potassium chloride. This concentration was chosen based on preliminary data from an experiment on various concentration of potassium chloride in solution.

Briefly, a subset of animals was sacrificed and divided into 5 groups each receiving pre-fixative solution with different potassium concentrations: potassium free phosphate buffered saline, 10 mM kcl, 25 mM kcl, 50 mM kcl and 75 mM kcl. Since fixative is known to cause contraction of skeletal muscle, it was hypothesized that muscle cell cross sectional area would be highest in the potassium free group, and would incrementally decline with increasing amounts of potassium, and plateau. Indeed, average cross sectional areas decreased as potassium chloride concentration increased, except in the 50 mM and 75 mM groups, which were not different (Data not shown). Therefore 50 mM was chosen as the optimal concentration of potassium for pre-fixative solution.

Following perfusion with 10 mL of 50 mM potassium chloride in phosphate buffered saline, animals were perfused with 10mL of formalin (VWR, Canada) *in situ*, at low pressure. The reason for *in situ* fixation is twofold. First, cross linking skeletal muscle proteins while attached to the skeleton combats fixative induced contraction, preserving the shape of the muscle. Second, it ensures proper penetration of fixative by exploiting the integral nature of

the vasculature. Because formalin is a relatively large molecule, it does not diffuse easily or deeply into tissues, therefore perfusion through the vasculature ensures optimal penetration. As a secondary measure, tissues were post fixed with skeletal muscle samples still attached to bones, for a further 48 hours. To post fix, a tissue to formalin ratio of 1:20 was used to further ensure adequate fixative penetration. To avoid over fixing samples, which is known to cause tissue artifacts such as brown granules, tissues were carefully dissected and transferred to 70% ethanol until processing.

Compound	**Amount** for 1L
NaCl	8g
KCl	0.2g
KH_2HPO_4	1.44g
KH_2PO_4	0.24g
Deionized H_2O	~1L

Table 4. Recipe for 1 liter of 1x phosphate buffered saline

Compound	**Amount** for 1L
KCl	3.7275g
Deionized H_2O	~1L

Table 5. Recipe for 1 liter of 50mM potassium chloride

Tissue Preparation: Heart

Following 48 hours of post fix, hearts were cut into three equal transverse sections, and the middles, containing the mid papillary region, were packed into cassettes, labelled and placed in 70% ethanol until processing.

Tissue Preparation: Diaphragm

After perfusion fixation, the diaphragm was excised, attached to the ribcage in order to prevent deformation caused by the fixative and processing procedures. After 48 hours of post fix in formalin at 1:20 ratio, diaphragms were placed in cassettes, labelled and packed down with tissue to maintain structural integrity during dehydration.

Tissue Preparation: Lungs

Upon removal of lungs and intact trachea, a cannula was inserted and secured into the trachea. The lungs were then suspended and perfusion fixed at a pressure of 20cmH_2O overnight. Following pressurized perfusion fixation, the lungs and intact trachea were stored in formalin at a ratio of 1:20 tissue weight to formalin volume, for 48 hours and then transferred into labelled cassettes in 70% ethanol until tissue processing.

Tissue Preparation: Limb Muscle

Once perfused with formalin, the lower leg was skinned to expose hind limb musculature. The entire limb was post fixed for 48 hours. Following, the achilles tendon was clamped with a hemostat, while the gastrocnemius and soleus were carefully separated and removed. Tissues were then packed into cassettes, labelled and placed into 70% ethanol until processing.

Paraffin Block Preparation

Samples were dehydrated and paraffinized in a Thermo Scientific Excelsior tissue processor (Fisher Scientific, USA). Following processing, tissues were cut to expose cross sectional surfaces and mounted on cassette backing in paraffin (VWR, Canada). Once blocks were oriented on the microtome, (Thermo Shandon, Fisher Scientific, Canada) they were trimmed ~100μm before sectioning, to ensure maximum tissue exposure. Cross sectional slices (5μm) were obtained from the mid papillary region of the heart, belly of the medial costal diaphragm, middle of each lobe of the right lung, or belly of the gastrocnemius or soleus. The right side of the diaphragm and lungs were always used to ensure that cardiac injury and remodeling did not directly impact morphology. Sections were mounted on charged Superfrost slides (Fisher Scientific, Canada) with each slide containing 2-3 serial sections. Slides were set overnight at 37^{o}C and stored at room temperature until staining.

Tissue Staining

All staining protocols began with removal of paraffin in two changes of xylene for 5 minutes each. Next, slides were rehydrated in alcohol, 2 changes of absolute ethanol at 5 minutes each, then one change in 95% for two minutes, finishing with 1 change in 70% for two minutes. Slides were then washed in deionized water.

Hematoxylin and Eosin

Modified Harris Hematoxylin (VWR, Canada) and Eosin (Table 5, Sigma-Aldrich, Canada) were used to examine general muscle morphology of the diaphragm. Once removed from deionized water, slides were stained for 8 minutes in Modified Harris Hematoxylin. Once rinsed in running water for 10 minutes, staining was differentiated in 1% acid alcohol for 30

seconds and then rinsed again for one minute. Ammonia water was then used to 'blue' the samples. The slides were dipped repeatedly until tissues appeared blue; 30-60 seconds. After 5 minutes of rinsing in tap water and dipping 10 times in 95% alcohol, slides were counterstained in Eosin working solution for 1 minute. Then tissues were dehydrated, in 70%, 95% and absolute alcohol, for the same intervals described above, cleared in 2 changes of xylene, mounted with xylene based medium (VWR, Canada) and covered with glass. In bright field microscopy, this stain results in bright pink muscle fibers and dark purple nuclei allowing observation of gross muscle morphology.

	Compound	**Amount**
Eosin Stock	Eosin Y	1g
	Distilled H_2O	100mL
Phloxine Stock	Phloxine B	1g
	Distilled H_2O	100mL
Eosin Working Solution	Eosin Stock	100mL
	Phloxine Stock	10mL
	95% Ethanol	780mL
	Glacial Acetic Acid	4mL
1% Acid Alcohol Solution	Hydrochloric Acid	1mL
	70% Ethanol	50mL
Ammonia H_2O Solution	Ammonium Hydroxide	2mL
	Distilled H_2O	1L

Table 6. Recipes for Hematoxylin and Eosin staining protocol

Picrosirius Red

To evaluate muscle cross sectional area and fibrosis, Picrosirius Red (Table 6, Sigma Aldrich, Canada) was chosen. The direct red 80 within the stain binds to the extracellular matrix allowing for the borders of each cell to be clearly defined and measured. For this same reason, this stain is ideal for visualizing interstitial and perivascular fibrosis. The staining protocol was initiated as described above. Briefly, slides were deparaffinized and rehydrated to water, and stained in Modified Harris Hematoxylin for 8 minutes. After rinsing in running tap water for 10 minutes, slides were counterstained in Picrosirius Red for 1 hour. Next the slides were washed in 2 changes of 5% glacial acetic acid for 2 minutes each. After being shaken dry, slides were dehydrated, cleared and mounted as described above. This stain results in red collagen, pale yellow cytoplasm and brown nuclei. The most common staining artefact is the non-specific binding of direct red 80 to the cytoplasm, making fibrosis quantification difficult.

Compound	**Amount for 500mL**
Direct Red 80	**0.5g**
Aqueous Picric Acid	**500mL**

Table 7. Recipe for 500 mL of Picrosirius Red tissue stain.

Gomori's Trichrome

To isolate lung fibrosis, one step Gomori's One Step Trichrome (Sigma-Aldrich, Canada) was chosen, as it allowed for clear differentiation of nuclei, alveolar tissue and fibrosis. When stained with Picrosirius Red, lung tissue appears light brown with darker brown nuclei, making tissue differentiation and thus analysis of fibrosis impossible. The staining protocol is very similar to Picrosirius Red; slides were deparaffinized, rehydrated and stained with Modified Harris Hematoxylin as previously described. Following 10 minutes of rinsing, slides were placed in Gomori's one step trichrome for 15 minutes. Next, slides were rinsed, dehydrated and cleared, then mounted.

Once mounted and cover slipped, slides were left to dry overnight in a fume hood before being stored at room temperature until analysis.

Image Analysis

Images were acquired using an Olympus FSX 100 light microscope (Olympus, Japan).

Fibrosis

To analyze fibrosis, images (~10 per animal) were uploaded into Cell Sense software (Olympus, Tokyo, Japan). Samples were analyzed for percentage of fibrosis if they were free from (1) artefacts related to processing, (2) mechanical damage from sectioning, and (3) intercellular direct red 80 binding. For each animal, 5 images were used to calculate average fibrosis, expressed as a percentage of total tissue area.

Atrophy

Cross sectional area was blindly calculated using 10 random muscle sample images within Image J software. From each animal, approximately 5 images were used to calculate cross sectional area, and from each image approximately20 cells were analyzed resulting in about100 cells per animal being measured. Inclusion criteria for muscle cell measurement was as follows: (1) the area of the cell was approximately circular, indicating a cross-sectional view, (2) cell was free of artefacts such as cracking or splitting (3) cell displayed clear border, indicating that they were not disrupted by the sectioning process, and allowing for accurate circumference measurement. Atrophy (reduction of the cross-sectional area of the whole muscle) can be caused by either reduction of contractile proteins, namely myosin heavy chain (the most abundant contractile protein), or muscle cell death; the latter results in a smaller muscle cell while the former results in fewer total muscle cells.

To investigate the possibility of decreased myofibril population in TAC, muscle cell counts were performed. The same images used to calculate myocyte cross-sectional area were analyzed for total myocyte population. For each image, 3 lines were drawn directly across the width of the muscle from the thoracic to abdominal borders, in the sagittal plane, and any cell in contact with the line was counted (Figure 11).

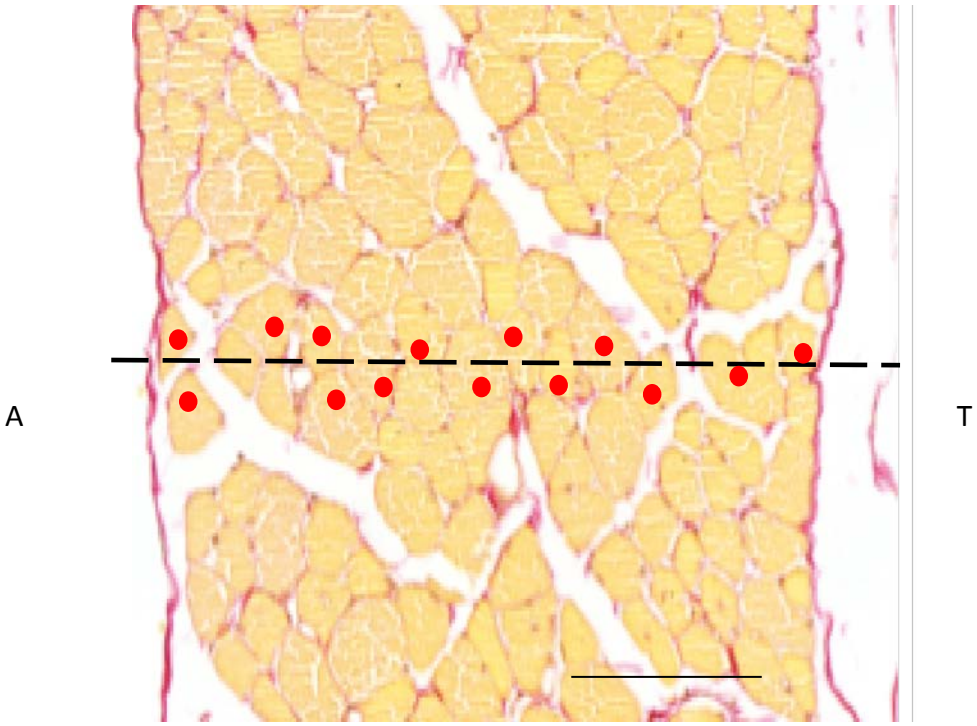

Figure 11. Representative image used to analyze myocyte population. Dashed line used as analysis guide.
A Denotes abdominal side of diaphragm. **B** Denotes Thoracic side.
Red circles mark cells included in the count. Scale bar: 100µm

Statistical Analysis

All statistical analyses were performed using Prism 6 (GraphPad Software Inc., USA) and significance was defined as $p < 0.05$.

Data that is expressed as a mean of multiple samples (heart rate, inspiratory time, blood pressure, dT/dt, etc.) is presented as mean ± standard error of the mean (SEM) to reflect variability within the data point. Absolute measures (weights, fibrosis and cell counts) are expressed as mean ± standard deviation (SD) to highlight the variability between animals. Two tailed student's T-tests were used for comparison between two groups in figure 13D and 14D. One tailed Student's T-tests and ANOVAs were selected *a priori* for comparison between two groups in figures 12C, 12D, 13B, 13C, 13E, 18A and 18B, based on the volume of literature confirming the deleterious effects of HF on muscle structure and function (Adams et al, 1999; Anker, Steinbor & Straaburg, 2004; Breitbart, Auger-Messier, Molkentin, & Heineke, 2011; Chen et al., 2012; Coirault et al, 2007; Farkas et al., 1994; Howell et al., 1995). When differences were found by ANOVA, a protected Least Square Difference (protected LSD) post-hoc test was performed.

To compare cross sectional areas (Figures 13, 15, 16, 17, 18 & 19), a Wilcoxin signed rank test was performed. Muscle cell cross section sizes vary based on fiber type and duration of TAC. Since the diaphragm is a mixed muscle and several groups have established selective atrophy to specific fiber types in HF (Coirault et al., 2007; Howell et al., 1995; Stassijins et al, 1998), cross sectional area data cannot be assumed as normally distributed. The Wilcoxin test corrects for skewed distribution allowing comparison between groups.

CHAPTER IV: RESULTS

Histomorphometric and Hemodynamic Analysis of Animals

TAC is designed to recapitulate pressure-overload HF and is characterized by cardiac hypertrophy, reduced contractility and drastic changes in cardiac blood pressure.

In order to confirm our model, both systolic and diastolic pressures were measured and mean arterial pressure (MAP) calculated (Table 7). TAC model exhibited a bi-phasic progression of function with early compensation, characterized by increased MAP, followed by a progressive decline in function indicated by reduced arterial pressure (Table 7) that eventually culminated in HF; cardiac hypertrophy (Figure 12 A & B), reduced contractility (Figure 12 C) and elevated left ventricular pressure (Figure 12 D).

One of the hallmark features of pressure-overload HF is cardiac hypertrophy. In order to confirm the development of hypertrophy, hearts were weighted and histologically imaged. Gross examination of hearts was done from sections taken at the mid papillary region. Sham and 18 week TAC hearts, stained with Picrosirius Red, revealed increased wall thickness and chamber size, characteristic of HF (Figure 12A). Further, quantitative comparison of heart weights reveals a significant increase in total heart weight compared to sham (Figure 12B). To adjust for any differences in growth between the animals, heart weights are divided by tibial length to normalize differences in size. Decreased contractility is characteristic of HF. As such, to further confirm the development of HF, dP/dt_{MAX} was used to directly assess contractility. Importantly, by 18 weeks of TAC, contractility was significantly decreased (Figure 12C), further confirming the presence of decompensated HF.

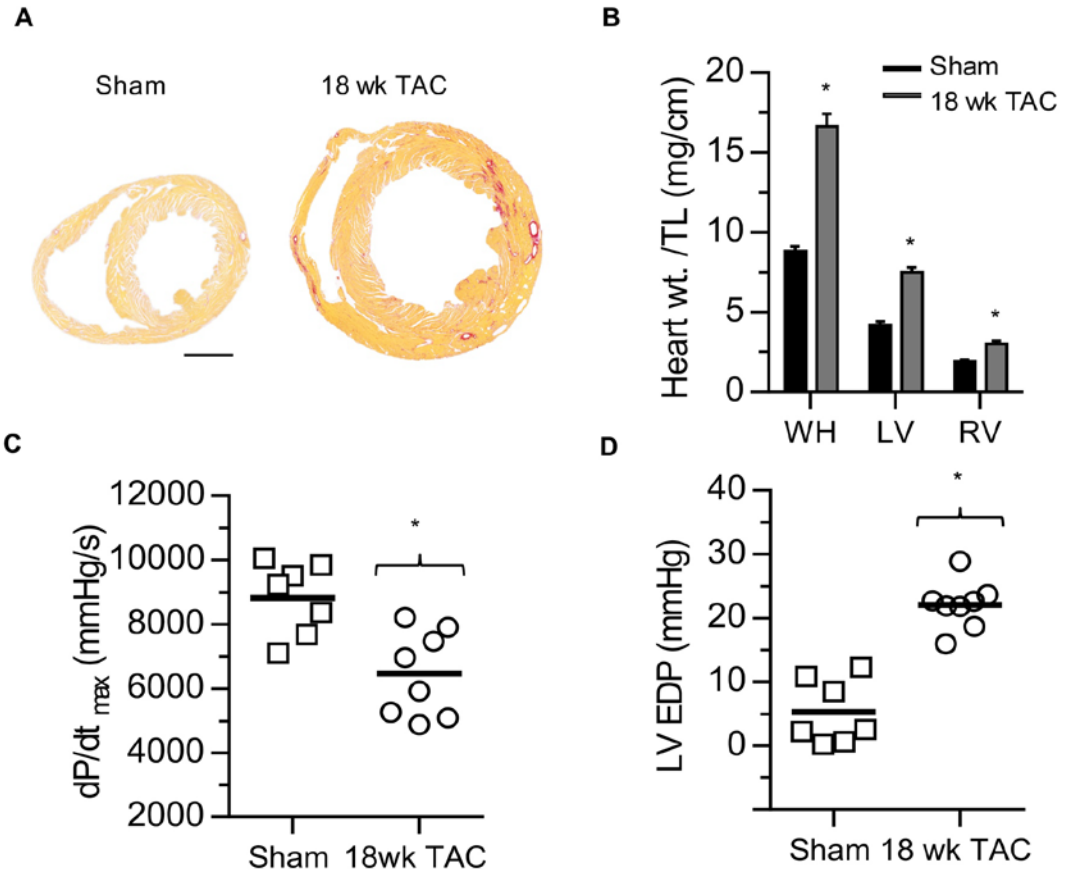

Figure 12. Histomorphometric and hemodynamic analysis of TAC induced heart failure. (A) Representative cross sectional images of sham and 18 wk TAC hearts at mid-papillary region stained with Picrosirius Red. (B) Normalized cardiac weights of whole heart, left and right ventricle of sham (n=8) and 18 wk TAC (n=8) mice. (C & D) Left ventricular pressure and the first derivative of pressure development in sham (n=8) and 18 wk TAC (n=8) mice. * Indicates significance vs. sham; $p<0.05$ as determined by student's T-test. Scale bars: (A) 2mm

	Sham *(n=8)*	2 wk TAC *(n=8)*	4 wk TAC *(n=8)*	9 wk TAC *(n=8)*	18 wk TAC *(n=8)*
Left Ventricle					
LVP (mmHg)	102 ± 5	142 ± 3*	176 ± 5*	145 ± 5*	128 ± 6*
EDP (mmHg)	5 ± 2	19 ± 1*	22 ± 4*	20 ± 2*	22 ± 1*
Hemodynamic					
MAP (mmHg)	81 ± 5.3	87 ± 3.1	98 ± 3.2*	87 ± 2.8	78 ± 4
-Systolic BP (mmHg)	100 ± 4.8	140 ± 1.6*	170 ± 4.6*	143 ± 4.5*	128 ± 5.8
-Diastolic BP (mmHg)	71 ± 5.6	60 ± 4.1	61 ± 4.2	59 ± 2.7*	53 ± 3.6*
Heart rate (beats/min)	576 ± 12	613 ± 13	607 ± 15	583 ± 15	597 ± 25
Morphometric					
Body Weight (g)	39.1 ± 0.9	38.9 ± 0.7	40.5 ± 0.3	48.4 ± 2.6*	41.4 ± 2.2
Heart Weight (mg)	16.4 ± 0.5	19.7 ± 0.4*	24.0 ± 1.3*	28.2 ±1.3*	32.1 ± 1.6*
Respiratory					
P_{Imax} (cmH_2O)	86 ± 5.7	88.4 ± 3.2	57.9 ± 3.1*	61.9 ± 1.2*	43.2 ± 3.9*
T_I (s)	0.14 ± 0.003	0.13 ± 0.005	0.13 ± 0.005	0.15 ± 0.007	0.14 ± 0.01
T_E (s)	0.72 ± 0.06	0.72 ± 0.07	0.61 ± 0.06*	0.85 ± 0.1	0.86 ± 0.1
T_{TOT} (s)	0.86 ± 0.06	0.85 ± 0.07	0.75 ± 0.07	1.0 ± 0.1	1.0 ± 0.1

Table 8. Hemodynamics, morphometric and metabolic parameters during 18 weeks TAC. Tissue weights, Mean ± SD, all others are Mean ± SEM. * Indicates significance vs. sham; $p<0.05$, as determined by protected LSD.

Diaphragmatic Remodeling Evident by 18 weeks of TAC

After confirming the presence of cardiac dysfunction, the effect of TAC on diaphragm atrophy and fibrosis was investigated. Diaphragms were sectioned and stained with Picrosirius Red in order to visualize cell borders and collagen content. Quantification of histological sections displayed levels of interstitial fibrosis ~ 3 fold of sham (Figure 13A & B). Additionally, TAC animals exhibited significant diaphragmatic atrophy (Figure 8C), a finding which is in agreement with several groups (Coirault et al., 1997; Howell et al., 2009; Lindasy et al, 1996; Picard et al., 2012). As diaphragmatic atrophy has been attributed to increased work of breathing caused by pulmonary edema, lung weights in sham and 18 week TAC were investigated. Lung wet to dry weight is a relative way to measure pulmonary edema as it inherently normalizes for variance in lung size. Specifically, should pulmonary edema be present, we would expect to see an increase in wet to dry weight ratios, indicating increased fluid content in the lungs. However, there was no change in lung wet to dry ratio. Interestingly, absolute lung weights (wet and dry) were clearly increased in TAC (Figure 13 D&E).

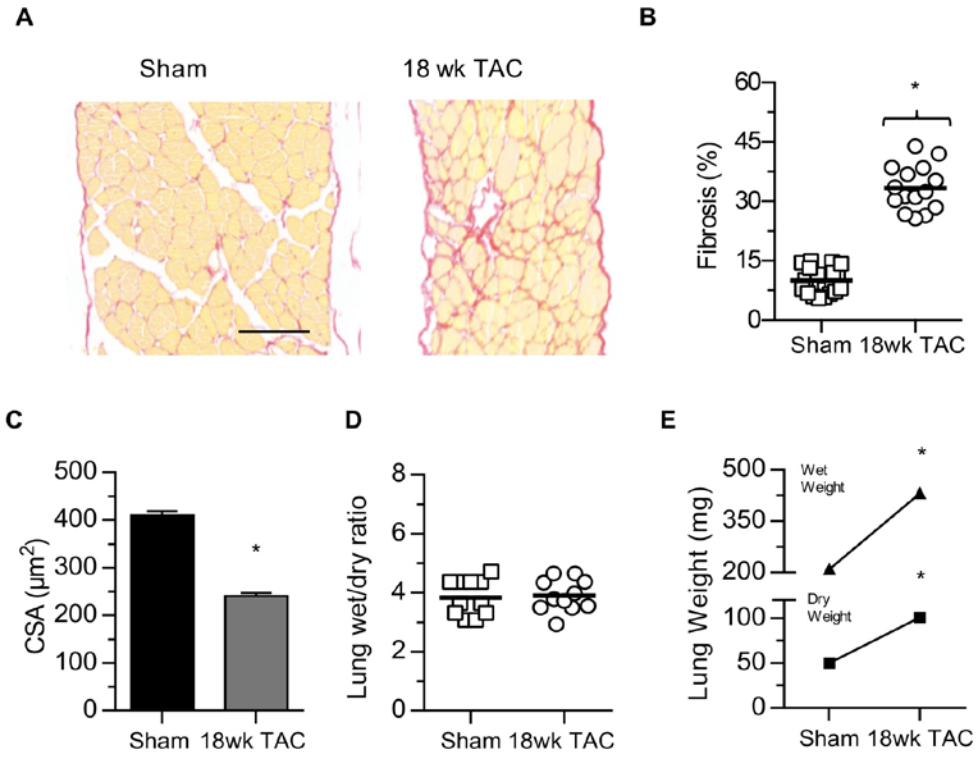

Figure 13. Diaphragmatic Remodeling Evident by 18 weeks of TAC in the absence of pulmonary edema. **(A)** Representative images of sham and 18 wk TAC diaphragms stained with picrosirius red. **(B)** Percent fibrosis of sham (n=5) and 18 wk TAC (n=5) diaphragms. **(C)** Mean cross sectional area of sham (n=5) and 18 wk TAC (n=5) diaphragms. **(D)** Wet to dry weight ratio of lungs from sham (n=8) and 18 wk TAC (n=8) mice. **(E)** Wet and dry weight of sham (n=8) and 18 wk TAC (n=8) lungs. **(B, D, E)** Mean ± SD, **(C)** Mean ± SEM * Indicates significance vs. sham; $p<0.05$ as determined by student's T-test. Scale bars: **(A)** 100μm

Progressive Development of Diaphragmatic Weakness

The presence of respiratory muscle weakness is well noted in clinical HF (Buller et al., 1991; Chua et al., 1995; Dall'Ago et al., 2006; Josiak et al., 2014; Mancini et al., 1992; Ponikowski et al., 2001; Ribero et al., 2009). Several groups have further characterized this phenomenon in experimental models of HF. First, Supinski at al. (1994) showed impaired *in vitro* function in dogs after 6 weeks of ventricular pacing as did Coirault et al. (1997). Howell et al. (1995) then showed that limb muscle and diaphragm muscle adapt differently to HF, namely the latter presents with atrophy of type 1 muscle fibers, while the former with type II atrophy, exposing the difference between respiratory and limb muscles, a finding confirmed a year later by Stassijins et al. (1996) who went on to theorize that diaphragm weakness was caused by decreased cross sectional area. Lecarpentier's group (1999) also found weakness and *in vitro* dysfunction that was associated with decreased cross bridge formation and impaired calcium handling. Finally, Chen et al. (2012) noted profound lung remodeling in rats exposed to TAC, suggesting a critical role for the lungs in increased work of breathing in HF. Yet, over the last nearly 3 decades of thoroughly characterizing diaphragmatic adaptations to HF, the incipient cause remains elusive.

In agreement with the literature, muscle wasting (Figure A & C), fibrosis (Figure 13 B) and changes in absolute lung weight (Figure 13 E) occur by 18 weeks of TAC. Yet the simple presence of these adaptations late in the development of HF provides no indication of their cause. Therefore, we explored the time course development of changes in the morphology and function of the diaphragm in our model.

Mancini et al. (1992) first described an increased diaphragmatic load as increased TTI in HF caused by increased PI and decreased PI_{OCC} with no change in duty cycle. Therefore, the components of TTI in this model for congruence with clinical HF were investigated. To assess

diaphragm strength in response to TAC, *in vivo* trans diaphragmatic pressure during eupenic breathing (PI) and occlusion (PI_{OCC}) were measured. These methods were chosen as an analogue to clinical methods of PI and PI_{OCC} evaluation as they require volitional inspiratory maneuvers (Caruso, 2015).

Gross observation of sham breathing and occlusion (Figure 14A, top) reveals increased pressure generation during occlusion. Comparison of each time point (Figure 14A, bottom) indicates reduced pressure generation during occlusion by 4 weeks of TAC, deteriorating through to 18 weeks. To examine inspiratory pressure development over the duration of occlusion, pressure measurements at 5 second intervals were taken. Pressure development in sham and 2 week TAC animals were not statistically different at any time interval including max. However, by 4 weeks TAC, pressure development was attenuated past 10 seconds of occlusion, and maximum pressure was decreased. In both the 9 and 18 week TAC animals, pressure generated at each interval was significantly lower than sham (Figure 14B). Maximal pressure generated during eupneic breathing gives insight into work of breathing at rest, with more pressure indicating more muscle activity or a greater metabolic demand on the muscle. At all time points, inspiratory pressure was increased from sham (Figure 14C). Notably, while all time points were elevated above sham, 9 week TAC animals generated pressures statistically higher than all other time points, indicating increased effort during inspiration. Clinical respiratory muscle dysfunction in HF is characterized by increased tension time index with no changes in duty cycle. Therefore, measuring duty cycle allowed comparison between this model and the clinical manifestation of HF. No differences in inspiratory time or total breath cycle time were observed at any point between TAC and sham (Figure 14D & Table 7),

These findings are consistent with clinical observations in HF, as elevated tension time index is commonly observed and also attributed to changes in inspiratory pressure and maximal inspiratory pressure, but not duty cycle. Finally, both the finding of *in vivo* muscle weakness

and the fact that other groups have described *in vitro* dysfunction in HF, (Coirault et al., 2007; Howell et al., 1995; Lecaperteier et al., 1999; Supinski et al., 1994) prompted the examination of *in vitro* force production as the cause for weakness. Interestingly, TAC did not diminish *in vitro* function at any time point (Figure 14E). Unexpectedly, enhanced muscle fiber force production was found in 2 week TAC animals an occurrence that, to our knowledge, was first observed in this study. However, *in vitro* force at all other time points are unchanged from sham. Temporally, respiratory alterations in HF begin with increased resting PI, followed by decreased maximal force *in vivo*, without impaired *in vitro* muscle fiber function or changes in duty cycle. Therefore, the cause of diaphragm weakness in our model is not due to *in vitro* dysfunction.

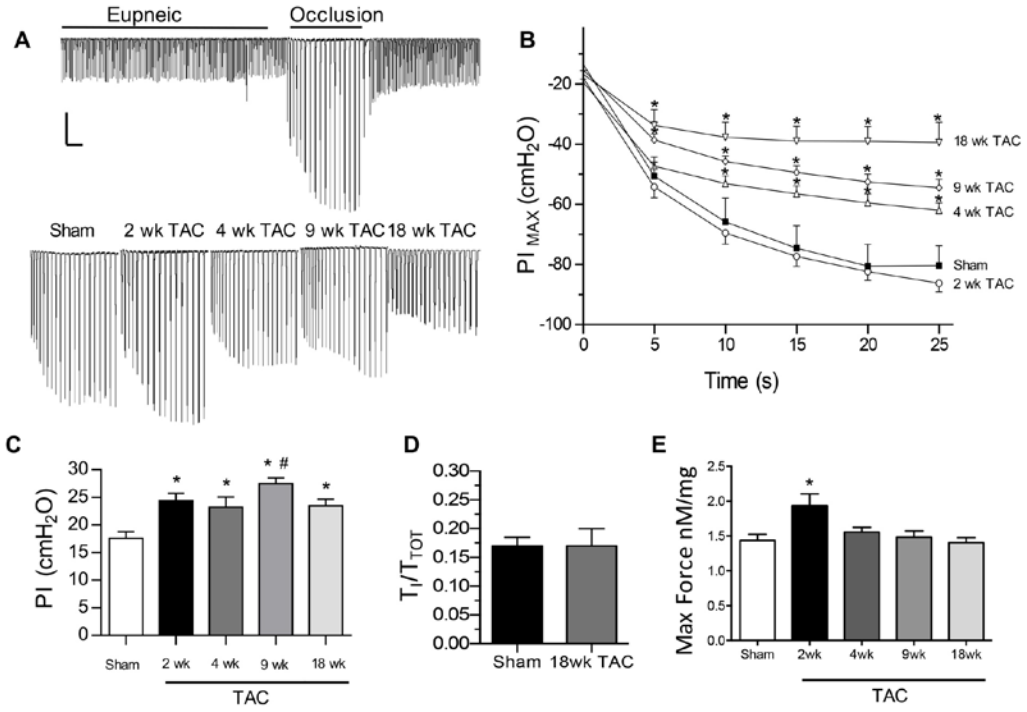

Figure 14. Diaphragmatic weakness progressively develops throughout the duration of 18 weeks TAC and is characterized by decreased PI_{OCC}, increased P_I with no change in duty cycle. (**A**) Representative tracings of inspiratory pressure at baseline during anaesthetized eupneic breathing (P_I) and maximum inspiratory pressure (PI_{OCC}) during a 25s airway occlusion followed by representative tracings of inspiratory pressure development during airway occlusion in TAC and sham mice. (**B**) Inspiratory pressure development in sham (n=10) and TAC (n= > 6) mice during the 25s airway occlusion. **(C)** *In vivo* inspiratory pressure of sham (n=10) and TAC (n=>6) mice during eupnic breathing. **(D)** Duty cycle of Sham (n=8) and 18 wk TAC (n=5) **(E)** *In vitro* force production of diaphragm from sham (n=12) and TAC (n=>6) mice during stimulation protocol. Mean ± SEM, * Indicates significance vs. sham; $p<0.05$ as determined by protected LSD. Scale bars: **(A)** 10 cm_{H2O}

Progressive Diaphragmatic Atrophy Begins Early in the Development of HF

Diaphragmatic atrophy is a well-accepted consequence of clinical (Hughes et al., 1999; Lindasy et al., 1996) and experimental HF (Coirault et al., 1997; Howell et al., 1995; Lecarpentier et al., 1999; Magner et al, 2015; Stassijins et al., 1998; Supinski et al., 1994), yet its onset relative to the pathogenesis of the disease is yet to be established. Since skeletal muscle cross sectional area is positively correlated with force generation capabilities (Minotti et al, 1992), hematoxylin and eosin stained diaphragm strips were used to visualize gross changes in muscle morphology (Figure 15A). Myocyte cross sectional area was measured to quantify the observed changes. Picrosirius Red stained diaphragms were used to measure fiber area since it differentially stains the cytoplasm of cells yellow and their borders red. The histograms in Figure 15B distinctly indicate a progressive leftward shift in muscle fiber area beginning at 4 weeks of TAC. Clearly, diaphragmatic atrophy begins early on in the development of pressure-overload HF. While gross examination of muscle samples did not reveal evidence of muscle fiber necrosis, we still sought to confirm that atrophy was not caused by cell death. To do this, the number of cells spanning the thickness of the diaphragm were counted (Figure 15C). This established that at no time point had the cell population decreased, confirming our theory that atrophy was not caused by apoptosis or necrosis.

Finally, to explore the relationship between atrophy and weakness, a stepwise linear regression analysis (Figure 15D) was performed which revealed an exceedingly strong negative correlation, implicating atrophy as the primary cause of reduced diaphragmatic strength. Therefore, the precipitating mechanism initiating the development of respiratory myopathy in HF has been uncovered. According to the analysis of the results, 97.8% of the variability in strength can be attributed to muscle atrophy.

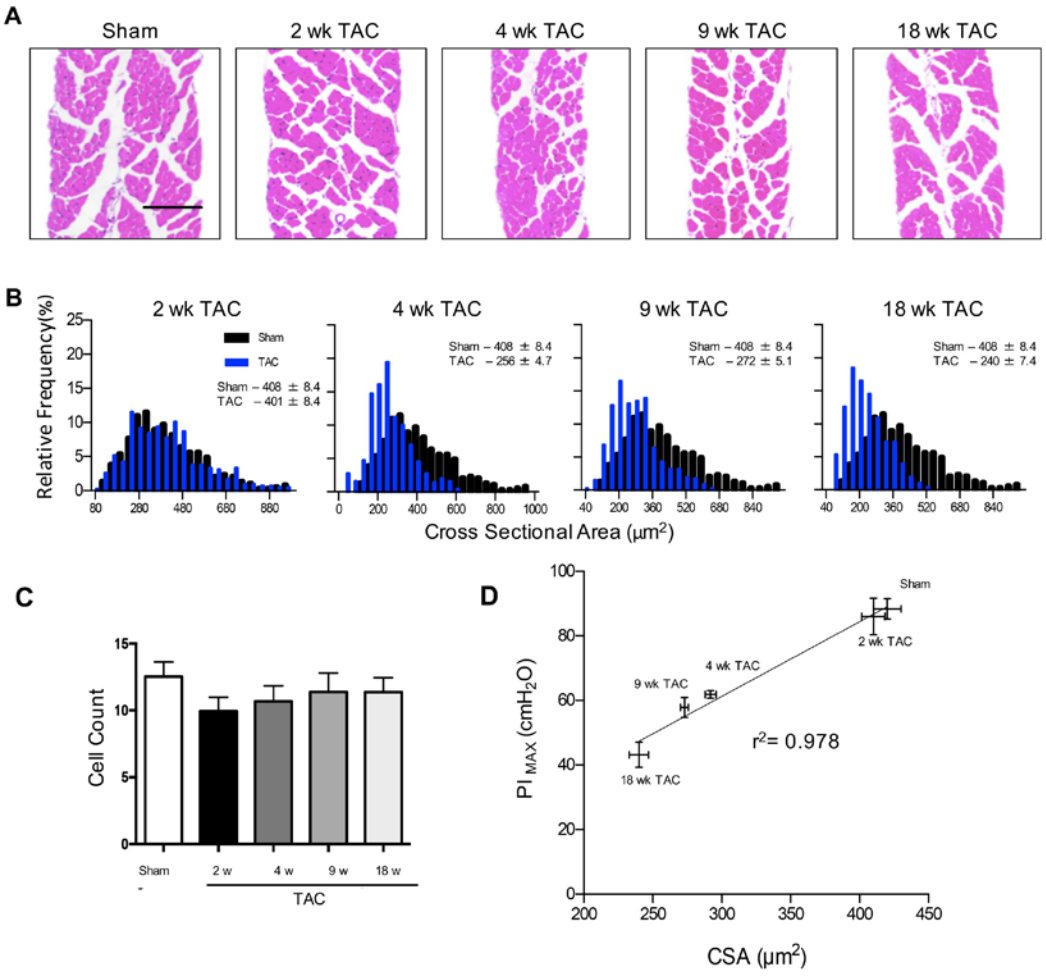

Figure 15. Diaphragmatic atrophy progressively develops throughout the duration of 18 weeks TAC and is strongly correlated with muscle weakness **(A)** Representative images of sham and TAC diaphragms stained with hematoxylin and eosin **(B)** Diaphragm muscle fiber cross sectional area histogram of sham (n=5) vs. TAC (n=5) mice. **(C)** Cell count of myofibrils spanning the sagittal plane of the diaphragm. (**D)** Linear regression plot highlights strong positive correlation between muscle cross sectional area and inspiratory strength. Scale bar **(A)** represents 40μm

Lung Remodeling in Late Stage TAC

Pulmonary edema was not found in our model at end stage HF (Figure 13D) however, it is possible that changes in lung fluids or tissue earlier in the development of HF could be causing the increased work of breathing.

Chen et al. (2012) were the first to observe significant lung remodeling in TAC. As such, changes in lung tissue throughout the pathogenesis of HF were investigated as part of this study. Whole tissue lung weights were taken immediately following sacrifice, and then allowed to dehydrate and weighted again. Fibrosis and tissue morphology were investigated histologically. Comparison of lung weights show significant and progressive increases in both wet and dry weight 9 and 18 weeks of TAC (Figure 16A), indicating pulmonary remodeling by 9 weeks. Importantly, lung wet to dry weight ratios remained stable, ruling out pulmonary edema at any stage. Quantification of histological sections revealed increased fibrosis (Figure 16B). Gross inspection of histological sections stained with Gomori's Trichrome display large deposits of fibrosis (blue staining) and alveolar distension in 9 and 18 week animals (Figure 16C). Moreover, the increased nuclei content is indicative of an inflammatory response (Jacobson et al., 2005). Certainly, quantification of histological sections confirms increased alveolar size (Figure 16 D) in 9 and 18 week TAC animals. Clearly, significant changes in lung tissue weights and morphology occur by 9 weeks of TAC, worsening by 18 weeks. Since evidence of pulmonary remodeling becomes apparent after the onset of diaphragm weakness, it is unlikely that it is a factor in the onset of diaphragm myopathy.

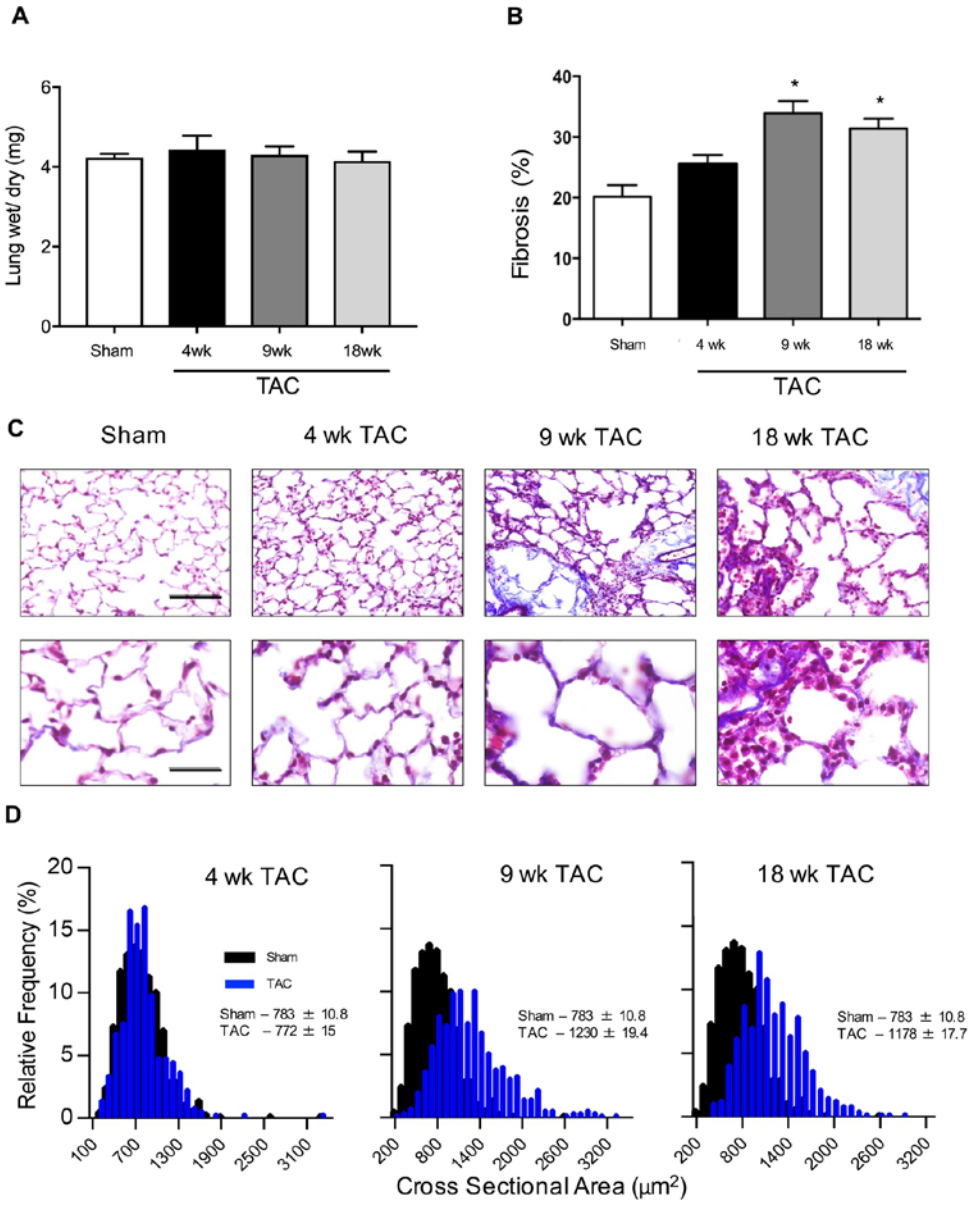

Figure 16. TAC induces progressive and profound lung remodeling in late stage HF. (A) Lung wet and dry weights of sham and TAC mice. (B) Interstitial/alveolar pulmonary fibrosis (n=5). (C) Representative images of lung tissue stained with Gomori's trichrome. in sham (n=5) and TAC (n=5) mice. (D) Histogram of alveolar cross sectional area. Mean ± SEM, * Indicates significance vs. sham; $p<0.05$ as determined by protected LSD. Scale bars: (B) Top panel 30 μm Bottom panel 15 μm

No Locomotor Muscle Atrophy at 4 Weeks of TAC

Many researchers have proposed that the increased ventilatory drive observed in HF is resultant from metabolic factors caused by alterations in limb muscle (Mancini et al., 1992; Pipoli et al.,1996). Certainly, limb muscle atrophy is a widely accepted outcome of HF (Josiak et al, 2014; Stassijins, Lysens & Decramer, 1996), specifically of slow twitch fibers, which results in increased ergo-receptor activation, causing dyspnea. However, this theory is based on the assumption that skeletal muscle atrophy of limb and respiratory muscles occurs concomitantly. To address this, histological sections of limb muscles of sham and 4 week TAC animals (Figure 16 A & C) were examined, as this is when diaphragmatic atrophy first becomes apparent. Moreover, both a predominantly fast twitch muscle (the glycolytic portion of the gastrocnemius was isolated), and a predominately slow twitch muscle (soleus) were examined since there is evidence to suggest that limb muscle atrophy is fiber type specific (Ciciliot et al., 2013; Stassijins, Lysens & Decramer, 1996). Quantification of muscle cross sectional area revealed no change in cross sectional area between sham and 4 week TAC animals (Figure 16 B & D) in either fast twitch or slow twitch muscle. Hence, diaphragmatic atrophy occurs before the development of limb muscle wasting. Moreover, since peripheral muscles are unchanged by 4 weeks of TAC, it is not likely that an augmented ergo-reflex is the cause of increased ventilatory drive early on in HF.

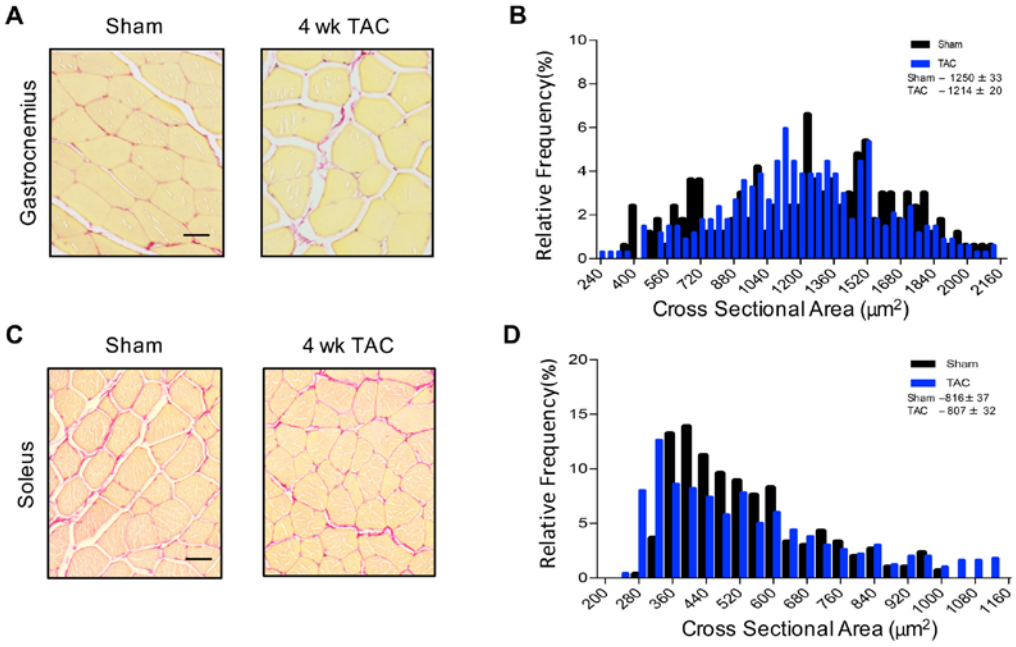

Figure 17. Analysis of skeletal muscle demonstrates no atrophy 4 weeks following TAC **(A)** Histological cross sections of gastrocnemius tissue stained with PSR and the corresponding **(B)** CSA histograms (*n=4* for each group). Scale bars: **(A&C)** 30μm

Effect of Aortic and Abdominal Banding on the Development of Diaphragm Myopathy

Rockman et al. (1991) demonstrated that the hypertensive stress caused by banding is greatest proximal to the band, suggesting that while TAC places a hypertensive stress on the heart, the rest of the vasculature does not experience elevated pressures. In fact, it is likely that blood flow to the diaphragm in TAC animals was significantly reduced. Therefore, we sought to investigate whether the atrophy found in the diaphragms of TAC animals was a consequence of HF, or hypotension driven. Consequently, in a subset of animals, the abdominal aorta (AAC) was banded to induce HF. Representative histological sections of sham and AAC diaphragms indicate significant atrophy and fibrosis (Figure 17A). Indeed, when quantified, fibrosis was significantly elevated in AAC mice (Figure 17B). Further, 18 weeks of AAC also induced diaphragmatic atrophy (Figure 17C). TAC and ACC both resulted in comparable diaphragmatic atrophy and fibrosis, indicating that the atrophy and fibrosis observed in the TAC model is not caused by reduced blood flow.

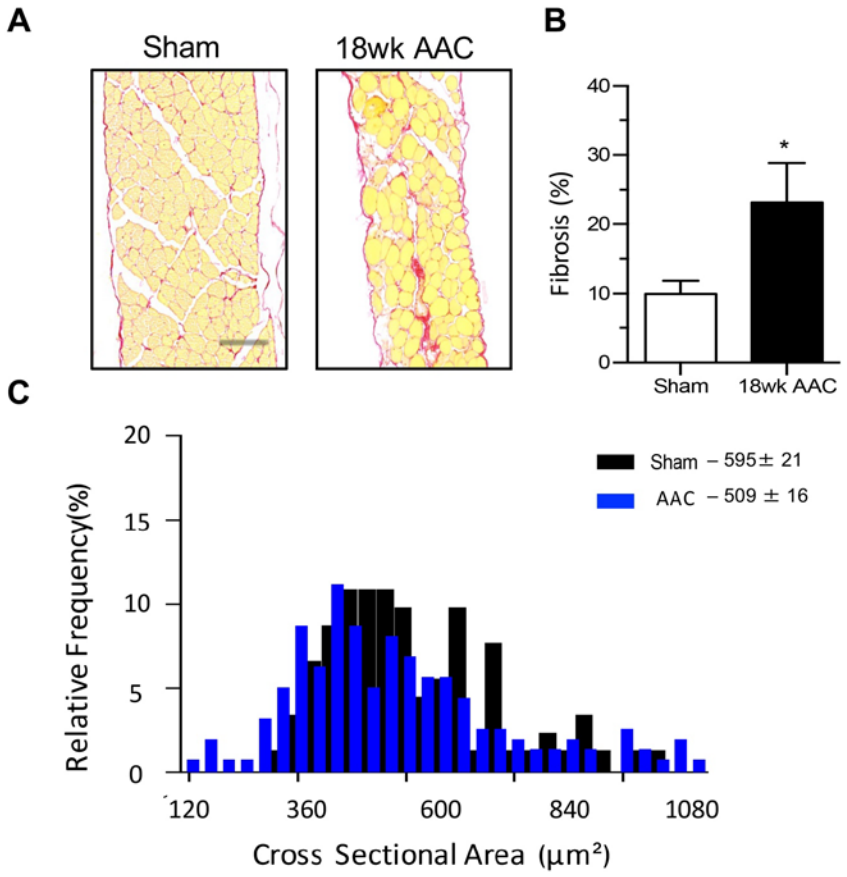

Figure 18. Abdominal aortic constriction (AAC) induces diaphragmatic atrophy and fibrosis. (**A**) Representative images of sham (*n=6*) and 18 wk AAC (*n=3*) diaphragm muscles stained with PSR. **(B)** Percent fibrosis of sham (*n=6*) and 18 wk AAC (*n*=3) diaphragm. (**C**) Diaphragm muscle fiber cross sectional area histogram of sham (*n=6*) and 18 wk AAC (*n=3*) mice. Mean ± SD, * Indicates significance vs. sham; $p<0.05$ as determined by protected LSD or students T-test. Scale bars: **(A)** 50µm.

	Sham *(n=8)*	**9 wk TAC** *(n=8)*	**18 wk TAC** *(n=8)*	**18 wk AAC** *(n=3)*
Left Ventricle				
LVP (mmHg)	102 ± 5	145 ± 5*	128 ± 6*	148 ± 5*
LV-EDP (mmHg)	5 ± 2	20 ± 2*	22 ± 1*	16 ± 3*
LV-dP/dt Max (mmHg/s)	9294 ± 387	7896 ± 432*	6794 ± 508*	8016 ± 124*
Morphometric				
Body Weight (g)	39.1 ± 0.9	48.4 ± 2.6*	41.4 ± 2.2	47.0 ± 2.3*
Heart weight (mg)	16.4 ± 0.5	24.0 ± 1.3*	32.1 ± 1.6*	24.2 ± 1.7*
HW/TL (mg/cm)	8.8 ± 0.3	14.8 ± 0.7*	16.6 ± 0.8*	12.9 ± 0.9*
MAP(mmHg)	81 ± 5.3	87 ± 2.8	78 ± 4	112 ± 12*
-Systolic BP (mmHg)	100 ± 4.8	143 ± 4.5*	128 ± 5.8*	145 ± 4.8*
-Diastolic BP (mmHg)	71 ± 5.6	59 ± 2.7	53 ± 3.6	96 ± 4.5*
Heart rate (beats/min)	576 ± 12	583 ± 15	597 ± 25	592 ± 15
Lung Wet wt. (mg)	21 ± 1.0	34.1 ± 4.7*	43.9 ± 6.6*	26.8 ± 1.2*
Lung Dry wt. (mg)	5.2 ± 0.1	7.7 ± 0.9*	10.6 ± 1.4*	5.9 ± 0.1*
Lung wet wt./dry wt.	4.0 ± 0.2	4.4 ±0.2	4.1 ± 0.3	4.5 ± 0.1

Table 9. Cardiac hemodynamic function in sham, 18wk TAC and 18wk AAC mice. Tissue weights, Mean ± SD, all others are Mean ± SEM, * Indicates significance vs. sham; $p<0.05$, as determined by protected LSD.

Diaphragmatic Atrophy Is Ameliorated by Chronic B-Adrenergic Blockade

In HF, neurohormonal dysfunction is classically associated with catecholamines. Therefore, animals were chronically treated for 4 weeks following TAC with propranolol, a non-selective β-adrenergic blocker to systemically attenuate β-adrenergic signaling. We then compared respiratory muscle morphology and function between the three groups (Figure 19A). Chronic β-blockade maintained both muscle cross sectional area (Figure 19B) and peak inspiratory pressure (Figure 19C), yet did not completely stop the genesis of HF. Despite β-adrenergic blockade, cardiac pressures nevertheless increased and contractility decreased (Table 9) similarly in all TAC animals, confirming that β-adrenergic overdrive is a significant contributor to respiratory muscle dysfunction in TAC induced HF.

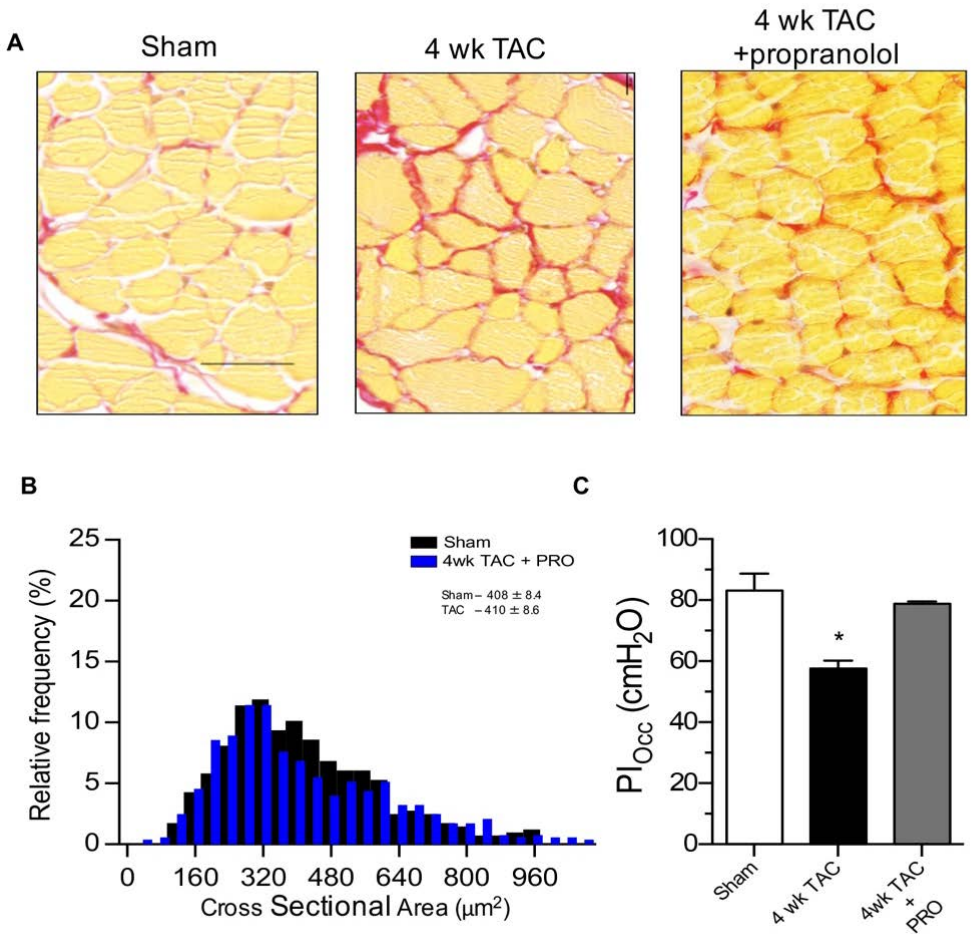

Figure 19. Chronic β-adrenergic blockade in TAC mice ameliorates diaphragm atrophy maintaining inspiratory strength (A) Representative cross sectional images of diaphragm from sham, 4wk TAC and 4wk TAC+propranolol stained with picrosirius red. (B) Diaphragm muscle fiber cross sectional area histogram of sham (n=5) vs. 4wk TAC+propranolol mice (n=4) (C) Maximal inspiratory pressure during a 25s airway occlusion in sham (n=10), 4wk TAC (n=8), 4wk TAC+propranolol (n=6) mice. Mean ± SEM, * Indicates significance vs. sham; $p<0.05$, as determined by protected LSD. Scale Bars: (A) 50 μm

	Sham *(n=8)*	**2 wk TAC** *(n=8)*	**2 wk TAC + propranolol** *(n=6)*	**4 wk TAC** *(n=8)*	**4 wk TAC + propranolol** *(n=8)*
LVP (mmHg)	102 ± 5	142 ± 3*	150 ± 3*	176 ± 5*	164 ± 4*
LV EDP (mmHg)	5 ± 2	19 ± 1*	14 ± 2*	22 ± 4*	17 ± 2*
LV +dP/dt (mmHg/s)	9294 ± 387	7919 ± 207*	6638 ± 120*	10136 ± 470	6599 ± 233*
Heart Rate (beats/min)	576 ± 12	613 ± 13	468 ± 14*	607 ± 15	460 ± 13*
LV +dP/dt/ Heart rate	16	13	14	17	14

Table 10. Effect of propranolol treatment on hemodynamic function on 2 and 4 wk TAC mice. Mean ± SEM, *Indicates significance vs. sham; $p<0.05$, as determined by protected LSD.

CHAPTER V: DISCUSSION

Here we show, in agreement with our hypothesis, that TAC induced respiratory muscle weakness is a progressive phenomenon, caused by atrophy, in the absence of pulmonary edema and preceding limb muscle alterations. A summary of the time course development of respiratory alterations associated with TAC induced HF can be found in Table 10. We have demonstrated that atrophy is the sole cause of diaphragmatic weakness as over 97% of the variance in diaphragmatic strength is explained by atrophy (Figure 15 D) making the cause of atrophy a critical target in the treatment of hypertension induced respiratory weakness.

	2 wk TAC	**4 wk TAC**	**9 wk TAC**	**18 wk TAC**
PI	↑	→	↑	↓
PI_{MAX}	S	↓	→	↓
Intrinsic diaphragmatic force	↑	S	S	S
Diaphragm myocyte CSA	S	↓	→	↓
Pulmonary Edema	ND	ND	ND	ND
Limb Muscle Atrophy	-	ND	-	-
Lung fibrosis	S	S	↑	→
Alveolar CSA	S	S	↑	→

Table 11. Temporal progression of diaphragm dysfunction in TAC induced HF

↑ indicates: values increased from previous time point
↓ indicates: values decreased from previous time point
→ indicates: values consistent from previous time point
S indicates: values similar to sham
ND indicates: not detected

Although HF is classified with respect to exercise tolerance, treatment goals are often aimed at improving cardiac function, which, arguably, has negligible effects on skeletal and respiratory muscle alterations and ultimately, quality of life. Often, dyspnea and exercise intolerance in HF are attributed to skeletal muscle myopathy (Josiak et al., 2014; Piepoli et al., 2013; Ponikowski, Chua & Francis, 2001), or pulmonary edema (Ingram & Braunwald, 2005; Mulrow, Lucey & Farnett, 1993), despite significant evidence to implicate respiratory muscle dysfunction as a substantial factor (Howell et al., 1995; Mangner et al, 2015; Wilson, Mancini & Dunkman 1993). Therefore, this thesis was aimed at characterizing the temporal evolution of TAC-induced respiratory muscle dysfunction with the goal of elucidating the incipient cause of respiratory weakness. Our data indicates that TAC causes progressive diaphragmatic fibrosis and atrophy. We have shown a substantial decrease in diaphragmatic strength, correlating strongly with atrophy, without *in vitro* dysfunction. While diaphragmatic weakness is thought to arise from over-activation of the diaphragm as a results of increase work of breathing owing to pulmonary edema, here we have shown diaphragm weakness (primary atrophy) occurring independent of pulmonary edema. However, while the mechanism for increased work of breathing and diaphragm weakness remains to be investigated, we further show that blocking the β-adrenergic system, using propranolol, prevented the development of diaphragm weakness, implicating this as a causal mechanism. Ultimately, any improvement in diaphragm force production will lead to improvements in patients' quality of life and exercise tolerance. This is important as exercise therapy is emerging as a new therapeutic strategy for managing heart failure.

This work demonstrates that respiratory muscle dysfunction develops much earlier in the progression of HF than previously thought, is progressive in nature and occurs independent of pulmonary edema or limb muscle atrophy. Furthermore, our work implicates β-adrenergic

overdrive as a key mediator of HF induced respiratory muscle atrophy. This thesis is the first multi-time point investigation into the genesis of respiratory dysfunction resulting from TAC

Enhanced in vitro *Function Precedes Atrophy*

Impaired *in vitro* function has been widely reported by other groups investigating diaphragm dysfunction in animal models of HF (Coirault et al., 1997; Coirault et al., 2007; Howell et al., 1995; Lecarpentier et al., 1999; Mangner et al., 2015; Supinski et al., 1994). In order to understand the role of *in vitro* dysfunction in the genesis of diaphragm myopathy, we sought to identify the temporal onset. However, we found no dysfunction at any time point. Rather, at 2 weeks of TAC animals present with increased *in vitro* force production, a novel finding which has not been reported previously. In a collaborative study with our lab, Gillis et al. (2015) investigated the acute (2 weeks) and long term (18 weeks) effects of TAC on myofilament and intact *in vitro* muscle preparations in mice. Interestingly, they found both enhanced force production at 2 weeks of TAC (normalized by 18 weeks), and impaired myofilament function by 18 weeks of TAC. The authors theorize that compensatory adaptations with calcium handling proteins are occurring within the muscle, resulting in enhanced function in intact muscle strips; a theory also proposed by Lecarpentier et al. (1999) to explain the impaired relaxation in their rabbit model of volume overload. Why our group did not find reduced *in vitro* function while other did is unclear, however, it may be related to the TAC model as most other work is done in myocardial infarction or ventricular pacing models (Coirault et al., 1997; Howell et al., 1995; Lecarpentier et al., 1999; Mangner et al., 2015; Supinski et al., 1994). It is possible that while respiratory muscle dysfunction occurs ubiquitously in HF, certain aspects are specific to the etiology of HF. For example, HF arising from myocardial infarction may cause diaphragmatic *in vitro* dysfunction, whereas hypertensive HF may result in normal, or enhanced *in vitro* function.

Critically, our observation of enhanced *in vitro* performance directly precedes the development of atrophy. It is possible that the cause of the transient increase in function is related to the mechanism of atrophy. Enhanced *in vitro* function caused by altered calcium handling is a viable theory because it seems to parallel with how the heart remodels in HF. In early stages of cardiac dysfunction, neurohormonal activation is designed to rescue cardiac function. When cardiac output drops, sympathetic activation increases cardiac contractility and enhances relaxation to increase cardiac output. This is accomplished by catecholamine mediated increase in calcium release and reuptake. Over time, however, intracellular calcium stores become depleted, and reuptake diminished (Middlekauff, 2010), resulting in decreased contractility (Kushner & Marks, 2010; Weherns & Marks, 2004). It is possible that neurohormonal overdrive is also involved in the pathogenesis of diaphragm myopathy in the same way. HF causes substantial increases in circulating catecholamines (Colucci et al., 1988). Perhaps over exposure to catecholamines, which is known to be toxic to cardiomyocytes, is also toxic to respiratory muscle. Indeed, over exposure to catecholamines induces fibrosis, apoptosis and reduces inotropic responses to β-adrenergic stimulation in the heart (Brouri et al., 2004; Communal et al., 1998). Importantly, TAC diaphragms also show increased fibrosis, reduced strength and atrophy. The skeletal muscle of late stage HF patients displays decreased expression of SERCA (Middlekauff et al., 2012), a key contractile related calcium handling protein. Perhaps catecholamine overexposure results in adaptations which initially enhance contractile function, but ultimately lead to SERCA down-regulation, eventually contributing to muscle atrophy. Therefore, future work aimed at the effects of β-adrenergic blockade on *in vitro* function and expression of calcium handling proteins in diaphragm muscle in HF is certainly warranted. Specifically, the effect of catecholamine exposure on diaphragm contractility and the long term effects of catecholamine exposure on

diaphragm atrophy. By identifying the mechanism of diaphragm atrophy, we can improve treatment strategies for patients with respiratory muscle weakness caused by atrophy.

Peripheral Muscle Adaptation

Both experimental and clinical HF induce drastic changes to limb muscle (Drexler et al., 1991; Howell et al., 1995; Josiak et al, 2014; Mancini et al., 1998; Piepoli et al., 1996) and the diaphragm (Dimopoulou et al., 1998; Howell et al., 1995), which collectively result in significant exercise limitation.

In limb muscle, there is an adaptive shift towards a greater proportion of fast twitch type II fibers, whereas the diaphragm increases its relative proportion of slow twitch type I fibers (Howell et al., 1995) indicating a distinction between the two phenomena. While disuse is thought to be a contributing factor to limb muscle myopathy (Josiak et al, 2014; Piepoli et al., 2013; Simonini et al., 1996; Vescovo et al., 1996) it is not a viable mechanism in the diaphragm since it is responsible for inspiration. Despite key differences between limb and diaphragm muscles, research in this area continues to operate under one major assumption: that limb and respiratory muscle myopathy occur concomitantly. The reason for this is twofold; (1) the diaphragm is classified as a skeletal muscle, and (2) skeletal muscle dysfunction is always investigated using a single time point as an outcome. This results in respiratory and peripheral muscle dysfunction being considered as single temporal phenomenon. For example, the muscle hypothesis, (Josiak et al, 2014; Piepoli et al., 2013) suggests that limb and respiratory muscle myopathy occur concomitantly (Figure 3) and that they share a common mechanism, cardiac cachexia (HF induced muscle wasting). Critically, cachexia is a phenomenon exclusive to end stage HF, while dyspnea is not. To date, there has been no investigation to delineate the time course development of respiratory myopathy relative to limb muscle dysfunction making it impossible to confirm the mechanism

responsible. Understanding the temporal series of events in the development of skeletal muscle dysfunction in HF will provide substantial clarity with respect to cause and treatment strategies.

Indeed, in our model, by 18 weeks of TAC diaphragm dysfunction manifests as atrophy, fibrosis and reduced strength. While diaphragmatic atrophy is evident by 4 weeks of TAC (Figure 15), neither the gastrocnemius nor soleus muscles display any evidence of atrophy or fibrosis (Figure 17), eliminating the possibility of a common mechanism for the initial cause of limb and respiratory muscle atrophy in HF.

The Influence of Banding Location on Respiratory Muscle Myopathy

TAC may result in transient hypotension in diaphragmatic circulation which may have mediated the atrophy seen in our model. Therefore, we banded the abdominal aorta in a subset of animals to investigate whether diaphragmatic atrophy was caused by pressure-overload HF, or by design of our experimental model. While both TAC and abdominal aortic constriction models clearly result in HF (Table 8), the stress on the heart is directly related to the distance of the constriction from the heart (Brekenridge, 2010). Therefore, with abdominal aortic constriction, less pressure stress is placed on the heart, resulting in less severe progression of HF. Abdominal aorta constriction did result in fibrosis and atrophy in the diaphragm (Figure 18) indicating that diaphragm atrophy in TAC was not the result of any potential hypotension-induced hypoperfusion atrophy but indeed related to the development of HF per se. Notably, the diaphragms of abdominally banded mice displayed cores and central nuclei in some samples in contrast to the TAC diaphragms where none were evident (data not shown). Typically, cores and central located nuclei are hallmarks of cell apoptosis/necrosis, which have been reported in respiratory muscle in clinical HF.

Why signs of cell degradation may be present in abdominal aorta constriction but not TAC is unclear. One possible explanation is that the endothelium of the diaphragm from AAC

animals is exposed to pathologically high blood pressure (i.e., hypertension) that is absent in the diaphragm of the TAC animals. This may directly lead to damage or dysfunction of the endothelium. Therefore, it is possible that the increased blood pressure in the diaphragm of abdominally banded animals is responsible for the phenotypic variation between the diaphragms of TAC and abdominally banded animals. During hypertension, damage to the endothelium, a single cell layer that lines the interior surface of all blood vessels, occurs (Park, Charbonneau & Schiffrin, 2000; Schiffirin. Park & Intengan, 2001). In a healthy state, the endothelium mediates endothelium-dependent vasodilation (via the molecule nitric oxide), nutrient and water absorption and suppresses vascular inflammation and hypertrophy (Wilson & Lerman, 2001). When damaged, the endothelium becomes dysfunctional, promoting a pro-inflammatory state and reduced nitric oxide balance which diminishes vasodilatory ability. Endothelial dysfunction results in significant oxidative stress (Münzel et al., 2015) which can leave the endothelium overly permeable, allowing toxins to pass into other tissues (Rubanyi & Vanhoutte, 1986) such as skeletal muscle. Over exposure of skeletal muscle to free radicals causes apoptosis and necrosis (Adhihetty & Hood, 2003). Indeed, there is evidence to suggest that apoptosis occurs in the diaphragm in both clinical (Adams et al., 1999; Vescovo et al., 2000) and experimental HF (Dalla Libera et al., 1999; Vescovo et al., 1998). However, the factors mediating apoptosis in skeletal muscle in HF are not well understood. The possibility exists that endothelial stress causing excessive free radical formation could be an important factor in the damage of respiratory muscle in HF. Indeed, defective nitric oxide signaling has been implicated as a factor in the pathogenesis of skeletal muscle dysfunction in canines with HF (Shen, Wolin & Hintze, 1997) but this area of research is extremely limited and does not extend to respiratory muscles. Additional investigation is warranted to further distinguish the presence and role endothelial dysfunction or defective nitric oxide signaling in respiratory muscle atrophy in HF.

Effect of β-Blockade on Diaphragm Function

In our experiments, chronic β-blockade was able to prevent the atrophy and loss of maximal strength in the diaphragm seen by 4 weeks of TAC. Importantly, while β-blockade did rescue diaphragm mass and function, it did not prevent the development of HF. This is important because if β-blockade treated HF, then the absence of diaphragm atrophy would most likely be explained by the absence of the primary disease - HF.

In cardiac muscle, chronic β- adrenergic activation leads to reductions in contractile proteins (Bristow, 1997). The success of β-blockers in attenuating diaphragmatic atrophy seems to suggest a similar mechanism at play. Critically, the ability for chronic β-blockade to attenuate atrophy suggests that β-adrenergic overdrive is the key factor causing atrophy in TAC diaphragm, not errant cardiac function. However, it is still unclear as to the mechanism behind the success of β-blocker therapy on diaphragm atrophy. Specifically, from this work it is not possible to identify which β-receptors were responsible for the development of atrophy. There are 3 subtypes of β-adrenergic receptors: β_1, β_2 and β_3 (Bylund et al., 1994). The predominant subtype in the human heart is β_1, comprising approximately 80% of the receptor population, followed by β_2, representing 15-18% and the remainder represented by β_3 (Brodde, 1993). Unfortunately, the proportions of these subtypes in the diaphragm and peripheral muscle have not yet been defined. Moreover, it is unclear if propranolol treatment attenuated a toxic effect of circulating catecholamines directly on the diaphragm. This begs the question; if β-receptor overstimulation is a systemic factor, why was the diaphragm affected and not the limb muscle? One possible explanation is that the receptor population between the heart, diaphragm and limb muscles is different and therefore the effective concentration of circulating catecholamines may have divergent effects on these tissues. Further, the diaphragm is constantly active while the limb muscles are purely voluntary muscles. Therefore, it is possible that the constant activation of the diaphragm may predispose this muscle to rapid development

of atrophy. While we did not identify limb muscle atrophy by 4 weeks TAC, it is very likely that limb muscle atrophy does occur at with prolong development of HF. Of interest, Breitbart et al. (2011) demonstrated that TAC-induced limb muscle atrophy was caused, at least in part, by cardiac over-expression of myostatin, a negative regulator of skeletal muscle growth. Future studies aimed at β-blockade for prevention of limb muscle atrophy will help to elucidate if the development of diaphragm and limb muscles atrophy share a common pathway or if they have completely different mechanism. Certainly, the success of β-blocker therapy in treating HF-induced diaphragmatic atrophy is a significant contribution to the understanding of exercise intolerance in HF. However, in order to translate these findings into clinical management of HF, work must be done to delineate the proportions of β-receptor subtypes in the diaphragm and skeletal muscles of healthy and HF patients.

What's 'Lung' Got to do with it?

It is commonly believed that pulmonary congestion, caused by HF, results in increased work of breathing (PI) leading to fatigue related injury to the diaphragm (Ingram & Braunwald, 2005; Mulrow, Lucey & Farnett, 1993). This work clearly demonstrates that increased PI in early HF is not caused by pulmonary edema. Lung wet to dry ratios were unchanged between sham and 18 week TAC animals (Figure 13 D) indicating no change in lung water content, therefore pulmonary edema did not develop. However, absolute lung weights were significantly higher in HF animals, indicating an increase in lung tissue (Figure 16A). Similar findings were reported both by Coirault et al. (1997) and Chen et al. (2012) in their murine models of TAC HF. Coirault et al. (1997) reported decreased lung compliance and increased airway resistance, but failed to examine the lungs histologically and only reported absolute lung weights. Because of this, they attributed their findings to pulmonary edema. Chen et al. (2012) reported significant lung fibrosis and inflammation after 14 weeks of TAC resulting in

a restrictive lung phenotype. They could not entirely rule out the development of transient pulmonary edema, as they did not measure lung weights throughout the progression of HF in their mice. Our data proves that rather than congestion, HF causes lung remodeling, since at no time point did we observe increased wet weight to dry weight ratio in lung tissue. Certainly, there are marked changes in lung structure at 9 and 18 weeks of TAC, however since atrophy preceded lung remodeling, it cannot be implicated as the initial cause for respiratory muscle atrophy.

There is also the possibility that β-adrenergic stimulation also contributes to lung remodeling. While we have established that respiratory muscle dysfunction in TAC is not caused by lung remodeling, it is possible that further in the progression of HF, lung remodeling does exacerbate respiratory muscle dysfunction and exercise intolerance. If so, in clinical aortic stenosis, lung remodeling could be an important target for treatment. To further explore this hypothesis, future work should be done to examine the incidence of lung remodeling in other forms of experimental and clinical HF, and the potential impact of β-adrenergic overdrive in the development of lung remodeling.

Histological Assessment of Atrophy

This work indicates a pivotal role of atrophy in the pathogenesis of respiratory muscle dysfunction in HF. Currently, histology in the study of respiratory muscle dysfunction is astoundingly underused given the substantial pay off of information it affords. Often, groups investigate function and protein content, leaving the morphology of the muscle unexplored. Critically, without histological assessment, the finding of atrophy as the cause of muscle weakness would not have been possible. Therefore, this thesis demonstrates the substantial value of histological data in characterizing the development of muscle myopathy. Certainly, other techniques can be employed for the detection of atrophy such as

total muscle weights and western blot. However, the former lacks sensitivity, as changes in non-cachectic HF may be too slight to detect. The latter may provide insight into the total content of specific proteins within muscle, but may be overly specific, as there are a substantial amount of proteins that could be affected by atrophy. Histology represents a valid and reliable method to visualize changes in whole muscle fibrosis, myocyte cross sectional area, and provides opportunity to elucidate changes to specific fiber types. It is unknown if the measurement of atrophy using molecular methods in this study would have yielded similar results as histology, certainly there is merit in comparing the two methods. While histology is not a standard component in the evaluation of muscle dysfunction, this work powerfully suggests that, moving forward, it should be. Importantly, there are very few standards and limited reporting in research on the methods used to fix and dissect tissues for histological investigation. If histology were to be included in future work, there are several considerations that must be made. First, fixative induces muscle contraction, the cross linking of muscle proteins often results in distortion of the structure of the muscle. This can be avoided by first, preparing tissues *in* situ, second, using a relaxing solution of 50 mM potassium chloride, and finally, leaving tissues attached to skeletal structures until processing. This thesis demonstrates the considerable value of histology, and the methods necessary for standardization of histological protocols, for valid and reliable reporting of morphological changes in muscle tissue induced by HF.

Limitations

While the TAC model of HF is useful for investigating the effects of pressure-overload on the heart, there are many factors that separate it from clinical HF. Firstly, hypertension progresses into HF over years or even decades, whereas with TAC, hypertension develops instantaneously. The immediate and sudden onset of cardiac stress likely results in phenotypic

variations between our TAC model and clinical HF. Moreover, our model is developed over a single genomic background which does not reflect the diversity of HF patients. Indeed, HF develops in genetically diverse populations and exists with many, often multiple comorbidities (chronic obstructive pulmonary disease, diabetes mellitus, obesity, metabolic disease, coronary artery disease, etc.). All of these comorbidities can contribute to the pathogenesis of respiratory dysfunction (Anther et al., 2012). Moreover, they may confound or contraindicate treatment strategies, which makes the translation of our results difficult. Indeed, chronic obstructive pulmonary disease causes respiratory muscle dysfunction (Mann et al., 2009; Ottenheijm et al., 2005; Orozco-Levi et al., 2001), as does morbid obesity (Parameswaran, Todd & Soth, 2006; Pelosi et al., 1997; Tenório et al., 2013;) and diabetes mellitus (Meo et al., 2006). As such, temporal characterization of respiratory muscle myopathy in a variety of underlying conditions is necessary to identify whether atrophy is a universal phenomenon or is specific to pressure-overload HF.

Also, while we have shown that chronic β-adrenergic blockade from the onset of cardiac stress can prevent TAC induced respiratory muscle atrophy, this strategy is not feasible with clinical populations. Often, patients don't seek medical attention until late in the progression of HF (Sueata et al., 2005). Here, in our model, we show that respiratory myopathy manifests early in disease progression, meaning that prophylactic treatment of diaphragm atrophy is relatively unfeasible. Exercise training has been found to improve skeletal and respiratory muscle function in exercise (Coats et al., 1992; Middlekauff et al., 2011), but whether treatment with properly titrated doses of β-blockers would enhance the effects of exercise or produce similar results is yet to be investigated.

As mentioned in our methods chapter, we chose to limit our use of animals, and thus, compared the same group of shams to all TAC time points, abdominal aortic constriction animals and to our propranolol treated animals. This means that the same group of shams are

represented in several data sets. While we view this as an ethical strength of our work, it doesn't account for variability between litters, or between age groups. Moreover, during our propranolol experiments, we chose not to employ a vehicle group to control for the possible effects of stress caused by repeated injections. The reason for this is, again, to limit the use of animals. However, since the effects of propranolol were exceedingly positive, we are confident in our decision to omit a vehicle control subgroup from the propranolol experiment.

An Appropriate Model of Skeletal Muscle Dysfunction in HF

The exploration of HF related diaphragm myopathy occurs in several species and in several models of HF. It is possible that discrepancies in findings between studies are due to genetic and model variability. Gillis et al. (2015) noted differences between TAC and myocardial infarction induced HF on intrinsic diaphragm function in mice. Namely, 18 weeks of TAC resulted in substantial reductions in maximum calcium stimulated force generation whereas 18 weeks post myocardial infarction showed no change as compared to sham. In rats, myocardial infarction causes no intrinsic dysfunction, but does result in selective atrophy of type I and type IIb fibers (Stassijins et al., 1998). In Yucatan mini pigs, myocardial infarction results in generalized fiber atrophy (Howell et al., 1996). In clinical HF, some groups do not find atrophy (Lindasy et al., 1996), while others do and describe gender differences in patterns of atrophy (Middlekauff et al. 2012). Still, the underlying question is: what is the ideal animal model for investigating skeletal and respiratory muscle dysfunction in HF? Certainly, myocardial infarction represents a significant contribution to HF (Velagaleti et al., 2008) but this thesis indicates that TAC may not be the ideal model to investigate skeletal muscle adaptations to hypertensive HF. In fact, TAC most closely models aortic stenosis, a relatively rare cause of HF (Thaden, Nkomo & Enriquez-Sarano, 2014), where blood pressure is only elevated in the heart and tissues proximal to the constriction. In hypertensive HF, blood

pressure is increased in all organs and tissues. Even abdominal aortic constriction may not be sufficient to accurately recapitulate the elevated systemic blood pressure seen in clinical pressure overload as tissues distal to the tie (lower limbs, kidney) would see normal or lower physiological pressures. As such, a model in which systemic blood pressure is chronically elevated, such as spontaneously hypertensive or salt sensitive rats, may better represent limb and respiratory myopathy in HF.

Conclusions and Future Directions

Through this work, we have successfully established that TAC-induced HF causes diaphragmatic dysfunction before the development of limb muscle dysfunction and in the absence of pulmonary edema. Notably, we were able to successfully preserve diaphragm function in the face of HF by non-selective blockade of β-adrenergic receptors. β-blockers are nearly ubiquitously recommended in the clinical management of HF (AHA, 2016), however it is unknown if the approved drugs will attenuate respiratory muscle atrophy as we have yet to investigate the effect of β-blockers on respiratory outcomes. Indeed, HF severity is determined by the degree of dyspnea and exercise limitation, yet these factors are not considered in clinical drug trails. Importantly, our animals were treated with 10 times the standard dose of propranolol used to treat hypertension. Considering this, future work should consider pharmacology, as the therapeutic dose for management of blood pressure may not be efficacious for treating respiratory muscle weakness. Finally, while β-blockers are recommended first line treatment for HF, they are dramatically under-prescribed (Yilmaz et al., 2007). This work represents a new pharmacological target for the use of β-blockers in HF and highlights the importance of this under-prescribed therapy.

Also, there is evidence to suggest that the development of respiratory muscle weakness is specific to the cause of HF. Therefore, it is important to determine if the temporal

development of respiratory muscle dysfunction occurs similarly in other pathological iterations of HF.

This thesis establishes that the manifestation of respiratory muscle dysfunction in HF is progressive in nature and specific to the cause of HF. Further investigations into the temporal development of diaphragm myopathy in response to other forms of HF (eg. myocardial infarction, other forms of pressure overload HF) and comorbidities (eg. obesity, diabetes, chronic obstructive pulmonary disease) are necessary in order to fully understand and successfully treat patients with chronic illnesses. Respiratory muscle dysfunction has a significant impact on quality of life and because of this, is a vital target for the management of chronic disease.

CHAPTER VI: REFERENCES

ACCF/AHA guideline for the management of heart failure: a report of the American College of Cardiology Foundation/American Heart Association Task Force on Practice Guidelines. Circulation. 2013;128(16):e240-e327.

Adams, V., Jiang, H., Yu, J., MÃķbius-Winkler, S., Fiehn, E., Linke, A.& Hambrecht, R. (1999). Apoptosis in skeletal myocytes of patients with chronic heart failure is associated with exercise intolerance. *Journal of the American College of Cardiology*, 33(4), 959-965.

Adhihetty, P. J., & Hood, D. A. (2003). Mechanisms of apoptosis in skeletal muscle. *BAM-PADOVA-*. 13(4), 171-180.

Agostoni, P. G., Bussotti, M., Palermo, P., & Guazzi, M. (2002). Does lung diffusion impairment affect exercise capacity in patients with heart failure? *Heart*, 88(5), 453-459.

Ahmed A. (2007) A propensity matched study of New York Heart Association class and natural history end points in heart failure. *American Journal of Cardiology*, 99(4):549-553.

Allen, D.L., Cleary, A.S., Speaker, K.J., Lindsay, S.F., Uyenishi, J., Reed, J.M., Madden, M.C. & Mehan, R.S. (2008). Myostatin, activin receptor IIb, and follistatin-like-3 gene expression are altered in adipose tissue and skeletal muscle of obese mice. *American Journal of Physiology, Endocrinology and Metabolism*, 294(5), 918-27.

Allen, D., L., Hittel, D.,S. & McPheron, A.C. (2011). Expression and function of myostatin in obeisty, diabetes and exercise adaptation. *Medicine and Science in Sports and Exercise*, 43(10), 1828-35.

Anker, S., Steinborn, W., & Strassburg, S. (2004). Cardiac cachexia. *Annals of medicine*, 36(7), 518-529.

Anker, S. D., Chua, T. P., Ponikowski, P., Harrington, D., Swan, J. W., Kox, W. J. & Coats, A. J. (1997). Hormonal changes and catabolic/anabolic imbalance in chronic heart failure and their importance for cardiac cachexia. *Circulation*, 96(2), 526-534.

Ather, S., Chan, W., Bozkurt, B., Aguilar, D., Ramasubbu, K., Zachariah, A. A., ... & Deswal, A. (2012). Impact of noncardiac comorbidities on morbidity and mortality in a predominantly male population with heart failure and preserved versus reduced ejection fraction. *Journal of the American College of Cardiology*. 59(11), 998-1005.

Beaudoin, M.S., Snook, L., A., Arkell, A.M., Simpson, J.,A., Holloway, G.,P., & Wright, D.,C. (2013). Resveratrol supplementation improves white adipose tissue function in a depot-specific manner in zucker diabetic fatty rats. *American Journal of Physiology, Regulatory, Integrative and Comparative Physiology*, 305(5), 542-51.

Bellotti, P., Badano, L. P., Acquarone, N., Griffo, R., Pinto, G. L., Maggioni, A. P., & Mombelloni, P. (2001). Specialty-related differences in the epidemiology, clinical profile, management and outcome of patients hospitalized for heart failure. The OSCUR study. *European heart journal*, 22(7), 596-604.

Bennett, J. A., Riegel, B., Bittner, V., & Nichols, J. (2002). Validity and reliability of the NYHA classes for measuring research outcomes in patients with cardiac disease. *Heart & Lung: The Journal of Acute and Critical Care*, 31(4), 262-270.

Bernardo, B. C., Weeks, K. L., Pretorius, L., & McMullen, J. R. (2010). Molecular distinction between physiological and pathological cardiac hypertrophy: experimental findings and therapeutic strategies. *Pharmacology & therapeutics*. 128(1), 191-227.

Bilandzic, A., & Rosella, L. (2017). The cost of diabetes in Canada over 10 years: applying attributable health care costs to a diabetes incidence prediction model. *Chronic Diseases and Injuries in Canada*. 37(2).

Bo Li, Z., Kollias, H. D., & Wagner, K. R. (2008). Myostatin directly regulates skeletal muscle fibrosis. *The Journal of Biological Chemistry*, 283(28), 19371-19379.

Booth, F. W. (1977). Time course of muscular atrophy during immobilization of hind limbs in rats. *Journal of Applied Physiology*, 43(4), 656-661.

Breckenridge, R. (2010) Heart failure and mouse models. *Disease Models & Mechanisms* 3: 138-143

Breitbart, A., Auger-Messier, M., Molkentin, J. D., & Heineke, J. (2011). Myostatin from the heart: local and systemic actions in cardiac failure and muscle wasting. *American Journal of Physiology-Heart and Circulatory Physiology*, 300(6), H1973-H1982.

Brink, M., Anwar, A., & Delafontaine, P. (2002). Neurohormonal factors in the development of catabolic/anabolic imbalance and cachexia. *International journal of cardiology*, *85*(1), 111-121.

Bristow, M. R. (1997). Mechanism of action of β--blocking agents in heart failure. *The American journal of cardiology*, *80*(11), 26L-40L.

Brodde, O. E. (1993). Beta-adrenoceptors in cardiac disease. *Pharmacology & therapeutics*. 60(3), 405-430.

Brouri, F., Hanoun, N., Mediani, O., Saurini, F., Hamon, M., Vanhoutte, P. M., & Lechat, P. (2004). Blockade of β 1-and desensitization of β 2-adrenoceptors reduce isoprenaline-induced cardiac fibrosis. *European journal of pharmacology*. *485*(1), 227-234.

Brunotte, F., Thompson, C.H. & Adamopoulous, S. (1995) Rat skeletal muscle metabolism in experimental heart failure. *Acta Pysiologica Scandinavia.* 154, 439-447.

Buller, N.P., Jones, D. & Poole-Wilson, P.A. (1991) Direct measure of skeletal muscle fatigue in patients with chronic heart failure. *British Heart Journal.* 65, 20-24.

Bylind-Fellenius, A., Walker, P., Elander, A., Holm, S., Holm, J., Schersten, T. (1981) Energy metabolism in relation o oxygen partial pressure in human skeletal muscle during exercise. *Journal of Biochemistry.* 200, 247-255.

Bylund, D. B., Eikenberg, D. C., Hieble, J. P., Langer, S. Z., Lefkowitz, R. J., Minneman, K. P. & Trendelenburg, U. (1994). International Union of Pharmacology nomenclature of adrenoceptors. *Pharmacological reviews*. 46(2), 121-136.

Carretero, O. A., & Oparil, S. (2000). Essential hypertension part I: definition and etiology. Circulation, 101(3), 329-335.

Chen, Y., Guo, H., Xu, D., Xu, X., Wang, H., Hu, X. & Huo, Y. (2012). Left Ventricular Failure Produces Profound Lung Remodeling and Pulmonary Hypertension in Mice Heart Failure Causes Severe Lung Disease. *Hypertension*, *59*(6), 1170-1178.

Chlif, M., Keochkerian, D., Choquet, D., Vaidie, A., & Ahmaidi, S. (2009). Effects of obesity on breathing pattern, ventilatory neural drive and mechanics. *Respiratory Physiology & Neurobiology*, *168*(3), 198-202.

Chua, T. P., Anker, S. D., Harrington, D., & Coats, A. J. (1995). Inspiratory muscle strength is a determinant of maximum oxygen consumption in chronic heart failure. *British heart journal*, 74(4), 381-385.

Coats, A.J., Adamopoulos, S., Radaelli, A., McCance, A., Meyer, T.E., Bernardi, L., Solda, P.L., Davey, P., Ormerod, O., Forfar, C. (1992) Controlled trial of physical training in chronic HF: exercise performance, hemodynamics, ventilation, and autonomic function. *Circulation*. 85, 2119–2131.

Coats, A. J. (2001). What causes the symptoms of heart failure?. *Heart*. 86(5), 574-578.

Cohen-Solal, A., Beauvais, F., & Tabet, J. Y. (1994). Cardiopulmonary exercise testing in chronic heart failure. *Cardiovascular Prevention and Rehabilitation*. 99.

Cohn, J. N., Levine, T. B., Olivari, M. T., Garberg, V., Lura, D., Francis, G. S. & Rector, T. (1984). Plasma norepinephrine as a guide to prognosis in patients with chronic congestive heart failure. *New England journal of medicine*. 311(13), 819-823.

Coirault, C., Chemla, D., Pourny, J., Lambert, F., Riou, B., & Lecarpentier, Y. (1997). Relaxation is impaired in the diaphragm muscle of the cardiomyopathic Syrian hamster. *American Journal Of Respiratory And Critical Care Medicine, 155*(5), 1575-1582.

Coirault, C., Guellich, A., Barbry, T., Samuel, J., Riou, B., & Lecarpentier, Y. (2007). Oxidative stress of myosin contributes to skeletal muscle dysfunction in rats with chronic heart failure. *American Journal of Physiology. Heart and Circulatory Physiology*. 292(2), H1009-17.

Communal, C., Singh, K., Pimentel, D. R., & Colucci, W. S. (1998). Norepinephrine stimulates apoptosis in adult rat ventricular myocytes by activation of the β-adrenergic pathway. *Circulation*. 98(13), 1329-1334.

Costa, D., Barbalho, M.c., Miguel, G.P.S., Forti,E.M.P. Moreira, J.L., Azevedo, C. (2008). The impact of obesity on Pulmonary function in adult women. *Clinics.* 63(6), 719-24.

Cowley AJ, Fullwood L, Stainer K, Hampton JR. (1991) Exercise tolerance in patients with heart failure—how should it be measured? *European Heart Journal*. 12(1): 50-4.

Dall'Ago, P., Chiappa, G. R., Guths, H., Stein, R., & Ribeiro, J. P. (2006). Inspiratory muscle training in patients with heart failure and inspiratory muscle weakness: a randomized trial. *Journal of the American College of Cardiology*. 47(4), 757-763.

Dalla Libera, L., Zennaro, R., Sandri, M., Ambrosio, G. B., & Vescovo, G. (1999). Apoptosis and atrophy in rat slow skeletal muscles in chronic heart failure. *American Journal of Physiology-Cell Physiology*, 277(5), C982-C986.

Davey, P., Meyer, T., Coats, A., Adamopoulos, S., Casadei, B., Conway, J., & Sleight, P. (1992). Ventilation in chronic heart failure: effects of physical training. *British Heart Journal*. 68(11), 473-477.

Denolin, H., Kuhn, H., Krayenbuehl, H., Loogen, F., & Reale, A. (1983). The definition of heart failure. *European Heart Journal*, 4(7), 445-448.

DeGroote, P., Dagirn, J., Soudan, B., Lamblin, N., McFadden, E. & Bauters, C. (2004) B-type nauretic peptide and peak oxygen consumption provide independent risk information for stratification in patients with stable congestive heart failure. *Journal of American Cardiology*. 43(9), 1584-1589.

DeTroyer, A., Estenne, M., Yernault, J.C. (1980) Disturbance of respiratory muscle function in patients with mitral valve disease. *American Journal of Medicine*. 69, 867-873.

Dimopoulou, I., Daganou, M., Tsintzas, O. K., & Tzelepis, G. E. (1998). Effects of severity of long-standing congestive heart failure on pulmonary function. *Respiratory medicine*. 92(12), 1321-1325.

Dorn, G.W. (2009) Novel therapies to abrogate postinfarction ventricular remodeling. *Nature Reviews Cardiology*. 6, 283-291.

Drazner, H.M, (2011) The Progression of Hypertensive Heart Disease. *Circulation*. 123, 327-334.

Drexler, H. (1991) Reduced exercise tolerance in chronic heart failure and its relationship to neurohormonal factors. *European Heart Journal.* 12, 12-28.

Drexler, H., Faude, F, Hoing, S. & Just, H. (1987) Blood flow distribution within skeletal muscle during exercise in the presence of chronic heart failure: effect of milrinone. *Circulation.* 76, 1344-1352.

Drexler H, Banhardt U, Meinertz T, Wollschlager H, Lehmann M, Just H. (1989) Contrasting peripheral short-term and long-term effects of converting enzyme inhibition in patients with congestive heart failure. *Circulation.* 79, 491-502.

Farkas G., A., Gosselin, L.,E., Zhan, W.,Z., & Schlenker, E.,H. and SieckG.,C. (1994). Histochemical and mechanical properties of diaphragm muscle in morbidly obese zucker rats. *Journal of Applied Physiology*. 77(5), 2250-2259.

Fauci AS, Braunwald E & Kasper DL. (2008) Harrison's Principles of Internal Medicine. 17th ed. New York: McGraw-Hill.

Flegal, K. M., Kruszon-Moran, D., Carroll, M. D., Fryar, C. D., & Ogden, C. L. (2016). Trends in obesity among adults in the United States, 2005 to 2014. *Jama*. 315(21), 2284-2291.

Florea, V.G. & Cohn, J.N. (2014) The autonomic nervous system and heart failure. *Circulation.* 114, 1815-1826.

Fonarow, G. C., Yancy, C. W., Hernandez, A. F., Peterson, E. D., Spertus, J. A., & Heidenreich, P. A. (2011). Potential impact of optimal implementation of evidence-based heart failure therapies on mortality. *American heart journal*. 161(6), 1024-1030.

Franciosa, J.A., Park, M. & Levine, T.B. (1981). Lack of correlation between exercise capacity and indicies of resting left ventricular performance in heart failure. *The American journal of cardiology*. 47, 33-39.

Francis, G. S. (1985). Neurohumoral mechanisms involved in congestive heart failure. *The American journal of cardiology*. 55(2), A15-A21.

Frey, N., & Olson, E. N. (2003). Cardiac hypertrophy: the good, the bad, and the ugly. *Annual review of physiology*, *65*(1), 45-79.

Fujii, Y., Guo, Y., & Hussain, S. N. (1998). Regulation of nitric oxide production in response to skeletal muscle activation. *Journal of Applied Physiology*, *85*(6), 2330-2336.

Gelberg, H. J., Rubin, S. A., Ports, T. A., Brundage, B. H., Parmley, W. W., & Chatterjee, K. (1979). Detection of left ventricular functional reserve by supine exercise hemodynamics in patients with severe, chronic heart failure. *The American journal of cardiology*. 44(6), 1062-1067.

Gheorghiade, M., Colucci, W.S., Swedberg, K.S. (2003) β--Blockers in Chronic Heart Failure. *Circulation*. 107, 1570-1575.

Gillis, T. E., Klaiman, J. M., Foster, A., Platt, M. J., Huber, J. S., Corso, M. Y., & Simpson, J. A. (2016). Dissecting the role of the myofilament in diaphragm dysfunction during the development of heart failure in mice. *American Journal of Physiology-Heart and Circulatory Physiology*. 310(5), H572-H586.

Gosker, H. R., Wouters, E. F., van der Vusse, G. J., & Schols, A. M. (2000). Skeletal muscle dysfunction in chronic obstructive pulmonary disease and chronic heart failure: underlying mechanisms and therapy perspectives. *The American journal of clinical nutrition*. 71(5), 1033-1047.

Hambrecht, R., Schulze, P. C., Gielen, S., Linke, A., Möbius-Winkler, S., Yu, J. & Schuler, G. (2002). Reduction of insulin-like growth factor-I expression in the skeletal muscle of non-cachectic patients with chronic heart failure. *Journal of the American College of Cardiology*. 39(7), 1175-1181.

Harms, C. A. (2000). Effect of skeletal muscle demand on cardiovascular function. *Medicine and science in sports and exercise*. 32(1), 94-99.

Ho, K.K., Anderson, K.M., Kannel, W.B., Grossman, W., & Levy, D. (1993). Survival after the onset of congestive heart failure in Framingham Heart Study subjects. *Circulation*. 88(1), 107-115.

Hittel DS, Berggren JR, Shearer J, Boyle K, Houmard JA. (2009). Increased secretion and expression of myostatin in skeletal muscle from extremely obese women. *Diabetes*, 58(1), 30-38.

Ho, K. K., Pinsky, J. L., Kannel, W. B., & Levy, D. (1993). The epidemiology of heart failure: the Framingham Study. *Journal of the American College of Cardiology*. 22(4), A6-A13.

Houser, S. R., Margulies, K. B., Murphy, A. M., Spinale, F. G., Francis, G. S., Prabhu, S. D., Rockman, H.A., Molkentin, J.D. & Koch, W. J. (2012). Animal models of heart failure. *Circulation research*. 111(1), 131-150.

Howell, S., Maarek, J., Fournier, M., Sullivan, K., Zhan, W., & Sieck, G. (1995). Congestive heart failure: Differential adaptation of the diaphragm and latissimus dorsi. *Journal of Applied Physiology*. 79(2), 389-97.

Hughes, P., Polkey, M., Harrus, M., Coats, A., Moxham, J., & Green, M. (1999). Diaphragm strength in chronic heart failure. *American Journal of Respiratory and Critical Care Medicine.* 160(2), 529-34.

Hunt SA, Baker DW, Chin MH, et al. (2001) ACC/AHA guidelines for the evaluation and management of chronic heart failure in the adult: executive summary: a report of the American College of Cardiology/American Heart Association Task Force on Practice Guidelines (Committee to revise the 1995 Guidelines for the Evaluation and Management of Heart Failure). *Journal of the Amerian Colege of Cardiology*. (38) 2, 2101–2113.

Hunt, S. A., Abraham, W. T., Chin, M. H., Feldman, A. M., Francis, G. S., Ganiats, T. G., & Oates, J. A. (2009). 2009 focused update incorporated into the ACC/AHA 2005 guidelines for the diagnosis and management of heart failure in adults: a report of the American College of Cardiology Foundation/American Heart Association Task Force on Practice Guidelines developed in collaboration with the International Society for Heart and Lung Transplantation. *Journal of the American College of Cardiology*. 53(15), e1-e90.

Ingelsson, E., Sundström, J., Ärnlöv, J., Zethelius, B., & Lind, L. (2005). Insulin resistance and risk of congestive heart failure. *Journal of the American Medical Association.* 294(3), 334-341.

Ingram, R. H., & Braunwald, E. (2005). Dyspnea and pulmonary edema. *HARRISONS PRINCIPLES OF INTERNAL MEDICINE*, *16*(1), 201.

Jacobson, J.R., Barnard, J.W., Grigoryev, D.N., Ma, S.F., Tuder, R.M., & Garcia, J.G. (2005). Simvastatin attenuates vascular leak and inflammation in murine inflammatory lung injury. *American Journal of Physiology-Lung Cellular and Molecular Physiology*. 288(6), L1026-L1032.

Jennings, D. B., & Lockett, H. J. (2000). Angiotensin stimulates respiration in spontaneously hypertensive rats. *American Journal of Physiology-Regulatory, Integrative and Comparative Physiology*. 278(5), R1125-R1133.

Johnson, B. D., Beck, K. C., Olson, L. J., O'Malley, K. A., Allison, T. G., Squires, R. W., & Gau, G. T. (2000). Ventilatory constraints during exercise in patients with chronic heart failure. *CHEST Journal*. 117(2), 321-332.

Jondeau, G., Katz, S. D., Zohman, L., Goldberger, M., McCarthy, M., Bourdarias, J. P., & LeJemtel, T. H. (1992). Active skeletal muscle mass and cardiopulmonary reserve. Failure to attain peak aerobic capacity during maximal bicycle exercise in patients with severe congestive heart failure. *Circulation*. 86(5), 1351-1356.

Josiak K., Jankowska, E.A., Piepoli, M.F., Banasiak W., Ponikowski, P. (2014). Skeletal myopathy in patients with chronic heart failure: significance of anabolic-androgenic hormones. *Journal of Cachexia and Sarcopenia in Muscle.* (5) 2, 287-296

Kang, P. M., & Izumo, S. (2000). Apoptosis and heart failure a critical review of the literature. *Circulation Research*. 86(11), 1107-1113.

Kitzman, D. W., Nicklas, B., Kraus, W. E., Lyles, M. F., Eggebeen, J., Morgan, T. M., & Haykowsky, M. (2014). Skeletal muscle abnormalities and exercise intolerance in older patients with heart failure and preserved ejection fraction. *American Journal of Physiology-Heart and Circulatory Physiology*. 306(9), H1364-H1370.

Klawitter, P. F., & Clanton, T. L. (2004). Tension-time index, fatigue, and energetics in isolated rat diaphragm: a new experimental model. *Journal of Applied Physiology*. 96(1), 89-95.

Komajda, M., Follath, F., Swedberg, K. O., Cleland, J., Aguilar, J. C., Cohen-Solal, A. & Korewicki, J. (2003). The EuroHeart Failure Survey programme—a survey on the quality of care among patients with heart failure in Europe. *European Heart Journal*. 24(5), 464-474.

Kubo S.H., Rector, T.S. & Bank A.J. (1991) Endothelium-dependent vasodilation is attenuated in patients with heart failure. *Circulation.* 84,1589–1596.

Kushnir, A., & Marks, A. R. (2010). The ryanodine receptor in cardiac physiology and disease. *Advances in pharmacology*. 59, 1-30.

Lecarpentier, Y., Coirault, C., Langeron, O., Blanc, F., Salmeron, S., Attal, P. &Chemla, D. (1999). Impaired load dependence of diaphragm relaxation during congestive heart failure in the rabbit. *Journal of Applied Physiology (Bethesda, Md. : 1985)*. 87(4), 1339-45.

Levine, S., Nguyen, T., Taylor, N., Friscia, M. E., Budak, M. T., Rothenberg, P., & Rubinstein, N. A. (2008). Rapid disuse atrophy of diaphragm fibers in mechanically ventilated humans. *New England Journal of Medicine*. 358(13), 1327-1335.

Levine, B., Kalman, J., Mayer, L., Fillit, H. M., & Packer, M. (1990). Elevated circulating levels of tumor necrosis factor in severe chronic heart failure. *New England Journal of Medicine*. 323(4), 236-241.

Levy D, Larson MG, Vasan RS, Kannel WB, Ho KK. (1996) The progression from hypertension to congestive heart failure. Journal of the *American Medical Association*. 275, 1557–62.

Light, R. W., & George, R. B. (1983). Serial pulmonary function in patients with acute heart failure. *Archives of internal medicine*. 143(3), 429-433.

Lindsay, D., Lovegrove, C., Dunn, M., Bennett, J., Pepper, J., Yacoub, M., & Poole-Wilson, P. (1996) Histological abnormalities of muscle from limb, thorax and diaphragm in chronic heart failure. *European Heart Journal.* 17(8), 1239-50.

Lipkin, D.P., Canepa-Anson, R., Stephens, M.R., Poole-Wilson, P.A. (1986) Factors determining symptoms in heart failure: comparison of fast and slow exercise tests. *British Heart Journal*. 55(5), 439-445.

Lipkin, D.P., Jones, D.A., Round, J.M., Poole-Wilson, P.A. (1988) Abnormalities of skeletal muscle in patients with chronic heart failure. *International Jouranl of Cardiology*. 18, 187-195.

Maak, C., Elter, T. & Bohm, M. (2003) B-blockertreatment of chronic heart failure: comparison of Carvedilol and Metoprolol. *Congestive Heart Failure.* 9, 5.

Maillet, M., van Berlo, J.H. & Molkentin, J.D. (2013) Molecular basis of physiological heart growth: fundamental concepts and new players. *Nature Reviews Molecular Cell Biology*. 14, 38-48.

Mancini, D.M., Ferraro, N., Tuchler, M., Chance, B. & Wilson, J.R. (1988) Detection of abnormal calf muscle metabolism in patients with heart failure using phosphorus-31 nuclear magnetic resonance. *American Journal of Cardiology*. 62, 1234-1240.

Mancini, D. M., Walter, G., Reichek, N., Lenkinski, R., McCully, K. K., Mullen, J. L., & Wilson, J. R. (1992). Contribution of skeletal muscle atrophy to exercise intolerance and altered muscle metabolism in heart failure. *Circulation*. 85(4), 1364-1373.

Mann, D. L., Kent, R. L., Parsons, B., & Cooper, G. (1992). Adrenergic effects on the biology of the adult mammalian cardiocyte. *Circulation. 85(*2), 790-804.

Man, W. D. C., Kemp, P., Moxham, J., & Polkey, M. I. (2009). Skeletal muscle dysfunction in COPD: clinical and laboratory observations. *Clinical science*. 117(7), 251-264

Mangner, N., Weikert, B.T., Bwoen, S., Sandri, M., Hollrigel, R., Erbs, S., Hambrecht, R., Adams, V. (2015) Skeletal muscle alterations in chronic heart failure: differential effects on quadriceps and diaphragm. *Journal of Cachexia and Sarcopenia.* 6(4), 381-390.

Maskin, C. S., Forman, R., Sonnenblick, E. H., Frishman, W. H., & LeJemtel, T. H. (1983). Failure of dobutamine to increase exercise capacity despite hemodynamic improvement in severe chronic heart failure. *The American journal of cardiology*. 51(1), 177-182.

Maskin CS, Kugler J, Sonnenblick EH, LeJemtel TH. (1983). Acute inotropic stimulation with dopamine in severe congestive heart failure: beneficial hemodynamic effect at rest but not during maximal exercise. *The American journal of cardiology.* 52(1),1028-1032.

Massie, B., Conway, M. & Younge R. (1985) ^{31}P Nuclear magnetic resonance imaging evidence of abnormal skeletal muscle metabolism in patients with congestive heart failure. *American Journal of Cardiology.* 60, 309-315.

Meo, S. A., Al-Drees, A. M., Arif, M., Shah, F. A., & Al-Rubean, K. (2006). Assessment of respiratory muscles endurance in diabetic patients. *Saudi medical journal*. 27(2), 223-226.

Metra, M., Raddino, R., Dei Cas, L. (1990). Assessment of peak oxygen consumption, lactate and ventilatory threshold and correlation with resting and exercise hemodynamic data in chronic congestive heart failure. *American Journal of Cardiology*. 65, 1127-1133.

Middlekauff, H. R. (2010). Making the case for skeletal myopathy as the major limitation of exercise capacity in heart failure. *Circulation: Heart Failure*. 3(4), 537-546.

Middlekauff, H. R., Vigna, C., Verity, M. A., Fonarow, G. C., Horwich, T. B., Hamilton, M. A. & Tupling, A. R. (2012). Abnormalities of calcium handling proteins in skeletal muscle mirror those of the heart in humans with heart failure: a shared mechanism? *Journal of cardiac failure*. 18(9), 724-733.

Mielniczuk, L. M., Lamas, G. A., Flaker, G. C., Mitchell, G., Smith, S. C., Gersh, B. J., & Pfeffer, M. A. (2007). Left Ventricular End-Diastolic Pressure and Risk of Subsequent Heart Failure in Patients Following an Acute Myocardial Infarction. *Congestive Heart Failure*, 13(4), 209-214.

Minotti, J.R., Christoph, I., Oka, R., Weiner, M.W., Wells, L. & Massie, B.M. (1991) Impaired skeletal muscle function in patients with congestive heart failure: relationship to systemic exercise performance. *Journal of Clinical Investigation.* 88, 2077-2082.

Minotti, J.R., Pillay, P., Chang, L., Wells, L. & Massie, B.M. (1992) Neurophysiological assessment of skeletal muscle fatigue in patients with congestive heart failure. *Circulation.* 86, 903-908.

Minotti, J.R., Pillay, P., Oka, R., Wells, L., Christoph, I. & Massie, B.M. (1993) Skeletal muscle size: Relationship to muscle function in heart failure. *Journal of Applied Physiology*. 75, 373-381.

Moriarty, T. F. (1980). The law of laplace. *Circulation Research.* 46, 321-322.

Mulrow, C. D., Lucey, C. R., & Farnett, L. E. (1993). Discriminating causes of dyspnea through clinical examination. *Journal of general internal medicine*. 8(7), 383-392.

Münzel, T., Gori, T., Keaney, J. F., Maack, C., & Daiber, A. (2015). Pathophysiological role of oxidative stress in systolic and diastolic heart failure and its therapeutic implications. *European heart journal*. ehv305.

Heineke, J., Auger-Messier, M., Xu, J., Sargent, M., York, A., Welle, S., & Molkentin, J. D. (2010). Genetic deletion of myostatin from the heart prevents skeletal muscle atrophy in heart failure. *Circulation*. 121(3), 419-425.

Nettlefold, L., Jensen, D., Janssen, I. & Wolfe, L. A. (2007) Ventilatory control and acid-base regulation across the menstrual cycle in oral contraceptive users. *Respiratory physiology & neurobiology.* 158, 51-58

Niebauer, J., Pflaum, C. D., Clark, A. L., Strasburger, C. J., Hooper, J., Poole-Wilson, P. A., ... & Anker, S. D. (1998). Deficient insulin-like growth factor I in chronic heart failure predicts altered body composition, anabolic deficiency, cytokine and neurohormonal activation. *Journal of the American College of Cardiology*. 32(2), 393-397.

Norman, H. S., Oujiri, J., Larue, S. J., Chapman, C. B., Margulies, K. B., & Sweitzer, N. K. (2011). Decreased cardiac functional reserve in heart failure with preserved systolic function. *Journal of cardiac failure*. 17(4), 301-308.

Ohtake, P. J., & Jennings, D. B. (1993). Angiotensin II stimulates respiration in awake dogs and antagonizes baroreceptor inhibition. *Respiration physiology*. 91(2), 335-351.

Okita, K., Yonezawa, K., Nishijima, H., Hanada, A., Ohtsubo, M., Kohya, T. & Kitabatake, A. (1998). Skeletal muscle metabolism limits exercise capacity in patients with chronic heart failure. *Circulation*. 98(18), 1886-1891.

Ottenheijm, C. A., Heunks, L. M., Sieck, G. C., Zhan, W. Z., Jansen, S. M., Degens, H., & Dekhuijzen, P. R. (2005). Diaphragm dysfunction in chronic obstructive pulmonary disease. *American journal of respiratory and critical care medicine*. 172(2), 200-205.

Orozco-Levi, M., Lloreta, J., Minguella, J., Serrano, S., Broquetas, J. M., & Gea, J. (2001). Injury of the human diaphragm associated with exertion and chronic obstructive pulmonary disease. *American journal of respiratory and critical care medicine*. 164(9), 1734-1739.

Osadchii, O. E., Norton, G. R., McKechnie, R., Deftereos, D., & Woodiwiss, A. J. (2007). Cardiac dilatation and pump dysfunction without intrinsic myocardial systolic failure following chronic β-adrenoreceptor activation. *American Journal of Physiology-Heart and Circulatory Physiology*. 292(4), H1898-H1905.

Panizzolo, F. A., Maiorana, A. J., Naylor, L. H., Lichtwark, G. A., Dembo, L., Lloyd, D. G. & Rubenson, J. (2015). Is the soleus a sentinel muscle for impaired aerobic capacity in heart failure. *Medical Science, Sports & Exercise.* 47, 498-508.

Patten, R.D. & Hall-Porter. (2009) Small animal models of heart failure. *Circulation, Heart Failure*. 2, 138-144.

Parameswaran, K., Todd, D. C., & Soth, M. (2006). Altered respiratory physiology in obesity. *Canadian respiratory journal*. 13(4), 203-210.

Park, J.B., Charbonneau, F. & Schiffrin, E.L. (2001) Correlation of endothelial function in large and small arteries in human essential hypertension. *Journal of Hypertension*. 19, 415–420.

Pelosi, P., Croci, M., Ravagnan, I., Cerisara, M., Vicardi, P., Lissoni, A., & Gattinoni, L. (1997). Respiratory system mechanics in sedated, paralyzed, morbidly obese patients. *Journal of Applied Physiology*. 82(3), 811-818.

Picard, M., Jung, B., Liang, F., Azuelos, I., Hussain, S., Goldberg, P. & Matecki, S. (2012). Mitochondrial dysfunction and lipid accumulation in the human diaphragm during mechanical ventilation. *American journal of respiratory and critical care medicine*. 186(11), 1140-1149.

Piepoli, M.F., Clark, A. L., Volterrani, M., Adamopoulos, S., Sleight, P., & Coats, A. J. (1996). Contribution of muscle afferents to the hemodynamic, autonomic, and ventilatory responses to exercise in patients with chronic heart failure effects of physical training. *Circulation*. 93(5), 940-952.

Piepoli, M.F., Ponikowski, P. & Clark, A.L. (1999) A neural link to explain the "muscle hypothesis" of exercise intolerance in chronic heart failure. *American Heart Journal*. 137, 1050–1056.

Piepoli, M. F., & Coats, A. J. (2007). Counterpoint: Increased metaboreceptor stimulation explains the exaggerated exercise pressor reflex seen in heart failure. *Journal of Applied Physiology*. 102(1), 494-496.

Piepoli, M. F., & Coats, A. J. (2013). The 'skeletal muscle hypothesis in heart failure' revised. *European Heart Journal.* 34(7), 486-488.

Ponikowski, P., Chua, T.P., Francis, D. (2001) Muscle ergo receptor over activity reflects deterioration in clinical status and cardiorespiratory reflex control in chronic heart failure. *Circulation.*104, 2324-2330.

Public Health Agency of Canada. (2009). Tracking Heart Disease and Stroke in Canada, 2009. Retrieved from: http://www.phac-aspc.gc.ca/publicat/2009/cvd-avc/pdf/cvd-avs-2009-eng.pdf

Rajendran, P., Rengarajan, T., Thangavel, J., Nishigaki, Y., Sakthisekaran, D., Sethi, G., & Nishigaki, I. (2013). The Vascular Endothelium and Human Diseases. *International Journal of Biological Sciences*, *9*(10), 1057–1069.

Rengo, G., Pagano, G., Parisi, V., Femminella, G. D., De Lucia, C., Liccardo, D. & Fusco, F. (2014). Changes of plasma norepinephrine and serum N-terminal pro-brain natriuretic peptide after exercise training predict survival in patients with heart failure. *International journal of cardiology*. 171(3), 384-389.

Rezk, B.M., Yoshida, T., Semprun-Prieto, L., Higashi, Y., Sukhanov, S., & Delafontaine, P. (2012). Angiotensin II infusion induces marked diaphragmatic skeletal muscle atrophy. *PLoS One*. 7(1), e30276.

Ribeiro, J., Chiappa, P., Neder, G., & Frankenstein, R. (2009). Respiratory muscle function and exercise intolerance in heart failure. *Current Heart Failure Reports.* 6(2), 95-101.

Roberto, S., Mulliri, G., Milia, R., Solinas, R., Pinna, V., Sainas, G. & Crisafulli, A. (2017). Hemodynamic response to muscle reflex is abnormal in patients with heart failure with preserved ejection fraction. *Journal of Applied Physiology*, *122*(2), 376-385.

Rockman, H. A., Ross, R. S., Harris, A. N., Knowlton, K. U., Steinhelper, M. E., Field, L. J. & Chien, K. R. (1991). Segregation of atrial-specific and inducible expression of an atrial natriuretic factor transgene in an in vivo murine model of cardiac hypertrophy. *Proceedings of the National Academy of Sciences*. 88(18), 8277-8281.

Roth, G. A., Forouzanfar, M. H., Moran, A. E., Barber, R., Nguyen, G., Feigin, V. L. & Murray, C. J. (2015). Demographic and epidemiologic drivers of global cardiovascular mortality. *New England Journal of Medicine*. 372(14), 1333-1341.

Rubanyi, G.M. & Vanhoutte, P.M. (1986) Superoxide anions and hyperoxia inactivate endothelium-derived relaxing factor(s). *American Journal of Physiology*. 250, H822–H827.

Sabbah, H.N., Hansesn-Smith, F. & Sharov, V.G. (1993) Decreased proportion of type I myofibers in in skeletal muscle of dogs with heart failure. *Circulation.* 87, 1729-1737.

Sakuma, K., & Yamaguchi, A. (2012). Sarcopenia and cachexia: The adaptations of negative regulators of skeletal muscle mass. *Journal of Cachexia Sarcopenia Muscle.* 3(2), 77-94.

Saval, M. A., Kerrigan, D. J., Ophaug, K. M., Ehrman, J. K., & Keteyian, S. J. (2010). Relationship between leg muscle endurance and VE/VCO2 slope in patients with heart failure. *Journal of Cardiopulmonary Rehabilitation and Prevention*. 30(2), 106-110.

Scano, G., Stendardi, L., & Bruni, G. I. (2009). The respiratory muscles in eucapnic obesity: Their role in dyspnea. *Respiratory Medicine.* 103(9), 1276-1285.

Schiffrin, E.L., Park, J.B. & Intengan, H.D. (2000) Correction of arterial structure and endothelial dysfunction in human essential hypertension by the angiotensin receptor antagonist losartan. *Circulation*, 101:1653–1659.

Scott, A.C., Wensel, R., Davos, C.H., et al. (2003) Skeletal muscle reflex in heart failure patients: role of hydrogen. *Circulation.* 107, 300-306.

Scott, A.C., Wensel, R., Davos, C.H., Georgiadou, P., Kemp, M., Hooper, J., Coats, A.J., Piepoli, M.F. (2003) Skeletal muscle reflex in heart failure patients: role of hydrogen. *Circulation.*107(2), 300-306.

Selig, S. E., Carey, M. F., Menzies, D. G., Patterson, J., Geerling, R. H., Williams, A. D. & Hare, D. L. (2004). Moderate-intensity resistance exercise training in patients with chronic heart failure improves strength, endurance, heart rate variability, and forearm blood flow. *Journal of Cardiac Failure*. 10(1), 21-30.

Sexton, W. L., & Poole, D. C. (1998). Effects of emphysema on diaphragm blood flow during exercise. *Journal of Applied Physiology.*, 84(3), 971-979.

Shan, K., Kurrelmeyer, K., Seta, Y., Wang, F., Dibbs, Z., Deswal, A. & Mann, D. L. (1997). The role of cytokines in disease progression in heart failure. *Current opinions in cardiology*. 12(3), 218-223.

Shelton, R. J., Ingle, L., Rigby, A. S., Witte, K. K., Cleland, J. G., & Clark, A. L. (2010). Cardiac output does not limit submaximal exercise capacity in patients with chronic heart failure. *European journal of heart failure*. 12(9), 983-989.

Shen, W., Wolin, M. S., & Hintze, T. H. (1997). Defective endogenous nitric oxide-mediated modulation of cellular respiration in canine skeletal muscle after the development of heart failure. *The Journal of heart and lung transplantation: the official publication of the International Society for Heart Transplantation*. 16(10), 1026-1034

Shishi, B., Loos, B., Smith, W., du Toit, E. F., & Engelbrecht, A. M. (2011). Diet-induced obesity alters signaling pathways and induces atrophy and apoptosis in skeletal muscle in a prediabetic rat model. *Experimental Physiology*. 96(2), 179-93.

Simonini, A., Long, C. S., Dudley, G. A., Yue, P., McElhinny, J., & Massie, B. M. (1996). Heart failure in rats causes changes in skeletal muscle morphology and gene expression that are not explained by reduced activity. *Circulation Research*. 79(1), 128-136.

Smart, S. C., Knickelbine, T., Malik, F., & Sagar, K. B. (2000). Dobutamine-Atropine Stress Echocardiography for the Detection of Coronary Artery Disease in Patients With Left Ventricular Hypertrophy Importance of Chamber Size and Systolic Wall Stress. *Circulation*. 101(3), 258-263.

Solaro, R. J., & Kobayashi, T. (2011). Protein phosphorylation and signal transduction in cardiac thin filaments. *Journal of Biological Chemistry*. 286(12), 9935-9940.

Solaro, R. J., Henze, M., & Kobayashi, T. (2013). Integration of troponin I phosphorylation with cardiac regulatory networks. *Circulation research*. 112(2), 355-366.

Stassijins, G., Lysens, R. & Decramer, M. (1996) Peripheral and respiratory muscles in congestive heart failure. *European Respiratory Journal.* 9, 2161-2167.

Stassijns, G., Gayan-Ramirez, G., De Leyn, P., Verhoeven, G., Herijgers, P., De Bock, V. & Decramer, M. (1998). Systolic ventricular dysfunction causes selective diaphragm atrophy in rats. *American journal of respiratory and critical care medicine*. 158(6), 1963-1967.

Strömberg, A., & Mårtensson, J. (2003). Gender differences in patients with heart failure. *European Journal of Cardiovascular Nursing*. 2(1), 7-18.

Sueta, C. A., Bertoni, A. G., Massing, M. W., Mcardle, J., Duren-Winfield, V., Davis, J. & Goff, D. C. (2005). Managed care patients with heart failure: spectrum of ventricular dysfunction and predictors of medication utilization. *Journal of cardiac failure*. 11(2), 106-111.

Sullivan, M.J., Knight, J.D., Higginbotham, M.B., Cobb, F.R. (1989) Relation between central and peripheral hemodynamics during exercise in patients with chronic heart failure. *Circulation.* (80)2, 769-781.

Sullivan, M. J., Green, H. J., & Cobb, F. R. (1990). Skeletal muscle biochemistry and histology in ambulatory patients with long-term heart failure. *Circulation*. 81(2), 518-527.

Supinski, G., Dimarco, A., & Dibner-Dunlap, M. (1994). Alterations in diaphragm strength and fatigability in congestive heart failure. *Journal of Applied Physiology*. 76(6), 2707-13.

Talaei, F., Hylkema, M.N., Bouma, H.R. and Boerema, & Schmidt, M. (2011). Reversible remodeling of lung tissue during hibernation in the syrian hamster *The Journal of Experimental Biology*. 214(8), 1276-1282.

Tenório, L.H., Santos, A.C., Neto, J.B.C., Amaral, F.J., Passos,V.M.M., Lima, A.M.J., and Brasileiro-Santos, M.S. (2013). The influence of inspiratory muscle training on diaphragmatic mobility, pulmonary function, and maximum respiratory pressures in morbidly obese individuals: A pilot study. *Disability and Rehabilitation.* 35(22), 1915-1920.

Thaden, J. J., Nkomo, V. T., & Enriquez-Sarano, M. (2014). The global burden of aortic stenosis. *Progress in cardiovascular diseases*. 56(6), 565-571.

Thom, T., Haase, N., Rosamond, W., Howard, V. J., Rumsfeld, J., Manolio, T. & Lloyd-Jones, D. (2016). Heart disease and stroke statistics--2016 update: a report from the American Heart Association Statistics Committee and Stroke Statistics Subcommittee. *Circulation*, *113*(6), e85.

Todd, G. L., Baroldi, G., Pieper, G. M., Clayton, F. C., & Eliot, R. S. (1985). Experimental catecholamine-induced myocardial necrosis. II. Temporal development of isoproterenol-induced contraction band lesions correlated with ECG, hemodynamic and biochemical changes. *Journal of molecular and cellular cardiology*. 17(7), 647-656.

de Tombe, P. P. (2003). Cardiac myofilaments: mechanics and regulation. *Journal of biomechanics*. 36(5), 721-730.

Toth, M. J., Ades, P. A., Tischler, M. D., Tracy, R. P., & LeWinter, M. M. (2006). Immune activation is associated with reduced skeletal muscle mass and physical function in chronic heart failure. *International Journal of Cardiology*, 109(2), 179-187.

Toth, M. J., Shaw, A. O., Miller, M. S., VanBuren, P., LeWinter, M. M., Maughan, D. W., & Ades, P. A. (2010). Reduced knee extensor function in heart failure is not explained by inactivity. *International Journal ofCcardiology*, 143(3), 276-282.

Towbin, J. A., & Bowles, N. E. (2002). The failing heart. *Nature*. 415(6868), 227-233.

Triposkiadis, F., Karayannis, G., Giamouzis, G., Skoularigis, J., Louridas, G., & Butler, J. (2009). The sympathetic nervous system in heart failure: physiology, pathophysiology, and clinical implications. *Journal of the American College of Cardiology*. 54(19), 1747-1762.

van Oort, R. J., & Wehrens, X. H. (2010). Transverse aortic constriction in mice. *JoVE, Journal of Visualized Experiments*. 38, e1729-e1729.

Velagaleti, R. S., Pencina, M. J., Murabito, J. M., Wang, T. J., Parikh, N. I., D'Agostino, R. B. & Vasan, R. S. (2008). Long-term trends in the incidence of heart failure after myocardial infarction. *Circulation*. 118(20), 2057-2062.

Vescovo, G., Serafini, F., Facchin, L. L., Tenderini, P., Carraro, U., Dalla Libera, L. & Ambrosio, G. B. (1996). Specific changes in skeletal muscle myosin heavy chain composition in cardiac failure: differences compared with disuse atrophy as assessed on microbiopsies by high resolution electrophoresis. *Heart*. 76(4), 337-343.

Vescovo, G., Zennaro, R., Sandri, M., Carraro, U., Leprotti, C., Ceconi, C., ... & Dalla Libera, L. (1998). Apoptosis of skeletal muscle myofibers and interstitial cells in experimental heart failure. *Journal of molecular and cellular cardiology*, *30*(11), 2449-2459.

Vescovo, G., Volterrani, M., Zennaro, R., Sandri, M., Ceconi, C., Lorusso, R. & Dalla Libera, L. (2000). Apoptosis in the skeletal muscle of patients with heart failure: investigation of clinical and biochemical changes. *Heart*, *84*(4), 431-437.

Volterrani, M., Clark, A. L., Ludman, P. F., Swan, J. W., Adamopoulos, S., Piepoli, M., & Coats, A. J. S. (1994). Predictors of exercise capacity in chronic heart failure. *European Heart Journal*. 15(6), 801-809.

Wannamethee, S.G., Shaper, A.G. and Whincup, P.H. (2005). Body fat distribution, body composition and respiratory function in elderly men. *American Society for Clinical Nutrition.* 82(5), 996-2003.

Weber, K.T., Kinasewitz, G.T., Janicki, J.S. (1982). Oxygen utilization and ventilation during exercise in patients with chronic cardiac failure. *Circulation*. 65, 1213-1223.

Wehrens, X., & Marks, A. (2004). Molecular determinants of altered contractility in heart failure. *Annals of medicine*. 36(sup1), 70-80.

Wilson, J.R., Rayos, G., Yeoh, T.K., Gothard, P. & Bak, K. (1995) Dissociation between exertional symptoms and circulatory function in patients with heart failure. *Circulation.* 92(1), 47-53

Wilson, J.R., Fink, L. & Marris, J. (1985) Evaluation of energy metabolism in skeletal muscle of patients with heart failure with grated phosphorous-31 nuclear magnetic resonance imaging. *Biochemistry Journal.*200, 247-255.

Wilson, J.R., Coyle, E.F. & Osbakken, M. (1992) Effect of Heart Failure on Skeletal Muscle in Dogs. *American Journal of Physiology.*262 (2)

Wilson, J.R. & Mancini, D.M. (1993) Factors contributing to the exercise limitation in heart failure. *American Journal of Cardiology.* 22, 93A-98A.

Wilson, J.R., Mancini, D.M. & Dunkman, W.B. (1993) Exertional fatigue due to skeletal muscle dysfunction in patients with heart failure. *Circulation.* 87, 470-475.

Wilson, J.R., Martin, J.L., Schwartz, D., Ferraro, N. (1984) Exercise intolerance in patients with chronic heart failure: role of impaired nutritive flow to skeletal muscle. *Circulation,* (69)1079-1087.

Wilson J.R., Ferraro, N. & Wiener, D.H. (1985) Effect of the sympathetic nervous system on limb circulation and metabolism during exercise in heart failure. *Circulation.* 72, 72-81.

Wilson, J.R. & Ferraro, N. (1985) Effect of the renin-angiotensin system on limb circulation and metabolism during exercise in heart failure. *Journal of the American College of Cardiology.* 6, 556-563.

Wilson, S.H. & Lerman, A. (2001) Function of Vascular Endothelium. *Heart Physiology and Pathophysiology*, 27.

Wolfe, L. A., Kemp, J. G., Heenan, A. P., Preston, R. J. &. Ohtake, P. J. (1998) Acid-base regulation and control of ventilation in human pregnancy. *Canadian journal of physiology and pharmacology.* 76, 815-827.

Yilmaz, M. B., Refiker, M., Guray, Y., Guray, U., Altay, H., Demirkan, B., & Korkmaz, S. (2007). Prescription patterns in patients with systolic heart failure at hospital discharge: why β- blockers are under prescribed or prescribed at low dose in real life? *International journal of clinical practice*. 61(2), 225-230.

Yusuf, S., Islam, S., Chow, C. K., Rangarajan, S., Dagenais, G., Diaz, R., ... & Kruger, A. (2011). Use of secondary prevention drugs for cardiovascular disease in the community in high-income, middle-income, and low-income countries (the PURE Study): a prospective epidemiological survey. *The Lancet*, *378*(9798), 1231-1243.

APPENDIX A

Hematoxylin and Eosin Staining Protocol

1. Deparaffinize sections in 2 changes of xylene for 5 minutes each.
2. Re-hydrate in 2 changes of absolute alcohol, 5 minutes each.
3. 95% alcohol for 2 minutes.
4. 70% alcohol for 2 miuntes.
5. Wash briefly in distilled water.
6. Stain in Modified Harris Hematoxylin solution for 8 minutes.
7. Wash in running tap water for 10 minutes.
8. Differentiate in 1% acid alcohol for 30 seconds.
9. Wash running tap water for 1 minute.
10. Bluing in 0.2% ammonia water for 30-60 seconds.
11. Wash in running tap water for 5 minutes.
12. Rinse in 95% alcohol, 10 dips.
13. Counterstain in eosin-phloxine working solution for 1 minute.
14. Dehydrate through 70-95% alcohol.
15. 2 changes of absolute alcohol, 5 minutes each.
16. Clear in 2 changes of xylene, 5 minutes each.
17. Mount with xylene based mounting medium and coverglass.

APPENDIX B

Picrosirius Red Staining Protocol

1. Deparaffinize sections in 2 changes of xylene for 5 minutes each.
2. Re-hydrate in 2 changes of absolute alcohol, 5 minutes each.
3. 95% alcohol for 2 minutes.
4. 70% alcohol for 2 miuntes.
5. Wash briefly in distilled water.
6. Stain in Modified Harris Hematoxylin solution for 8 minutes.
7. Wash in running tap water for 10 minutes.
8. Counterstain in Pircrosirius Red solution for 1 hour.
9. Differentiate in 2 changes of 5% glacial acetic acid water for 2 minutes each.
10. Shake water from slides.
11. Dehydrate through 95% alcohol.
12. 2 changes of absolute alcohol, 5 minutes each.
13. Clear in 2 changes of xylene, 5 minutes each.
14. Mount with xylene based mounting medium and coverglass.

APPENDIX C

Gomori's Trichrome Staining Protocol

1. Deparaffinize sections in 2 changes of xylene for 5 minutes each.
2. Re-hydrate in 2 changes of absolute alcohol, 5 minutes each.
3. 95% alcohol for 2 minutes.
4. 70% alcohol for 2 miuntes.
5. Wash briefly in distilled water.
6. Stain in Modified Harris Hematoxylin solution for 8 minutes.
7. Wash in running tap water for 10 minutes.
8. Counterstain in Gomori's One Step Trichrome for 15 minutes.
9. Wash briefly in distilled water.
10. Dehydrate through 95% alcohol.
11. 2 changes of absolute alcohol, 5 minutes each.
12. Clear in 2 changes of xylene, 5 minutes each.
13. Mount with xylene based mounting medium (VWR, Canada).